



**Renato Azevedo
Cardoso**

**DESIGN OF COMPOSITE STEEL AND CONCRETE
BRIDGES**

PROJETO DE PONTES MISTAS DE AÇO E BETÃO



**Renato Azevedo
Cardoso**

**DESIGN OF COMPOSITE STEEL AND CONCRETE
BRIDGES**

PROJETO DE PONTES MISTAS DE AÇO E BETÃO

Dissertação apresentada à Universidade de Aveiro para cumprimento dos requisitos necessários à obtenção do grau de Mestre em Engenharia Civil, realizada sob a orientação científica do Dr. Paulo Jorge de Melo Matias Faria de Vila Real, Professor Catedrático do Departamento de Engenharia Civil da Universidade de Aveiro e coorientação científica do Dr. Enrique Mirambell Arrizabalaga, Professor Catedrático do departamento de Engenharia Civil da Universidade Politécnica da Catalunha.

To my parents, my brother, my sisters and my nieces

o júri

presidente

Prof. Doutora Ana Luísa Pinheiro Lomelino Velosa
Professora Associada da Universidade de Aveiro

Prof. Doutor Paulo Jorge de Sousa Cruz
Professor Catedrático da Universidade do Minho

Prof. Doutor Paulo Jorge de Melo Matias Faria de Vila Real
Vice-Reitor da Universidade de Aveiro

agradecimentos

A realização do trabalho aqui apresentado só foi possível porque existiu sempre alguém pronto para me dar suporte e motivação durante a sua realização.

Primeiramente, gostaria de expressar o meu sincero agradecimento aos professores Paulo Jorge de Melo Matias Faria de Vila Real e Enrique Mirambell Arrizabalaga, pela sua assistência, paciência e suporte.

Gostaria ainda de expressar o meu agradecimento...

... aos meus pais, ao meu irmão e às minhas irmãs e sobrinhas, por todo o afeto e motivação durante a minha carreira académica,

... aos meus primos, Vicente, Marina e Isabel por toda a amizade e ajuda durante estes últimos anos.

Por fim mas não menos importante, gostaria de estender o meu agradecimento a todos os meus amigos e colegas por todos os bons momentos que a sua companhia proporcionou.

Muito Obrigado.

acknowledgments

The work presented herein became possible only because there was always someone ready to give me support and motivation during its preparation.

First of all, I would like to express my deepest thanks to the Professors Paulo Jorge de Melo Matias Faria de Vila Real and Enrique Mirambell Arrizabalaga, for their assistance, patience and support.

Also, I would like to express my deepest thanks...

... to my parents, my brother, my sisters, and to my nieces, for all the affection and motivation during my academic career,

... to my cousins, Vicente, Marina, and Isabel, for all the friendship and unquantifiable help during these last years.

Last but not least, I would like to extend my warmest thanks to all my friends and colleagues for all the good times that their companies provided.

Thanks so much.

palavras-chave

Pontes mistas de aço e betão, Ponte bi-viga, Eurocódigos, Serviço

resumo

O trabalho aqui apresentado visa dar uma compreensão didática do dimensionamento de pontes mistas de aço e betão, assim como avaliar a resposta estrutural sob condições de serviço de pontes mistas, quando sujeitas a diferentes processos construtivos. Tendo isto em consideração, é apresentada uma descrição teórica, seguindo-se um exemplo numérico e um estudo focado no comportamento em serviço de pontes mistas, quando sujeitas a diferentes processos construtivos.

A descrição teórica estabelece uma breve exposição das formas e dos elementos estruturais de uma ponte mista, seguindo-se as principais formas construtivas e as principais vantagens associadas a este tipo de pontes, terminando com uma descrição das etapas de cálculo de acordo com as metodologias preconizadas pelos Eurocódigos, com o intuito de desenvolver um conhecimento teórico relacionado com o dimensionamento de pontes mistas de aço e betão.

O exemplo numérico tem como objetivo aplicar o conhecimento adquirido, exemplificando as diferentes etapas de cálculo do dimensionamento de pontes mistas, dando especial ênfase às diferentes ações que atuam na ponte e a forma como estas são modeladas, assim como à verificação aos estados limite último e de serviço das seções transversais do tabuleiro misto.

O estudo focado no comportamento ao serviço das pontes mistas de aço e betão tem como finalidade analisar e avaliar a resposta estrutural das pontes mistas sob condições de serviço, quando sujeitas a diferentes processos construtivos. Assim sendo, o estado de tensões e as deformações devidas a cargas de curta e longa duração, bem como os efeitos da fissuração do betão sobre as zonas de suportes são analisados. Esta análise estrutural é efetuada com o programa de análise e dimensionamento MIDAS/Civil 2015 (V2.2).

keywords

Composite steel and concrete bridges, Twin-girder bridge, Eurocodes, Service

abstract

The work presented herein aims to give a didactical understanding related to the composite bridge designing according to the methodologies proposed by Eurocodes, as well as to evaluate the structural response under service conditions of composite bridges when considering different construction processes. Taking this into account, a theoretical description, followed by a numerical example, until a study focused on the serviceability behaviour of composite bridges when considering different construction processes are presented.

The theoretical description establishes a brief description related to the structural forms and structural elements of a composite bridge, followed by the main constructive forms and the advantages of such type of bridges, until description of the steps calculation according to the methodologies performed by Eurocodes, in order to develop a theoretical knowledge related to the steel concrete composite bridge designing.

The numerical example aims to apply the acquired knowledge, exemplifying the different calculation steps of a composite bridge designing, highlighting the various actions acting on the bridge, and how they are modelled, as well as the verification at ultimate and serviceability limit states of the deck cross sections.

The study focused on the serviceability behaviour of composite bridges aims to analyse and evaluate the structural response under service conditions when considering different construction processes. Taking this into consideration, short and long term stresses, deflections, as well as the effect of concrete cracking above supports are analysed. This study is solved through the analysis Program MIDAS/Civil 2015 (V2.2).

Contents

1. Introduction	1
1.1 Objectives	2
1.2 Thesis Lay-out	2
2. Steel – concrete composite bridges	5
2.1. Structural form	6
2.2. Structural elements of the bridge	6
2.2.1. Substructure	7
2.2.2. Superstructure	7
2.2.3. Other components	8
2.3. Construction forms	10
2.3.1. Erection of steel structure	10
2.3.2. Slab construction	15
2.4. Advantages of steel-concrete composite bridges	17
2.5. Structural materials	18
2.5.1. Concrete	18
2.5.2. Steel	20
3. Design of steel-concrete composite bridges	27
3.1. The Eurocodes and product standards	27
3.2. Limit state design	28
3.3. Actions	29
3.3.1. Traffic load	29
3.4. Combination of actions	34
3.4.1. Ultimate Limit States (ULS)	35
3.4.2. Serviceability Limit States (SLS)	36
3.5. Structural analysis of composite bridges	37

3.5.1.	Effect of shear lag	37
3.5.2.	Local buckling and cross-section classification	38
3.5.3.	Effect of cracking of concrete	40
3.5.4.	Effects of creep and shrinkage	40
3.5.5.	Stages and sequence of construction	41
3.6.	Verification by Ultimate Limit States	41
3.6.1.	Resistance of cross-sections	41
3.6.2.	Resistance to lateral-torsional buckling	43
3.6.3.	Resistance to shear buckling and in-plane forces applied to webs	45
3.6.4.	Resistance to longitudinal shear	47
3.6.5.	Resistance to fatigue.....	50
3.7.	Verifications by serviceability limit states	50
3.7.1.	Stresses	51
3.7.2.	Deflections	51
3.7.3.	Cracking of concrete	51
4.	Numerical Example	53
4.1.	Structural description.....	53
4.2.	Materials	54
4.3.	Fabrication and erection	57
4.4.	Normative standard used	57
4.5.	Actions.....	58
4.5.1.	Permanent actions	58
4.5.2.	Variable actions.....	59
4.6.	Effective width	63
4.7.	Global analysis	64
4.7.1.	Stages of construction	65

4.7.2.	Effect of creep	65
4.7.3.	Effect of cracking of concrete	65
4.7.4.	Mechanical characteristics of sections	66
4.7.5.	Model calculation	68
4.7.6.	Analysis results.....	69
4.7.7.	Safety factors and combination values	71
4.7.8.	Design value of the combined actions.....	72
4.8.	Verification by Ultimate Limit States (ULS)	75
4.8.1.	Cross section at Mid-span	75
4.8.2.	Cross section over pier	81
4.8.3.	Lateral torsional buckling.....	88
4.9.	Verification of Serviceability Limit States (SLS).....	93
4.9.1.	Deflections.....	93
4.9.2.	Stress limitations	93
4.9.3.	Cracking of concrete for longitudinal global bending.....	97
4.9.4.	Connection.....	101
5.	Influence of the construction process on the serviceability behaviour of composite bridges	105
5.1.	Description of the structural analysis.....	105
5.2.	General description of MIDAS/Civil.....	107
5.2.1.	Definition of construction stages.....	108
5.2.2.	Consideration of time-dependent material behaviour	108
5.2.3.	Running a construction stage analysis by MIDAS/Civil.....	110
5.3.	Considered construction process and loads applied at each stage	111
5.3.1.	Propped bridge.....	114
5.3.2.	Alternate slab concreting	115

5.3.3.	Continuous slab concreting	116
5.3.4.	Simultaneous slab concreting	117
5.3.5.	Propped bridge 2	118
5.4.	Conclusions related to the influence of the construction sequence	119
5.4.1.	Longitudinal bending moments.....	119
5.4.2.	Deflections and stresses at critical sections.....	121
5.4.3.	Effect of calculation method used to take into account the concrete cracking above supports	124
5.4.4.	Final considerations.....	126
6.	Conclusion	127
7.	References.....	129

List of Figures

Figure 2-1 - Schematic view of the structural elements of a composite twin girder bridge (Lebet & Hirt, 2013).....	5
Figure 2-2 - Span ranges for main bridge type (Lebet & Hirt, 2013).....	6
Figure 2-3 - Structural elements (Lebet & Hirt, 2013).....	6
Figure 2-4 – Types of bracing (Lebet, Hirt, 2013).....	7
Figure 2-5 - Plan bracing (Lebet, Hirt, 2013).....	7
Figure 2-6 - Types of shear connectors: studs, bars with bops and channels (Collings, 2005)	8
Figure 2-7 - Erection by launching principle (Lebet & Hirt, 2013).....	11
Figure 2-8 - Erection by crane principle (Sétra - Service d'études sur les transports, les routes et leurs aménagements, 2010).....	12
Figure 2-9 - Erection by shifting principle (Sétra - Service d'études sur les transports, les routes et leurs aménagements, 2010).....	13
Figure 2-10 - Erection by hoisting principle (Sétra - Service d'études sur les transports, les routes et leurs aménagements, 2010).....	14
Figure 2-11 - Example of mobile formwork (Lebet & Hirt, 2013).....	16
Figure 2-12 - Slab construction by precasting principle (Lebet & Hirt, 2013).....	16
Figure 2-13 - Longitudinal sections of joints in precast slabs (Lebet & Hirt, 2013).....	17
Figure 2-14 - Charpy test (Vayas & Iliopoulos, 2013).....	22
Figure 2-15 - Schematic comparison between the corrosion loss of weathering steel and ordinary structural steel (Steel Construction.info).....	25
Figure 3-1 Eurocodes to be used in a composite bridge design (COMBRI Design Manual, 2008).....	28
Figure 3-2- Example of lane numbering (Vayas & Iliopoulos, 2013).....	30
Figure 3-3 - Application of the Load model 2 (Vayas & Iliopoulos, 2013).....	32
Figure 3-4 - Length L_e and distribution of effective width of concrete along the span (Vayas & Iliopoulos, 2013).....	38
Figure 3-5 - Classes of cross sections (Vayas & Iliopoulos, 2013).....	39
Figure 3-6 - Effective class 2 web that was initially class 3 (Vayas & Iliopoulos, 2013)...	39
Figure 3-7 - Simplified method principle (Lebet & Hirt, 2013).....	40

Figure 3-8 - Examples of plastic stress distributions for a composite beam with a solid slab and full shear connection in sagging and hogging bending (EN 1994-2, 2005).....	42
Figure 3-9 - Summation of stresses acting on different resisting cross sections (Composite highway bridge design, 2010)	43
Figure 3-10 - U-frame model (EN 1994-2, 2005).....	44
Figure 3-11 - Modelling of the compression flange as a T-section column on rigid supports (Vayas & Iliopoulos, 2013).....	45
Figure 3-12 - Buckling of a panel in shear (Lebet & Hirt, 2013)	46
Figure 3-13 - Dimensions of headed studs (Vayas & Iliopoulos, 2013).....	47
Figure 3-14 - Longitudinal shear in inelastic regions (Vayas & Iliopoulos, 2013)	49
Figure 3-15 - Distribution of end shear due to shrinkage at an edge support (Vayas & Iliopoulos, 2013)	49
Figure 3-16- Failure mechanism and typical sections for checking shear failure (Vayas & Iliopoulos, 2013)	50
Figure 4-1 Cross section.....	54
Figure 4-2 - Structural arrangement of the steel-concrete composite bridge.....	56
Figure 4-3 - Positioning of the traffic loads in transverse position	59
Figure 4-4 - Effective width of the concrete flange	64
Figure 4-5 - Section Type 1 properties.....	66
Figure 4-6 - Section Type 2 properties.....	67
Figure 4-7 - Section Type 3 properties.....	67
Figure 4-8 - Model calculation.....	68
Figure 4-9 - Shrinkage loads model	70
Figure 4-10 – Location of plastic neutral axis.....	76
Figure 4-11 - Bottom flange geometry.....	81
Figure 4-12 - Location of plastic neutral axis	82
Figure 4-13 -Transverse and longitudinal stiffeners spacing	83
Figure 4-14 - Notations defining the modelled transverse frame.....	88
Figure 4-15 - Load cases modelling for the rigidity C_d calculation	88
Figure 4-16 - Geometric properties of section AA'.....	89
Figure 4-17 - Geometric properties of section BB'	89
Figure 4-18 - ULS shear force per unit length resisted by the shear connectors	103

Figure 5-1 - Creep Coefficient.....	109
Figure 5-2 - Shrinkage Strain	109
Figure 5-3 - Compressive strength	110
Figure 5-4 - Schematic representation of Propped bridge construction process	114
Figure 5-5 - Schematic representation of Alternate slab concreting	115
Figure 5-6 - Schematic representation of Continuous slab concreting.....	116
Figure 5-7 - Schematic representation of Simultaneous slab concreting	117
Figure 5-8 - Schematic representation of Propped bridge alternate slab concreting.....	118
Figure 5-9 - Bending moments due to Dead load at short and long term.....	119
Figure 5-10 - Bending moments at central span.....	119
Figure 5-11 - Bending moments at support	120
Figure 5-12 - Deflections due to Creep and Shrinkage in the bridge deck	122
Figure 5-13 - Time evolution of the stresses in the concrete slab at the centre of the central span.....	123
Figure 5-14 - Time evolution of the stresses in the bottom steel plate at the centre of the central span.....	123
Figure 5-15 - Final deflections at interior span and bottom steel stresses at support.....	124
Figure 5-16 - Influence of the calculation method on the bending moments at Central Span	125
Figure 5-17 - Influence of the calculation method on the bending moments at Support ..	126

List of Tables

Table 2-1 Types of bearings (Composite highway bridge design, 2010).....	10
Table 2-2 - Properties of concrete (Vayas & Iliopoulos, 2013)	18
Table 2-3 - Stress-strain relations for the capacity design of cross sections for C20/25 till C50/60 (concrete under compression) (Vayas & Iliopoulos, 2013).....	19
Table 2-4 - Properties of Structural Steel (Vayas & Iliopoulos, 2013).....	20
Table 2-5 - Mechanical properties of structural steels produced to EN 10025, in accordance with EN 1993-1-1 (Vayas & Iliopoulos, 2013).....	21
Table 2-6 - Definition of steel quality according to EN 10025 (Vayas & Iliopoulos, 2013)	22
Table 2-7 - Protective systems for bridges (Collings, 2005).....	24
Table 3-1 - Product standards.....	28
Table 3-2 - Number and width of notional lanes.....	30
Table 3-3 - Characteristic values of LM1 (adapted from (Vayas & Iliopoulos, 2013)).....	31
Table 3-4 - Characteristic values of centrifugal forces (Vayas & Iliopoulos, 2013).....	34
Table 3-5 - Groups of loads.....	34
Table 3-6 - Fundamental ULS combination of actions (Davaine, Imberty, & Raoul, 2007)	35
Table 3-7 - Characteristic SLS combination of actions (Davaine, Imberty, & Raoul, 2007)	36
Table 3-8 - Frequent SLS combination of actions (Davaine, Imberty, & Raoul, 2007)	37
Table 3-9 - Quasi-permanent SLS combination of actions (Davaine, Imberty, & Raoul, 2007).....	37
Table 3-10 - Shear resistance P_{Rd} (kN) of headed studs with $h_{sc}/d \geq 4$ in solid slabs at ULS (Vayas & Iliopoulos, 2013)	48
Table 4-1 - Maximum permissible thickness t [mm] according to EN 10025, as a function of the temperature and the Stress in the plate	55
Table 4-1 - Mechanical properties of section type 1	66
Table 4-2 - Mechanical properties of section type 2	67
Table 4-3 - Mechanical properties of section type 3	67
Table 4-4 - Properties for steel and composite cross sections.....	68
Table 4-5 - Results of action effects.....	69

Table 4-6 - Deflection values at mid span.....	70
Table 4-7 - Partial factors for actions.....	71
Table 4-8 - Partial factors for materials	71
Table 4-9 - Factors for combination values	71
Table 4-10 - Combined values at ULS.....	73
Table 4-11 - Combined values at SLS	74
Table 4-12 - Stresses in structural steel.....	94
Table 4-13 - Stresses in steel reinforcement	96
Table 4-14 - Longitudinal shear at an edge support.....	102
Table 5-1 - Loads applied at each stage	113
Table 5-2 - Area moment of inertia about the element local y-axis Scale factor.....	113
Table 5-3 - Cross-sectional area Scale factor.....	113
Table 5-4 - Input parameters to perform Propped bridge construction process.....	114
Table 5-5 - Input parameters to perform Alternate slab concreting.....	115
Table 5-6 - Input parameters to perform Continuous slab concreting	116
Table 5-7 - Input parameters to perform Simultaneous slab concreting	117
Table 5-8 - Input parameters to perform Propped bridge alternate slab concreting	118
Table 5-9 - Bending moments at central span and at support sections	120
Table 5-10 - Deflections and stresses at the critical sections.....	121
Table 5-11 - Deflection values at central span (mm).....	122
Table 5-12 - Influence of the bending moments on the bending moments.....	125

Chapter 1 Introduction

The history of bridge engineering is in part connected with the history of humanity, which, since the earliest times, has sought for ways to cross over barriers in order to communicate. Franklin D. Roosevelt once said: “There can be little doubt that in many ways the story of bridge-building is the story of civilization. By it we can readily measure an important part of a people’s progress”. (Weingardt, 2005, p. 53)

“The Romans understood that the establishment and maintenance of their empire depended on efficient and permanent communications. Building roads and bridges was therefore a high priority”. (Ryall, *et al*, 2000, p. 3)

Actually Romans were truly the first great bridge builders to use stones and, in some cases, cement to build arch bridges, their characteristic structural form of bridges. With the fall of the Roman Empire in the 5th century, bridge engineering did not have a major development until the 19th century.

The industrial revolution brought huge changes to all aspects of life and bridge design was not an exception. “Wood and stone were gradually replaced by cast iron and wrought iron constructions, which in turn was replaced by first steel and then concrete; the two primary materials of bridge building in the twentieth century”. (Ryall, *et al*, 2000, p. 17)

Of all types of bridges, steel-concrete composite ones have become most popular, particularly in Europe. “The greater majority of European countries now build composite bridges” (Sétra - Service d'études sur les transports, les routes et leurs aménagements, 2010, p. 13)

Thus, this dissertation aims to give an understanding of the behaviour of such type of bridges, including its advantages, followed by a description of the composite bridge designing, until the design of a composite bridge, highlighting the verification part of the design according to the methodologies proposed by Eurocodes, mainly by Eurocode 4 part 2, which is related to design of composite steel and concrete bridges. Moreover, a structural analysis focused on the structural response under service conditions of composite bridges when considering different construction processes is under scope.

1.1 Objectives

As it can be inferred by the above lines, the purpose of this dissertation is to present a didactical description about conceptual design of composite steel and concrete bridges, in order to give a better understanding of the behaviour of such type of bridges, followed by a numerical example which details the steps calculation according to methodologies proposed by Eurocodes, until the study of the influence of the construction process on the serviceability behaviour of composite bridges.

The general description aims to establish the main reasons to combine the two structural materials, concrete and structural steel, as well as the connection between these two materials. Moreover, a description related to the structural elements of a composite bridge, and their main functions, followed by the constructive forms and advantages of such type of bridges, until description of the steps calculation according to the methodologies performed by Eurocodes is under scope.

The numerical example is intended to exemplify the different calculation steps of a composite bridge designing, highlighting the various actions acting on the bridge, and how they are modelled, as well as the verification at ultimate and serviceability limit states of the deck cross sections.

On its turn, the goal of the structural analysis is to analyse and evaluate the structural response under service conditions of composite bridges when considering different construction processes.

1.2 Thesis Lay-out

The present thesis contains 6 chapters, including this introduction (Chapter 1) and conclusion (Chapter 6). Chapter 1, provides a brief reference to the importance of the bridge engineering in the people's progress, as well as it introduces the goals of this thesis.

The second and third chapters covers a literature review of steel and concrete composite bridge designing. In Chapter 2, a general overview of composite steel and concrete composites bridges is given, highlighting the structural forms and structural elements of a composite bridge, the constructive forms and the aspects that should be taken into consideration in order to adopt the most proper constructive structural system, the advantages of such type of bridges, until an overall analysis of the properties of the two structural materials (concrete and structural steel), which play an important role on the behaviour of composite structures. Chapter 3 includes the standards used (Eurocodes) in the

design of composite bridges, as well as a description related to the designing of a composite bridge process according to the methodologies performed by Eurocodes.

Chapter 4 provides a numerical example, which aims to illustrate the different steps of a twin composite girder bridge designing.

Chapter 5 includes the methodology of the evaluating of the influence of the construction process on the serviceability behaviour of composite bridges, as well as it discusses the results obtained.

Finally, Chapter 6 summarizes the work and provides a brief conclusion to this thesis.

Chapter 2

Steel – concrete composite bridges

“A bridge is a spatial object whose purpose is to cross an obstacle (valley, water, or road) with a communication route”. (Lebet, Hirt, 2013, p.13)

The concept of steel-concrete composite bridges, commonly designated as composite bridges (Figure 2-1), is that the bridge combines different materials, namely concrete and steel.

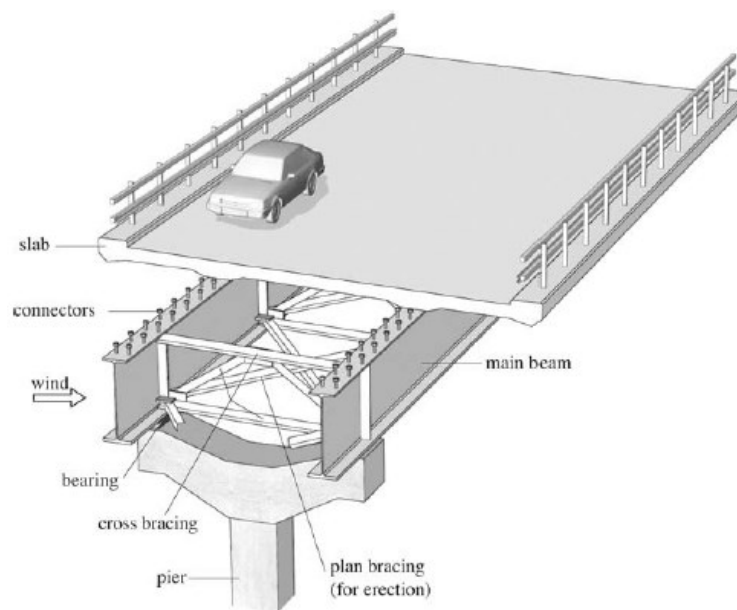


Figure 2-1 - Schematic view of the structural elements of a composite twin girder bridge (Lebet & Hirt, 2013)

The main reason to combine these materials is related to the benefits of both structural materials, because while concrete is excellent for dealing with compressive forces, steel also can carry large tensile stresses. (Vayas, Iliopoulos, 2013) Therefore, according to (Collings, 2005), to understand the basic behaviour of a composite structure, there are two primary points to consider:

- The differences between the materials;
- The connection of the two materials.

In order to have a better understanding of this type of bridges, both points listed above, as well other relevant points, such as the structural form, structural elements, and construction forms, are to be detailed on the following sections.

2.1. Structural form

“Most commonly, steel-concrete composite structures take a simple beam and slab form”. (Collings, 2005, p. 1) However, composite structures, allows the conception of a wide variety of possible solutions to different type of problems, such as truss beam, arch bridges, inclined leg bridge, cable stayed bridge and suspension bridge.

“The choice and configuration of the longitudinal structure of a bridge are primarily a function of the size of the obstacle to be crossed, the length of the spans, the accessibility of the location, and the possible methods of execution”. (Lebet, Hirt, 2013, p. 78) Figure 2-2, shows the most usual longitudinal structural forms, according to the span ranges.

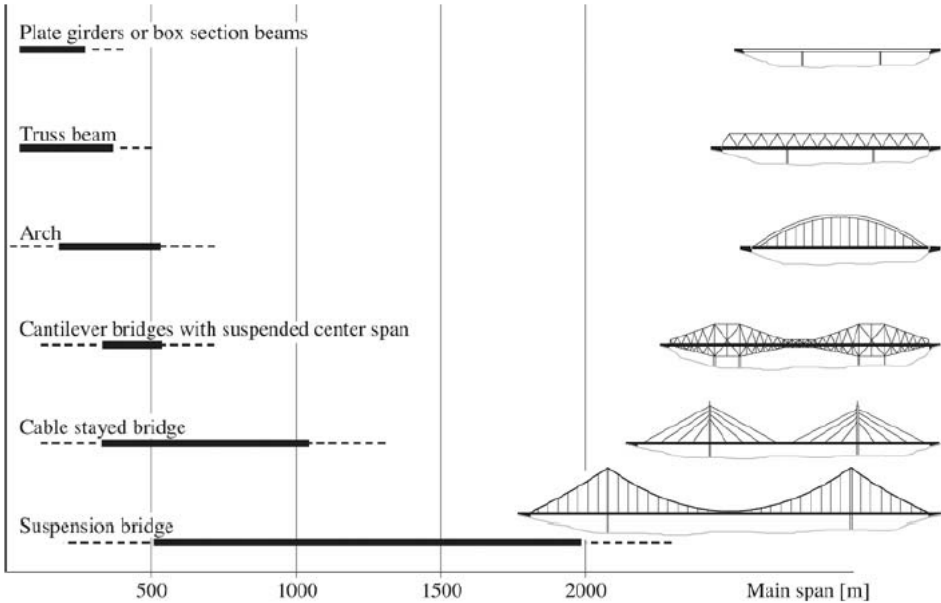


Figure 2-2 - Span ranges for main bridge type (Lebet & Hirt, 2013)

2.2. Structural elements of the bridge

The structural elements that constitute the bridges are the substructure and the superstructure as represented in Figure 2-3.

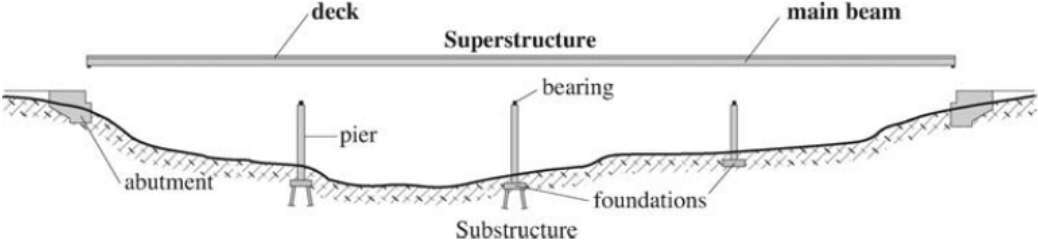


Figure 2-3 - Structural elements (Lebet & Hirt, 2013)

2.2.1. Substructure

The substructure is formed by the elements that support the bridges, such as the piers, abutments and foundations. The main function of these elements is to provide support to the superstructure and transfer the actions down to the ground. (Lebet, Hirt, 2013) These elements are generally of reinforced concrete and for this reason are not be detailed on the present work.

2.2.2. Superstructure

The superstructure comprises the individual elements such as the slab, the main beams with their shear connectors, the cross bracing and the plan bracing. (Lebet, Hirt, 2013)

The main function of the slab is essentially related to the transmission of the traffic loads to the primary structural elements of the bridge, while the main beams (longitudinal structural elements of the bridge) are responsible for the transference of the loads coming from the slab to the supports by bending, by shear, and by torsion. (Lebet, Hirt, 2013)

“The steelwork is relatively slender and usually requires bracing to ensure stability”. (Collings, 2005, p. 20) Depending on whether this bracing system is composed by planar elements perpendicular to the bridge axis or by horizontal elements, is defined as cross or plan bracing, respectively.

Cross bracing play an important role in composite bridges, because it prevents deformation of the bridge cross section, and transfers the horizontal forces which act on the main beams (due to wind, effects of curvature) to the plan bracing. Figure 2-4, illustrates the most common forms of cross bracing. (Lebet, Hirt, 2013)

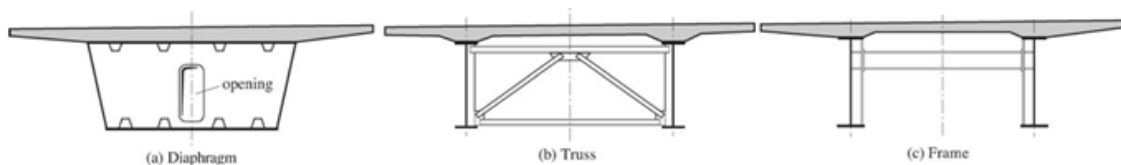


Figure 2-4 – Types of bracing (Lebet, Hirt, 2013)

Furthermore, the plan bracing, which sometimes is temporary used during construction (Figure 2-5), ensures the lateral behaviour of the bridge by stiffening the primary structure in the horizontal plane. (Lebet, Hirt, 2013)

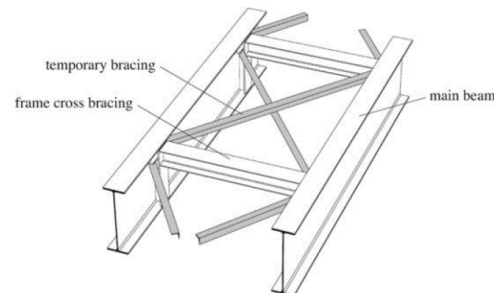


Figure 2-5 - Plan bracing (Lebet, Hirt, 2013)

The connection between the two structural materials (concrete and steel) has a fundamental role in composite behaviour, since that if is adequately connected, the two parts act as one whole structure, increasing the structural efficiency. This connection is achieved through shear connectors (Figure 2-6), which are defined as “devices for ensuring force transfer at steel-concrete interface that carry the shear and any connection between the materials”. (Collings, 2005, p. 13)

There are two basic forms of connectors: flexible or rigid. Flexible connectors, such as headed studs behave in a ductile manner, allowing significant movement or slip at the ultimate limit state, while the rigid connectors, such as bars behave in a more brittle fashion. Therefore, bops are an intermediate type between the rigid and the flexible connectors. (Collings, 2005)

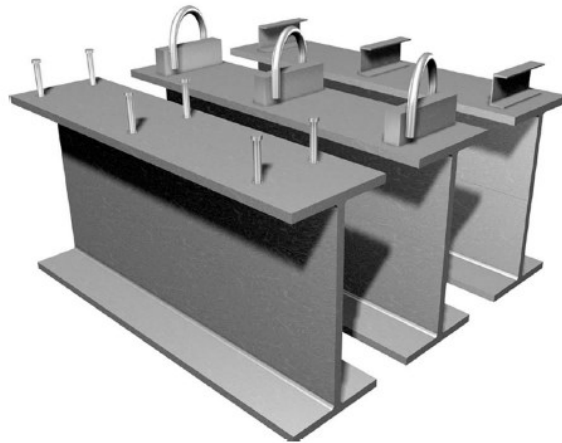


Figure 2-6 - Types of shear connectors: studs, bars with bops and channels (Collings, 2005)

2.2.3. Other components

Other components are used to ensure the proper functioning of a bridge, namely, expansion joints, bearings and water evacuation system. (Lebet & Hirt, 2013) A brief description of these elements is presented below.

2.2.3.1. Expansion joints

Expansion joints are flexible links that are used at the ends of the bridges to “assure the continuity of the rolling surface between the deck and abutments, or between two separate parts of the deck”. (Lebet, Hirt, 2013, p. 26) They must be able to allow movement of the superstructure relative the substructure, as well as to support the vertical loads from the traffic.

These flexible links should be manufactured and designed according to the regulations of the European Technical Approval (ETA), as well as not increase the degree of the bridge’s static indeterminacy by restraining degrees of freedom at supports, be waterproof and produce low noise when vehicles are passing over them. (Vayas, Iliopoulos, 2013)

Since expansion joints have a limited design life (mainly due to the effects of traffic) and their replacement is expensive, “the current trend is to reduce the number of expansion joints for a bridge”. (Lebet, Hirt, 2013, p. 26)

2.2.3.2. Water evacuation

With the purpose of preventing standing water on the rolling surface that can be dangerous for traffic, as well as can accelerate structural degradation (damage of the concrete due to either freeze-thaw action or chlorides in the water and in the case of the steel can lead to corrosion), it is necessary to conceive a complete system for water evacuation. (Lebet & Hirt, 2013)

2.2.3.3. Bearings

Bearings are structural devices placed at the interface between the superstructure and the substructure (Figure 2-3), which ensure the transfer of the vertical and horizontal forces from the superstructure to the piers and abutments as well as the necessary movements of the superstructure (e.g. due to temperature and humidity changes, creep, shrinkage, fatigue effects, dynamic load effects and overload). (Lebet & Hirt, 2013)

Generally, these devices have a short design life, during which require the necessity to “check them regularly, to provide the necessary maintenance, and if necessary to replace them”. (Lebet & Hirt, 2013, p. 25) Table 2-1, summarizes the most common types of bearings according to its major properties, as well as the typical use.

Type	Common capacity range (kN)	Typical friction	Use	Limitations	General comments
Pot	500-30000	0,05	>20 m span	Rotation capacity 0.01 radians	Widely used
Elastomeric strip	200-1000	4-10 kN/mm	Short span >10m	Limited translation and rotation	Economic for short spans
Elastomeric pad	10-500	0,5 - 5,0 kN/mm	Short span – light loads	Limited translation and rotation	Useful for light loads
Elastomeric laminated	100-1000	0,5 – 5,9 kN/mm	Short span	Heavy loads	Widely used
Cylindrical roller	1000-1500	0,01 (single roller hardened)	Minimal friction	Nil lateral translation or rotation	Limited used. Guides essential
Linear rocker	1000-10000	0,25	Fixed bearings. Rail bridges	High friction. Nil lateral rotation	Large rotation

Type	Common capacity range (kN)	Typical friction	Use	Limitations	General comments
Cylindrical knuckle	2000-10000	NA	Pinned bearings. Rail bridges	Unsuitable translation or lateral rotation	Little used
Plane sliding	100-1000	0,005	Sliding guides with large translation	Small rotation capacity	Suitable very short span (< 5m) where rotation negligible
Spherical sliding	1000-12000	0,05	>20 m span	More expensive than pot	Rotation capacity 0,05
Guided	150-1500	0.05	Horizontal load only	Carries no vertical load	Used when guide bearing essential, e.g. end of long viaduct of wide bridge
Pin	10-1000	NA	Fixed with uplift	Nil translation or lateral rotation	Useful for footbridge for security or uplift
Swing link	10-1000	Control by link length	Guided with uplift	Nil translation or lateral rotation	Useful for footbridge for security or uplift

Table 2-1 Types of bearings (Composite highway bridge design, 2010)

2.3. Construction forms

There exist multiple aspects that should be taken into consideration in order to adopt the most proper constructive structural system, such as the available construction depth and the geographical and topographical characteristics of the bridge location, as well as the future reconstruction activities and maintenance. Since the composite bridges are structures which comprises a concrete slab connected to the steel structure, the construction form corresponds to the erection of the steel structure, and to the slab construction. Both points listed above are detailed on the following.

2.3.1. Erection of steel structure

As stated by (Vayas & Iliopoulos, 2013, p.57), “the erection method is a complicated issue and cannot be covered in few paragraphs”, in such a way that it “defines the load history of the bridge and has a primary influence on the evolution of stresses and deformations”. Taking this into account, a brief description of the most common methods of the steel structure erection is present on the following, highlighting the fundamental characteristics, as well as its advantages and drawbacks.

2.3.1.1. Installation by launching

The method of erection by launching (Figure 2-7) is the most commonly implemented method, which consists on assembly the elements of the structure in an area that is in line with the bridge axis (located at one or both ends), and launching it up to its final position. (Lebet & Hirt, 2013) On its turn, according to (Sétra - Service d'études sur les transports, les routes et leurs aménagements, 2010) the steel structure can be moved by rolling over saddles incorporating rollers or by sliding on skids. In addition, a launching nose (temporary steel structure) is fixed to the front of the permanent steel frames, in order to reduce the cantilever loads.

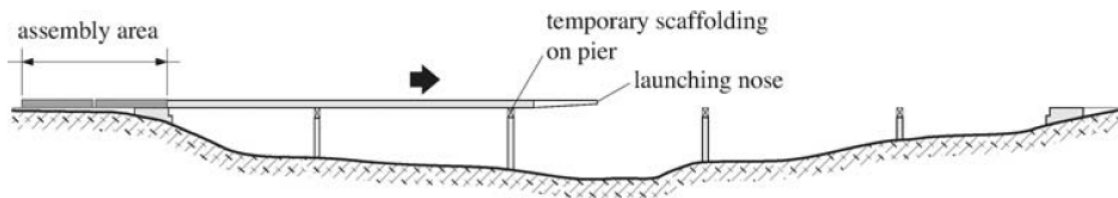


Figure 2-7 - Erection by launching principle (Lebet & Hirt, 2013)

On the following, the main advantages and drawbacks related to this erection method, according to (Vayas & Iliopoulos, 2013) and (Sétra - Service d'études sur les transports, les routes et leurs aménagements, 2010), are listed.

Advantages

- It does not requires special installations, except on the permanent pier heads and behind abutments;
- Allows all the steelwork elements to be assembled on the ground in the assembly area, which leads to optimum safety conditions;
- Adequate solution for traffic routes whit very small possibility of interrupting traffic.

Drawbacks

- Launching requires extensive technical capability and multiple specific equipment items;
- The time to install the steel frame is longer;
- Sufficient space is available behind an abutment and in line with the bridge axis for steelwork assembly;
- The bridge must be either straight or curved in plan with a constant radius if it is to be launched from a single abutment.

2.3.1.2. Crane installation

The method of erection by crane consists in lifting the steel structure and placing it on its permanent bearings using a crane. This method is possible either on a ground site, using mobile cranes on ground or on an aquatic site, using floating derricks, as illustrated in Figure 2-8. (Sétra - Service d'études sur les transports, les routes et leurs aménagements, 2010)

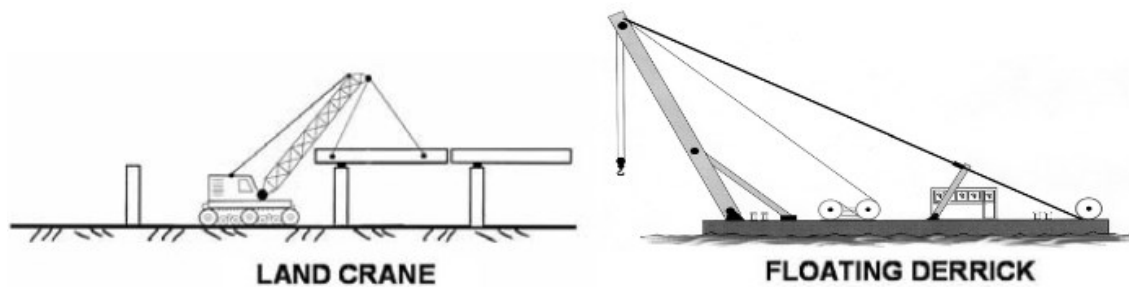


Figure 2-8 - Erection by crane principle (Sétra - Service d'études sur les transports, les routes et leurs aménagements, 2010)

On the following, the main advantages and drawbacks related to this erection method, according to (Sétra - Service d'études sur les transports, les routes et leurs aménagements, 2010), are presented.

Advantages

- Usually represents an economic solution;
- It is possible for all bridge geometries;
- It represents the installation method that applies the least stress to the steel frame;
- Allows steel structure installation in usually less than one day;
- It requires no launching area.

Drawbacks

- Post-installation operations are difficult and must effectively be performed at height and under less favourable conditions than at an assembly area;
- When ground is of poor quality, the crane can represent large zones to be prepared and this increase the construction cost;
- Floating derrick has a high cost associated;
- Usually the use of floating derricks require an interruption of navigable waterway traffic.

2.3.1.3. Installation by shifting

The method of erection by shifting consists in the construction of steel structure on temporary supports located parallel to its final position, and then sliding or shifting it for the final position using cables or jacks, as illustrated in Figure 2-9.

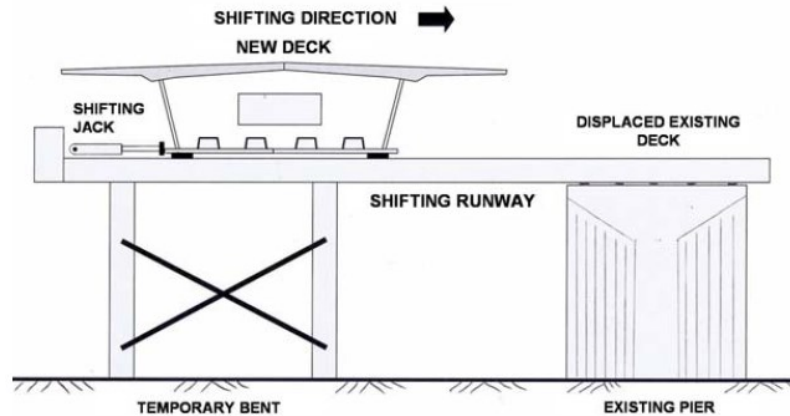


Figure 2-9 - Erection by shifting principle (Sétra - Service d'études sur les transports, les routes et leurs aménagements, 2010)

On the following, the main advantages and drawbacks related to this erection method, according to (Sétra - Service d'études sur les transports, les routes et leurs aménagements, 2010), are presented.

Advantages

- Very brief interruption of traffic on the supported road;
- No steel frame weight limitation because of low friction coefficient (5%), allowing shifting of both steelwork, slab and possible deck equipment;
- Very suitable method to replacing an existing bridge deck.

Drawbacks

- High cost;
- Sometimes it may be difficult to find a sufficient wide area along the bridge to be replaced.

2.3.1.4. Installation by hoisting

Installation by hoisting (Figure 2-10) is a method mainly appropriate for bridges crossing waterways, which consists in hoisting up the central parts of the bridge to their final level, through lifting devices attached to the cantilever parts of the bridge. (Vayas & Iliopoulos, 2013)

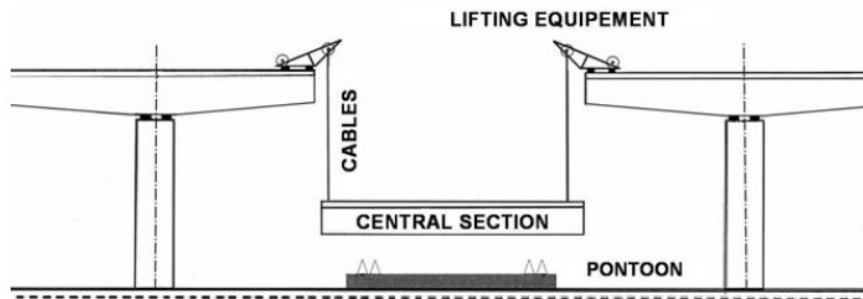


Figure 2-10 - Erection by hoisting principle (Sétra - Service d'études sur les transports, les routes et leurs aménagements, 2010)

On the following, the main advantages and drawbacks related to this erection method, according to (Sétra - Service d'études sur les transports, les routes et leurs aménagements, 2010), are listed.

Advantages

- The main assembly work is undertaken on the ground or at the fabrication shop, thus under optimum safety and quality conditions;
- Heavy and large elements can be hoisted in few hours, which leads to less interruption of river traffic.

Drawbacks

- Hoisting operations are complex and requiring particularly skilled work teams;
- High cost;
- The wind speed during erection must be very low (less than 5 m/s).

2.3.2. Slab construction

According to (Sétra - Service d'études sur les transports, les routes et leurs aménagements, 2010), there exist two major families of composite bridge slab construction methods: cast in-situ and precasting.

Both methods above mentioned offer many advantages, depending of the details required for a specific situation. Casting in-situ is the most common option for constructing the slab, in such a way that “minimises the number of joints in the slab, allows the steel frame imperfections to be corrected and optimises both the slab reinforcement tonnage and the frame steel consumption”. (Sétra - Service d'études sur les transports, les routes et leurs aménagements, 2010, p.148)

Precast slab construction ensures a quicker slab construction, a higher industrialised process of fabrication, and thus a better quality, as well as it reduces shrinkage effects, which leads greatly to slab cracking. On its turn, precasting has a number of major drawbacks, such as the reduction in the monolithic character of the slab, and multiplication of potentially weakening closing joints, particularly when the joints are not in compression. (Sétra - Service d'études sur les transports, les routes et leurs aménagements, 2010)

The following sections, provide a brief description of these two construction methods.

2.3.2.1. Slab construction by in-situ casting using mobile formwork

Slab casting in-situ with mobile formwork is a widely used solution for the majority of composite bridges, particularly to twin composite girder bridges. It is an advantageous solution for long bridges that are high above the ground, and consists in an equipment that supports the formwork for the slab cantilevers by means of hangers, which travels on the steel frame.

Furthermore, the formwork between the steel beams is often supported on the cross bracing, and is moved by sliding. Thus, the need to move the formwork should be taken into consideration during the conceptual design of the bridge cross section. Taking this into account, the cross bracing needs to be located in an appropriate position, in order to facilitate these operations. (Lebet & Hirt, 2013)

In Figure 2-11, an example of a typically mobile formwork, highlighting its main elements is represented.

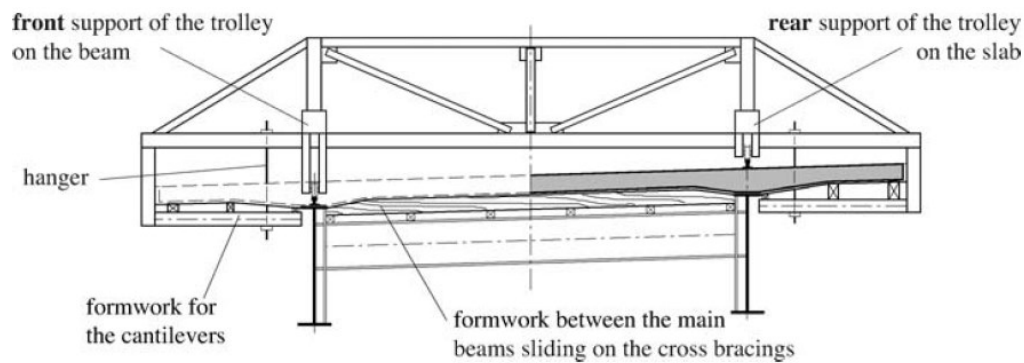


Figure 2-11 - Example of mobile formwork (Lebet & Hirt, 2013)

2.3.2.2. Slab construction by precasting

Slab construction by precasting is a method associated with rapid execution, which involves the construction of slab by adopting precast elements, fabricated either in a factory or in site, and then transported and placed on the steel beams, prior to finally concreting the closing joints designed between the precast slab connection. (Lebet & Hirt, 2013); (Sétra - Service d'études sur les transports, les routes et leurs aménagements, 2010)

Precast slab units have usually around 2 m long, weighing between 15 and 20 tonnes, and “are formed including voids, generally at 1 m centres, to facilitate subsequent creation of the steel to concrete connection using studs set out in groups”, as illustrated in Figure 2-12. (Lebet & Hirt, 2013, p. 162)

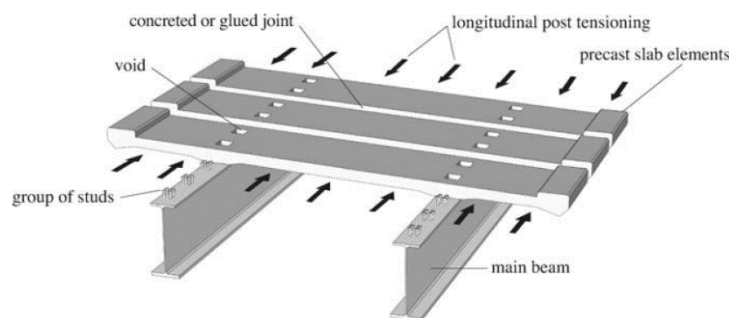


Figure 2-12 - Slab construction by precasting principle (Lebet & Hirt, 2013)

As it can be seen on 2.3.2, the main disadvantage of precast slab construction is related to the numerous slab joints between precast elements. There exist two main ways of forming the transverse joints: the traditional option and the glued joints (Figure 2-13). The traditional joints, known as concreted joints (Figure 2-13 a)), are detailed in such a way that they will act as formwork for the joint, provided by reinforcement in order to ensure continuity, and to carry the slab shear forces to which the joint is subjected. On other hand,

glued joints are “detailed to include the shear keys (Figure 2-13 b)), which marry up precisely with the form of the face of the preceding element”. (Lebet & Hirt, 2013, p.163)

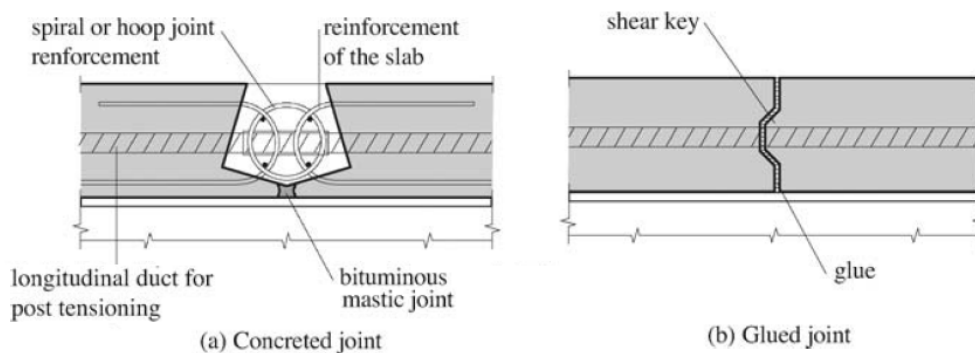


Figure 2-13 - Longitudinal sections of joints in precast slabs (Lebet & Hirt, 2013)

2.4. Advantages of steel-concrete composite bridges

According to (Vayas & Iliopoulos, 2013, p.13) the advantages of steel-concrete composite bridges are mainly connected with safety (S), economy (E), constructional simplicity (CS), functionality (F), and aesthetic (A), as follows:

- Low self-weight of superstructure
 - Cheaper foundations and bearings (E)
 - Lower seismic forces (E, S)
 - Cheaper reconstruction and retrofitting (E)
- Assembly capability on site
 - Lower transport and lifting costs (E)
 - Flexible site planning (F, E)
- No propping during construction
 - No traffic interruption (E, F)
 - Elimination of formworks (C, S)
- Big spans and low construction depth
 - Slender appearance (A)
 - Fewer piers (F)
- Maximum prefabrication
 - High quality (S)
 - Fewer Cast-in-place activities (CS)
 - High speed of construction (E)
 - Low labour costs (E)

2.5. Structural materials

As it can be inferred by the above sections, materials play an important role on the behaviour of composite structures. In order to give a better understanding of the differences between structural steel and concrete, this sub-chapter makes an overall analysis of the properties of these two materials, following its most important properties. Thus, the following sections begin with the reference to concrete and steel grades typically used in bridges, followed by a brief explanation about the symbols used to define the grade materials, as well as reference to other relevant characteristics.

2.5.1. Concrete

Concrete is a material formed of cement, aggregate and water which are used in different proportions to obtain the requirement strength (generally, the more cement and less water added, the stronger the resulting concrete). Sometimes it may be also possible the use of admixtures in concrete composition to change some properties, as to improve workability and retard strength gain. (Collings, 2005)

According to (EN 1994-2, 2005) the composite bridges design should be performed to concrete strength classes between C20/25 and C60/75. Also, the most common usual strength class of concrete slab is C35/45. (Vayas, Iliopoulos, 2013)

Some properties of concrete are presented in Table 2-2.

Specific weight	$\rho_c = 25 \text{ kN/m}^3$
Specific weight of wet concrete	$\rho_{c,wet} = 26 \text{ kN/m}^3$
Poisson ratio for uncracked concrete	$\nu_c = 0,2$
Poisson ratio for cracked concrete	$\nu_c = 0$
Coefficient of thermal expansion	$\alpha_c = 10 \times 10^{-6} \text{ per } ^\circ\text{C}$

Table 2-2 - Properties of concrete (Vayas & Iliopoulos, 2013)

2.5.1.1. Strength classes

For normal concrete, the strength classes are defined by the letter C followed by two figures, which express the characteristic (5%) cylinder strength f_{ck} and the cubes strength $f_{ck,cube}$ at 28 days. On its turn, lightweight concrete is denoted as LC followed the two figures of cylinder strength and the cube strength. (Vayas & Iliopoulos, 2013) The characteristic strengths for f_{ck} and the corresponding mechanical characteristics for normal concrete can be

found in the (EN 1992-1-1, 2004) (Table 3.1), while the properties of lightweight concrete can be determined according to (EN 1992-1-1, 2004) (chapter 11).

2.5.1.2. Stress-strain relations

The design value for the compressive stress of concrete is defined as:

$$f_{cd} = \alpha_{cc} \times \frac{f_{ck}}{\gamma_c} \quad (2.1)$$

Where:

f_{ck} is the characteristic value of the compressive stress;

α_{cc} is a reduction factor that takes into account the long-term effects on the compressive strength. The recommended value is 0,85 for unconfined concrete and 1,0 for confined one;

γ_c is the relevant safety factor, $\gamma_c = 1,5$

For the capacity design of composite cross sections, the stress-strain relations of Table 2-3, may be used. The parabola-rectangle diagram describes the “exact” behaviour of compressed concrete, however, it obviously makes the calculations more onerous. On the other hand, the bilinear diagram offers a more simplified approach. (Vayas & Iliopoulos, 2013)

Parabola-rectangle diagram	Bi-linear stress-strain relation
$\sigma_c = \begin{cases} f_{cd} \cdot \left[1 - \left(1 - \frac{\varepsilon_c}{2\text{‰}} \right)^2 \right], & 0 \leq \varepsilon_c \leq 2\text{‰} \\ f_{cd}, & 2\text{‰} \leq \varepsilon_c \leq 3.5\text{‰} \end{cases}$	$\sigma_c = \begin{cases} f_{cd} \cdot \frac{\varepsilon_c}{0.00175}, & 0 \leq \varepsilon_c \leq 1.75\text{‰} \\ f_{cd}, & 1.75\text{‰} \leq \varepsilon_c \leq 3.5\text{‰} \end{cases}$

Table 2-3 - Stress-strain relations for the capacity design of cross sections for C20/25 till C50/60 (concrete under compression) (Vayas & Iliopoulos, 2013)

2.5.1.3. Creep and shrinkage of concrete

Concrete is subject to time-dependent deformations, due to creep and shrinkage, which in turn, “depend on the ambient humidity, the dimensions of the element and the

composition of the concrete. Creep is also influenced by the maturity of the concrete when the load is first applied and depends on the duration and magnitude of the loading”. (EN 1992-1-1, 2004, p.37) The value of the creep coefficient and the total shrinkage may be determined from (EN 1992-1-1, 2004) (Chapter 3.1.4).

2.5.2. Steel

Steel used for building bridges and structures is a material that contains: iron, a small percentage of carbon and manganese, impurities that cannot be fully removed from the ore (namely sulphur and phosphorus), as well as some alloying elements that are added in very small quantities to improve the properties of the finished product (namely copper, silicon, nickel, chromium, molybdenum, vanadium and zirconium). (Chatterjee, 2003)

The most usual steel grade for structural members of bridges such as main beams is S355, delivered in a normalized state. “It is designated S335J2 + N or S355K2 + N for non-alloyed steels (EN 10025-2), and S355N or S355NL for fine grain steels (EN 10025-3). When thermomechanical steels are used, they are designated S355M or S355ML (EN 10025-4)”. (Lebet, Hirt, 2013, p.66)

In some situations, “higher strength steels (S460) are of interest in highly stressed regions of continuous beams, such as over intermediate supports”. On other hand, “steel grades inferior to S355 are not used in the construction of bridges, except perhaps for secondary elements that are only lightly stressed”. (Lebet, Hirt, 2013, p.66)

Some properties of structural steel are presented in Table 2-4.

Specific weight	$\rho_a = 78,5 \text{ kN/m}^3$
Modulus of elasticity	$E_a = 210 \text{ GPa}$
Poisson ratio	$\nu_c = 0,3$
Shear modulus	$G_a = 81 \text{ GPa}$
Coefficient of thermal expansion	$\alpha_c = 10 \times 10^{-6} \text{ per } ^\circ\text{C}$

Table 2-4 - Properties of Structural Steel (Vayas & Iliopoulos, 2013)

Structural steels used in bridges are particularly characterised by a grade (defined by the yield strength) and a quality (characterised by the resistance of the steel to bending impact as an indicator of the resistance to brittle fracture and to some degree the quality may also give an indicator of the weldability of steel).

2.5.2.1. Steel grade

Steel grades are defined by a system based in the European Standard EN 10025. According to this system, structural steel is designated by the letter S (initial for the English word Structural steel), followed by a number providing its yield strength (f_y) at thickness $t \leq 16$ mm in [MPa] and one or two symbols specifying the material toughness. (Vayas & Iliopoulos, 2013)

“The mechanical properties of structural steels are mainly characterized by the yield and the tensile strength that are defined in Eurocodes 3 and 4 as f_y and f_u correspondingly”. (Vayas & Iliopoulos, 2013, p.172)

The design rules of the Eurocode 4 Part 2 (EN 1994-2, 2005) only covers steel grades inferior or equivalent to S460, such as S235, S275, S355, S420 and S460. However, the use of steel grades above S460, up to S700, are also available. The last ones, are covered by EN 1993-1-12. (Steel Bridge Group, 2010)

Table 2-5 shows the mechanical properties of structural steels as a function of nominal thickness of the element and grade of steel, produced to EN 10025, in accordance with (EN 1993-1-1, 2005).

Steel grades to EN 10025	Nominal thickness of the element t in mm			
	$t \leq 40$ mm		$40 \text{ mm} \leq t \leq 80$ mm	
	f_y in MPa	f_u in MPa	f_y in MPa	f_u in MPa
S 235	235	360	215	360
S 275	275	430	255	410
S 355	355	510	335	470
S 275 N/NL	275	390	255	370
S 355 N/NL	355	490	335	470
S 420 N/NL	420	520	390	520
S 460 N/NL	460	540	430	540
S 275 M/ML	275	370	255	360
S 355M/ML	355	470	335	450
S 420 M/ML	420	520	390	500
S 460 M/ML	460	540	430	530

Table 2-5 - Mechanical properties of structural steels produced to EN 10025, in accordance with EN 1993-1-1 (Vayas & Iliopoulos, 2013)

2.5.2.2. Steel quality

According to (Lebet & Hirt, 2013, p. 63), “the notion of steel quality is used to define the particularities of the material's resistance to bending by impact of a test specimen containing a notch (Charpy test), which is an indication of its resistance to brittle fracture”.

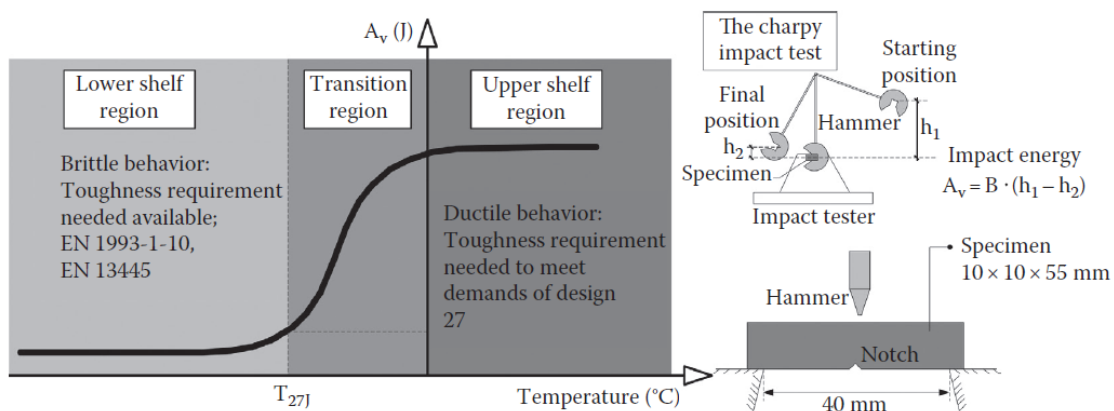


Figure 2-14 - Charpy test (Vayas & Iliopoulos, 2013)

As it can be seen in Figure 2-14, the Charpy test is carried out with a specimen at a specified (low) temperature, and measures the impact energy (in Joules) required to break a small notched specimen by a single impact blow from a pendulum. (Steel Bridge Group, 2010)

For each types of steel (non-alloy, normalized or thermomechanically treated), Standards EN 10025 in Parts 2 to 4, describes the qualities of steel as shown in Table 2-6.

EN 10025	Symbol	Longitudinal direction	
		Temperature T[°C]	Charpy V-notch Impact energy [J]
Part 2	JR	20	27
Non-alloy structural steel	J0	0	27
	J2	-20	27
	K2	-20	40
Part 3			
Normalized/ normalized rolled weldable fine-grain structural steels	N	-20	40
	NL	-50	27
Part 4			
Thermomechanically rolled weldable fine-grain structural steels	M	-20	40
	ML	-50	27

Table 2-6 - Definition of steel quality according to EN 10025 (Vayas & Iliopoulos, 2013)

2.5.2.3. Weldability

Weldability is a characteristic of steel that indicates the aptitude of the metal to be welded to another piece via an intermediary metal (electrode). This characteristic cannot be quantified, for this reason, is rather based on a qualitative judgement. (Lebet & Hirt, 2013)

As stated by (Steel Bridge Group, 2010, p.4), welding leads to a local heating of the steel, which subsequently cools. On its turn, the cooling can be quite fast, because the surrounding material that offers a large energy dissipation, as well as due to the weld (the heat introduced), which is usually relatively small. This situation can lead to hardening of the ‘heat affected zone’ (HAZ) and to reduced toughness. “The greater the thickness of material, the greater the reduction of toughness, because of the greater thermal conduction”.

Weldability also depends on the chemical composition. “Increased amounts of carbon and manganese, which are necessary for higher strengths, make the steel harder and consequently more difficult to weld”. For the purpose of measuring weldability of a metal, its ‘carbon equivalent value’ is given as an indicative measure. The ‘carbon equivalent value’ is given by the following formula:

$$C + \frac{Mn}{6} + \frac{Cr + Mo + V}{5} + \frac{Ni + Cu}{15} \quad (2.2)$$

Where C, Mn, etc. represent the percentage of the elements in the chemical composition of the steel. (Chatterjee, 2003, p.44)

Preheating (by blowtorch or combined series of torches) is always needed for steel grades S355 and above. The only exception are the thermomechanical steels, which due to their low carbon equivalent, do not need preheating. (Lebet & Hirt, 2013)

2.5.2.4. Thermomechanical Rolled Steels

Thermomechanical steels differ from traditional normalised steels, since for the same mechanical properties, they require less carbon and other hardening elements (lower carbon equivalent value), and for the same chemical composition, they have superior mechanical properties. (Lebet & Hirt, 2013)

2.5.2.5. Corrosion resistance

According to (Collings, 2005, p.68), “the corrosion of steel is defined as an electromechanical process, where the steel in presence of oxygen and water converts to a hydrated ferric oxide, or rust”. In order to protect the steel structure of composite bridges against corrosion, it is common to provide a protection by painting, as well as the use of steels with improved anti-corrosion characteristics, known as weathering steels.

- Protection by painting

Protection by paint is the most frequently form used to protect steel against the corrosion. Paint systems used to protect steel consists of three basic stages: a base layer, an intermediate layer (may be one thick coating or several thinner layers) and a finishing layer. (Lebet & Hirt, 2013); (Collings, 2005) Table 2-7, summarize some common protective systems for highway and railway structures.

Environment/ access	Preparation	First coat	Second coat	Third coat	Fourth coat	Thickness : μm
Protected (inferior of box)	Blast dean	Zinc epoxy primer	Micaceous iron oxide (MIO)			200
Inland with good access	Blast dean	Zinc epoxy primer	MIO	MIO	Polyure- thane finish	300
Inland with bad access	Blast dean	Epoxy primer	Glass flake epoxy	Polyure- thane finish		450
Marine or industrial	Blast dean, aluminium spray	Epoxy sealer	Zink epoxy primer	MIO	Polyureth ane finish	400

Table 2-7 - Protective systems for bridges (Collings, 2005)

- Weathering steels

Weathering steels are a low alloy steel (P, Cu, Cr, Ni, Mo), which present a good resistance to atmospheric corrosion. “This improved resistance to corrosion is due to the formation of a compact self-protective oxide film or ‘patina’ on the surface of the material”. (Lebet & Hirt, 2013, p.68)

The rust layers develops very quickly once the material is exposed to the atmosphere (Figure 2-15). While the rust layers formed on most ordinary structural steels are porous and detach from the metal surface after a certain time, for weathering steels, the rusting process is initiated in the same way, but the specific alloying elements in the steel produce a stable rust layer that adheres to the base metal, and is much less porous. (Steel Construction.info); (Lebet & Hirt, 2013)

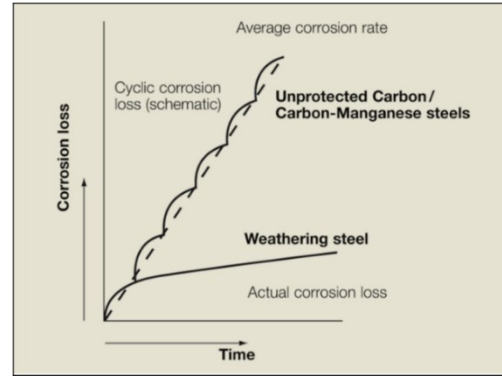


Figure 2-15 - Schematic comparison between the corrosion loss of weathering steel and ordinary structural steel (Steel Construction.info)

The main reasons for use of weathering steels in bridges design are related to: reduced first costs (saves painting costs and saves construction time) and reduced maintenance (no need to repaint, reduces traffic delays during maintenance, not as dependent on weather conditions, and reduces need for access). (Steel Bridge Group, 2010)

However, the experience gained from existing bridges, has shown that the use of weathering steels is not suitable for the following environments: (Steel Bridge Group, 2010); (Lebet & Hirt, 2013)

- Where there is an atmosphere of concentrated corrosive or industrial fumes;
- Where steelwork is continuously wet or damp;
- Where steel is exposed to high concentrations of chloride ions or salt spray;
- Where steelwork is located less than 500 m from the sea;
- Where steel is less than 1 m above ground level (vegetation) or less than 3 m above a river.

Chapter 3

Design of steel – concrete composite bridges

The designing of a composite bridge is a complex and long process, starting with the consideration of an appropriate design criterion in accordance with (EN 1990, 2002), followed by a definition and combination of actions in accordance with (EN 1991, 2001) and (EN 1990, 2002), respectively, and a determination of resistances, durability and serviceability in accordance with (EN 1994-2, 2005).

The calculation of the whole bridge in order to determine the internal forces and moments, as well as the corresponding stresses on its various sections is based on a structural model, which shall reflect the anticipated behaviour of the cross section, members, joints, and bearings. Eurocode 3, part 2 (EN 1993-2, 2006), recommends the use of elastic global analysis, except possibly on accidental design situations, however, (EN 1994-2, 2005) does not exclude the use of plastic global analysis at the ultimate limit state. (Composite highway bridge design, 2010) According to (EN 1994-2, 2005), the methods of global analysis should be taking into account the effect of shear lag, as well as the effect of local buckling. Furthermore, for a linear elastic analysis, appropriate allowance should be made for the effects of cracking on concrete, creep and shrinkage of concrete and sequence of construction. Taking this into account, the following sections provide a brief description of this process, as well as the standards used in the design of composite bridges.

3.1. The Eurocodes and product standards

Considering the importance of standards for a civil engineering designer, a set of structural design standards, commonly known as Eurocodes were developed by CEN (European Committee for Standardization) over the last 30 years, to cover the design of all types of structures in steel, concrete, timber, masonry and aluminium. (Composite highway bridge design, 2010)

There are 10 Eurocodes, starting at Eurocode 0 till Eurocode 9. The connection between Eurocodes in relation to bridges is created by EN 199X-2 (Part 2). “Consequently, the leading document for the design of composite bridges is Eurocode 4, part 2 (EN1994-2).

However, since composite construction combines the use of both structural steel and reinforced concrete, EN 1994 calls, besides the generic Eurocodes, both relevant material Eurocodes, EN 1992 and EN 1993”. (Vayas, Iliopoulos, 2013, p.67) In order to briefly summarize it, Figure 3-1 depicts a schematic representation of the Eurocodes to be used in the composite bridge designing.

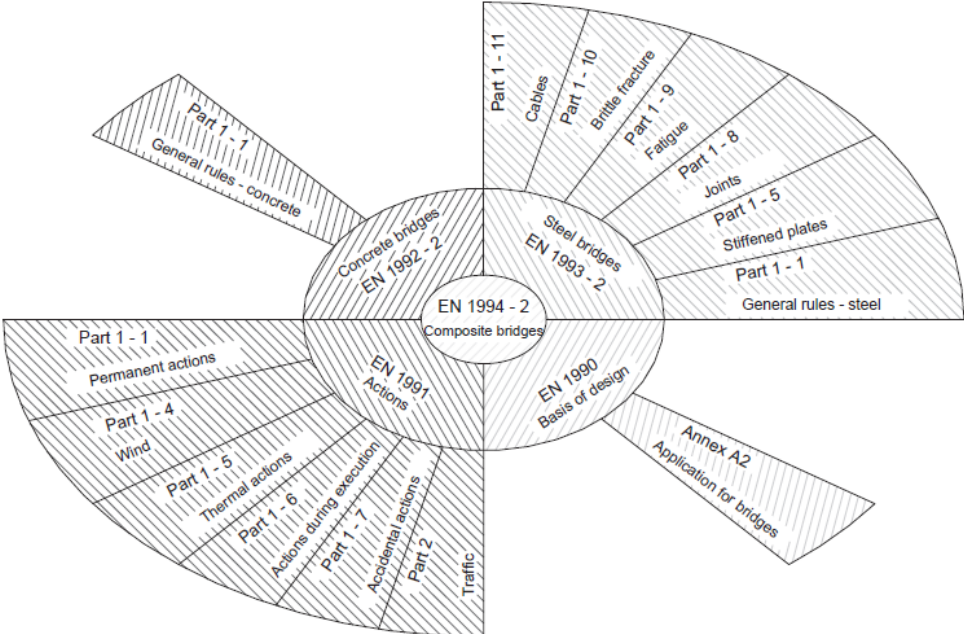


Figure 3-1 Eurocodes to be used in a composite bridge design (COMBRI Design Manual, 2008)

Standards of the products used in composite bridges are presented in Table 3-1.

Product	Standard
Steel	EN 10025
Bolts	EN 1993-1-8
Bearings	EN 1337
Concrete	EN 206

Table 3-1 - Product standards

3.2. Limit state design

The intended life for bridges is circa 100 years. During this span, bridges need to guarantee certain basic requirements related to structural resistance, serviceability and durability. According to (EN 1990, 2002), these requirements are based on consideration about ultimate and serviceability limit states. (Vayas, Iliopoulos, 2013)

Ultimate limit states (ULSs) are related whit the safety of people, as well as of the structure, and for composite bridges may be due to: (Vayas, Iliopoulos, 2013)

- EQU: Loss of static equilibrium of the structure or a structural element
- STR: Failure by collapse or excessive deformation of a structure or structural element
- GEO: Failure or excessive deformation of the ground where the strengths of soil or rock are significant in providing resistance
- FAT: Failure caused by fatigue of the structural elements

Serviceability limit states (SLSs) concern the functioning of the structure or structural members under normal use, the comfort of people and the appearance of the construction work, which are related with: (Vayas, Iliopoulos, 2013)

- Stresses;
- Deformations;
- Cracking of concrete.

3.3. Actions

Actions are classified according to (EN 1990, 2002) in relation to their duration, magnitude, and probability of occurrence as: (Vayas, Iliopoulos, 2013)

- Permanent (G), e.g. self-weight of structural members, fixed equipment and road surfacing, and indirect actions caused by shrinkage and uneven settlements;
- Variable (Q), e.g. traffic loads, wind loads, and snow loads;
- Accidental (A), e.g. vehicle impact;
- Seismic (AE), which develops during an earthquake ground motion.

As it can be noted by Figure 3-1, the different types of actions are defined by (EN 1991, 2001), except for seismic action which is covered by (EN 1998-1, 2004) and (EN 1998-2, 2011). Given the fact that explanation of all actions is long, and taking in to account the aim of this work, only traffic loads have been detailed on the following. However, on Chapter 4 a brief description about the determination of all actions considered for the global analysis of the numerical example is given.

3.3.1. Traffic load

Traffic loads correspond to the most relevant actions to take into account for bridge designing, which are determined in accordance to (EN 1991-2, 2003). Bearing in mind the purpose of this thesis, the methodology used to perform the traffic load actions for road bridges is described below. However, depending on the use of the bridge (roadway bridge,

railway, pedestrian or a combination of these), different traffic loads should be considered. Thus, the following guidelines begin with reference to the division of carriageway into notional lanes, followed by a brief explanation about determination of vertical and horizontal forces applied on the carriageway, as well as on footways and cycle tracks, until definition of groups of traffic loads on road bridges.

3.3.1.1. Division of carriageway into notional lanes

The first step in order to taken into account traffic loads when designing a bridge is to define the number of notional lanes on the carriageway, according to (EN 1991-2, 2003) (4.2.3).

The number of notional lanes depends on the carriageway width (w), which should be measured between kerbs or between the inner limits of vehicle restraint systems (Figure 3-2), and should not include the distance between fixed vehicle restraint systems or kerbs of a central reservation nor the widths of these vehicle restraint systems.

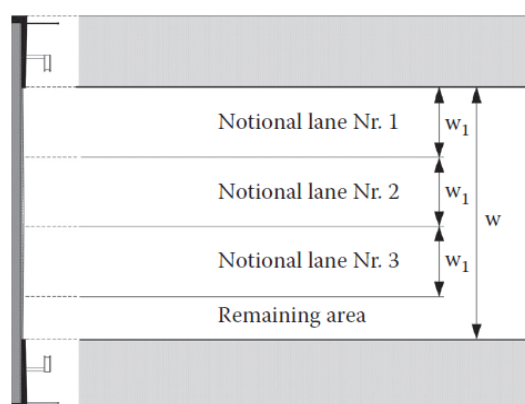


Figure 3-2- Example of lane numbering (Vayas & Iliopoulos, 2013)

Taking this into consideration, the number and width of notional lanes are determined in accordance with Table 3-2.

Carriageway width w	Number of notional lanes	Width of a notional lane w_1	Width of the remaining area
$w < 5,4m$	$n_1 = 1$	$3m$	$w - 3m$
$5,4m \leq w < 6m$	$n_1 = 2$	$\frac{w}{2}$	0
$6m \leq w$	$n_1 = \text{Int}\left(\frac{w}{3}\right)$	$3m$	$w - 3 \times n_1$

Table 3-2 - Number and width of notional lanes

The lane giving the most unfavourable effects is numbered Lane Number 1, followed by the second most unfavourable effect, which is numbered Lane Number 2, etc. As traffic loads are variable actions, they are placed in such a way that the most adverse effects are obtained.

3.3.1.2. Vertical loads on the carriageway

For vertical forces due to traffic loads, there are four models to consider: Load Model 1 (normal traffic), Load Model 2 (Single axle for short span members), Load Model 3 (Special vehicles) and Load Model 4 (Crowd loading). However, these Load Models apply for loaded lengths less than 200 m. For greater loaded lengths, the load model may be defined in the National Annex. Taking this into account, on the following, a brief description of these four Load Models is presented.

- Load Model 1 (LM1)

Load Model 1 is a model used for general and local verifications, which cover most of the effects of the traffic of lorries and cars. It comprises a double-axle concentrated loads (tandem system (TS)) with $\alpha_{Qi} \cdot Q_{ik}$ per axle, and a uniformly distributed loads (UDL) with $\alpha_{Qi} \cdot q_{ik}$, determined in accordance to Table 3-3.

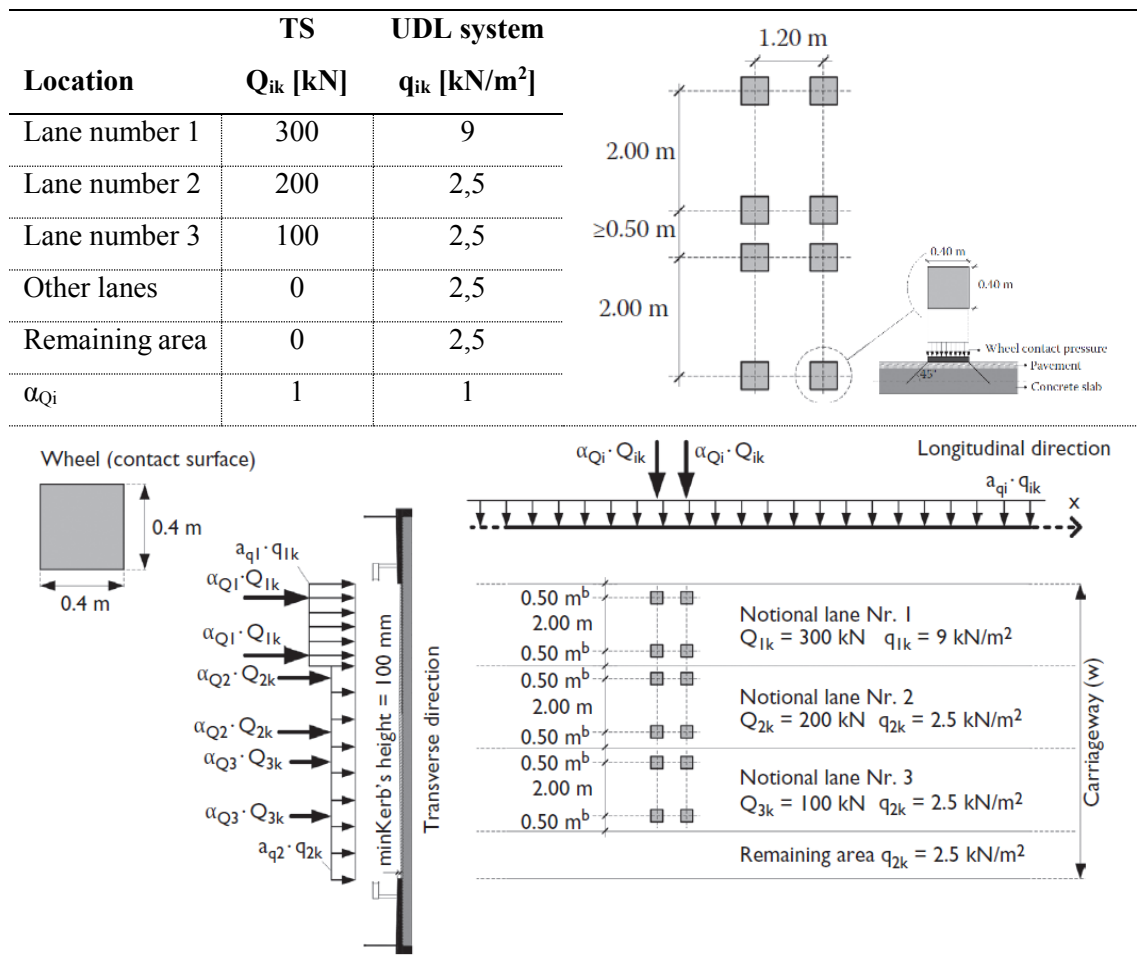


Table 3-3 - Characteristic values of LM1 (adapted from (Vayas & Iliopoulos, 2013))

- Load Model 2 (LM2)

Load model 2 consists in a single axle model, which is applied when a local verification for short structural elements (e.g. crossbeams, upper flange stiffeners of orthotropic decks, or deck panels of composite slabs with profile steel sheeting) is necessary. The magnitude of this single axle model may be defined in the National Annex, however (EN 1991-2, 2003) recommends that $\beta_Q \cdot Q_{ak} = \alpha_{Q1} \cdot Q_{ak}$ is equal to 400 kN. In order to brief summarize it, Figure 3-3 depicts a schematic representation of Load model 2 application. (Vayas & Iliopoulos, 2013)

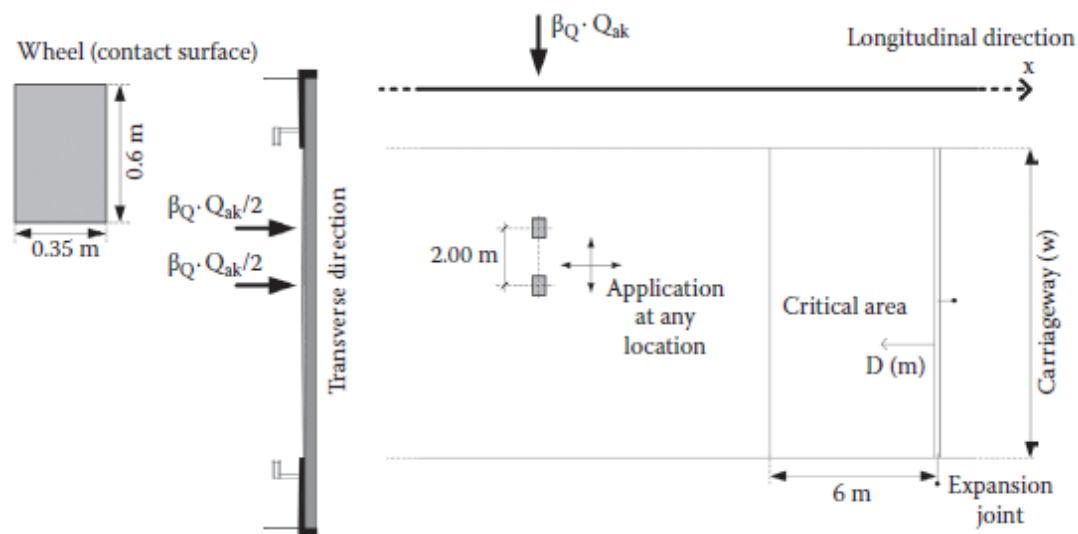


Figure 3-3 - Application of the Load model 2 (Vayas & Iliopoulos, 2013)

- Load Model 3 (LM3)

Load Model 3 is a model used for bridges that must be designed against special traffic loads, which is the case of bridges that may experience a military use during their lifetime. The standardized models of special vehicles, as well as their conditions of use may be defined in accordance with National Annex of (EN 1991-2, 2003).

- Load Model 4 (LM4)

Load model 4, commonly known as crowd loading is represented by a Load model consisting of a uniformly distributed load (which includes dynamic simplification) equal to 5 kN/m². Furthermore, load model 4 should be applied on the relevant parts of the length and width of the road bridge deck (the central reservation being included where relevant), and it should be associated only with a transient design situation.

3.3.1.3. Vertical loads on footways and cycle tracks

Vertical loads on footways and cycle tracks are represented by a uniform distributed load (UDL) equal to 5 kN/m^2 that acts on the unfavourable parts of the influence line in longitudinal and transverse directions. (Vayas & Iliopoulos, 2013)

3.3.1.4. Horizontal forces

The horizontal forces due to traffic loads, are defined in accordance with (EN 1991-2, 2003) (4.4), in order to represent braking / acceleration and centrifugal forces.

- Braking force

The braking force is taken as a force that acts at the surfacing level of the carriageway, which in turn is transferred to the expansion joints, the bearings, and the superstructure. (Vayas & Iliopoulos, 2013)

The characteristic value of the braking force Q_{1k} for the total width of the carriageway (limited to 900 kN for the total width of the bridge), is calculated according to (EN 1991-2, 2003) (4.4.1 (2)), as follows:

$$Q_{1k} = 0,6 \times \alpha_{Q1} \times (2Q_{1k}) + 0,1 \times \alpha_{q1} q_{1k} w_1 L \quad (3.1)$$

With:

$$180 \times \alpha_{Q1} \text{ kN} \leq Q_{1k} \leq 900 \text{ kN} \quad (3.2)$$

- Acceleration force

Acceleration forces are of the same magnitude as the braking forces but act in opposite direction, which means that both types of forces are considered as +/- Q_{1k} . (Vayas & Iliopoulos, 2013)

- Centrifugal force

According to (Vayas & Iliopoulos, 2013, p. 81), “the centrifugal force is a transverse force that acts at the level of the finished carriageway level and radially to the carriageway axis”. The characteristic value of Q_{tk} , in which dynamic effects are included, should be taken from Table 3-4.

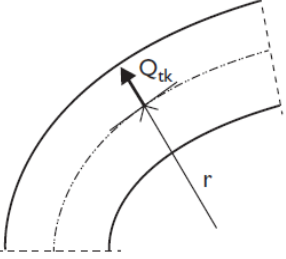
$Q_{tk} = 0,2Q_v$ (kN)	if $r < 200$ m	
$Q_{tk} = 40Q_v / r$ (kN)	if $200 \leq r \leq 1500$ m	
$Q_{tk} = 0$	if $r > 1500$ m	

Table 3-4 - Characteristic values of centrifugal forces (Vayas & Iliopoulos, 2013)

3.3.1.5. Groups of traffic loads on road bridges

As it can be seen by the above sections, the traffic loads include vertical and horizontal forces on the carriageway and on footways. Since the probability of those loads appear simultaneously with their characteristic values is small, groups of loads are considered. “A group of load is treated as a single variable and thus may be considered as the leading action, $Q_{k,1}$, or as an accompanying action”. (Composite highway bridge design, 2010, p. 45) The groups of loads are defined according to (EN 1991-2, 2003) (4.5), as shown in Table 3-5.

Load type	Carriageway					Footway	
	Vertical				Horizontal	Vertical	
Load system	LM 1	LM 2	LM 3	LM 4	Braking and acceleration	Centrifugal and transverse	UDL
gr 1 a	CV	-	-	-	Comb. Value	N.A.	N.A.
gr 1 b	-	CV	-	-	-	-	-
gr 2	FV	-	-	-	-	CV	CV
gr 1 b	-	-	-	-	Comb. Value	-	-
Gr 4	-	-	-	CV	-	-	-
Gr 5	CV	-	CV	-	-	-	-

CV – Characteristic value; FV – Frequent value; N.A. – See National Annex

Comb. Value – Combination value

Table 3-5 - Groups of loads

3.4. Combination of actions

The design values of the effects are determined for the combinations of actions that are considered to occur simultaneously. (EN 1990, 2002) “In the basic combination, one variable action is considered as leading variable action, the others being accompanying actions”. (Vayas & Iliopoulos, 2013, p. 124) The combination of action at ULS and SLS are presented on the following sections.

3.4.1. Ultimate Limit States (ULS)

At the ultimate limit state it must be verified that the design value of the effect of actions does not exceed the design value of the corresponding resistance. (Composite highway bridge design, 2010) According to (EN 1990, 2002) the following combinations should be considered:

- Fundamental combination (for persistent or transient situation)

$$\sum_{j \geq 1} \gamma_{G,j} G_{k,j} + \gamma_P P + \gamma_{Q,1} Q_{k,1} + \sum_{i \geq 2} \gamma_{G,i} \psi_{0,i} Q_{k,i} \quad (3.3)$$

- Accidental combination

$$\sum_{j \geq 1} G_{k,j} + P + A_d + (\psi_{1,1} \text{ or } \psi_{2,1}) Q_{k,1} + \sum_{i \geq 2} \psi_{2,i} Q_{k,i} \quad (3.4)$$

- Seismic combination

$$\sum_{j \geq 1} G_{k,j} + P + A_{Ed} + \sum_{i \geq 2} \psi_{2,i} Q_{k,i} \quad (3.5)$$

Thus, according to (eq. 3.3) the following fundamental ULS combination of actions should be considered:

Permanent actions	Shrinkage	Leading variable actions	Accompanying variable actions
1,35 G _{K,sup} or (1,0 G _{K,inf})	+ (1,0 or 0,0) S	+ 1,35 (UDL _k + TS _k + q _{fk,comb})	+ 1,5 min (F _w *; 0,6 F _{wk,T})
		+ 1,35 (UDL _k + TS _k + q _{fk,comb})	+ 1,5 (0,6 T _k)
		+ 1,35 gr1b	
		+ 1,35 gr2	+ 1,5 (0,6 T _k)
		+ 1,35 gr3	+ 1,5 (0,6 T _k)
		+ 1,35 gr5	
		+ 1,5 F _{wk}	
		+ 1,5 T _k	+ 1,35 (0,4.UDL _k + 0,75.TS _k + 0,4.q _{fk,comb})

Table 3-6 - Fundamental ULS combination of actions (Davaine, Imbert, & Raoul, 2007)

3.4.2. Serviceability Limit States (SLS)

At the serviceability limit state it must be verified that the design value of the effect of actions does not exceed some limiting criterion. (Composite highway bridge design, 2010)
There are three combinations of actions to consider:

- Characteristic combination (used to check the stresses in the structural steel, concrete and reinforcement)

$$\sum_{j \geq 1} G_{k,j} + P + Q_{k,1} + \sum_{i \geq 1} \psi_{0,i} Q_{k,i} \quad (3.6)$$

- Frequent combination (used to check the deformations on road bridges)

$$\sum_{j \geq 1} G_{k,j} + P + \psi_{1,1} Q_{k,1} + \sum_{i \geq 1} \psi_{2,1} Q_{k,i} \quad (3.7)$$

- Quasi-permanent combination (used to check deformations on road bridges and the crack widths on the deck slab)

$$\sum_{j \geq 1} G_{k,j} + P + \sum_{i \geq 1} \psi_{2,1} Q_{k,i} \quad (3.8)$$

3.4.2.1. Characteristic SLS combination of actions

According to (eq. 3.6) the following characteristic SLS combination of actions should be considered:

Permanent actions	Shrinkage	Leading variable actions	Accompanying variable actions
$G_{K,sup}$ or $(G_{K,inf})$	+ (1,0 or 0,0) S	+ (UDL _k + TS _k + q _{fk,comb})	+ min (F _w [*] ; 0,6 F _{wk,T})
		+ (UDL _k + TS _k + q _{fk,comb})	+ (0,6 T _k)
		+ gr1b	
		+ gr2	
		+ gr3	
		+ gr5	
		+ F _{wk}	
		+ T _k	+ (0,4.UDL _k + 0,75.TS _k + 0,4.q _{fk,comb})

Table 3-7 - Characteristic SLS combination of actions (Davaine, Imberty, & Raoul, 2007)

3.4.2.2. Frequent SLS combination of actions

According to (eq. 3.7) the following frequent SLS combination of actions should be considered:

Permanent actions	Shrinkage	Leading variable actions	Accompanying variable actions
$G_{K,sup}$ or $(G_{K,inf})$	+ (1,0 or 0,0) S	+ (0,4.UDL _k + 0,75.TS _k)	+ (0,5.T _k)
		+ 0,4 gr3	+ (0,5.T _k)
		+ 0,75 gr1b	
		+ 0,75 gr4	+ (0,5.T _k)
		+ 0,2 F _{wk}	
		+ 0,6 T _k	

Table 3-8 - Frequent SLS combination of actions (Davaine, Imberty, & Raoul, 2007)

3.4.2.3. Quasi-permanent SLS combination of actions

According to (eq. 3.8) the following quasi-permanent SLS combination of action should be considered:

Permanent actions	Shrinkage	Leading variable actions
$G_{K,sup}$ or $(G_{K,inf})$	+ (1,0 or 0,0) S	+ (0,5.T _k)

Table 3-9 - Quasi-permanent SLS combination of actions (Davaine, Imberty, & Raoul, 2007)

3.5. Structural analysis of composite bridges

As it was referred, the structural analysis of composite bridges is based on a model calculation that is performed to give the real behaviour of the structure, taking into account the effects of shear lag and cracking of concrete, as well as the effects of creep and shrinkage, and the staged construction. Thus, an explanation about this effects, is described on the following sections.

3.5.1. Effect of shear lag

The verification of cross-section should be determined taking into account the distribution of effective width between supports and mid span regions, due to non-uniform distribution of stresses over the total width of the slab, as a result of an effect known as shear lag (Figure 3-4).

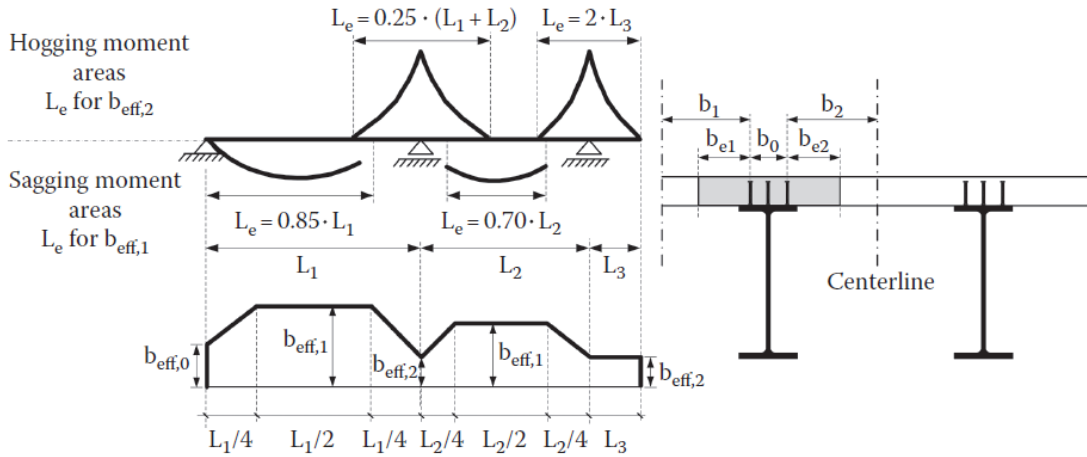


Figure 3-4 - Length L_e and distribution of effective width of concrete along the span (Vayas & Iliopoulos, 2013)

The effective width b_{eff} , at mid span or an internal support, as well as at an end support, may be defined by (EN 1994-2, 2005) (Chapter 5.4.1.2). At mid-span or internal support, it is determined by the following:

$$b_{eff} = b_0 + \sum b_{ei} \quad (3.9)$$

Where:

b_0 is the distance between the centres of outstand shear connectors;

b_{ei} is the value of the effective width of the concrete flange on each side of the web and taken as $L_e/8$ (but not greater than the geometric width b_i)

L_e may be assumed to be as shown in Figure 3-4.

On its turn, at an end support may be determined by:

$$b_{eff} = b_0 + \sum \beta_i b_{ei} \quad (3.10)$$

With:

$$\beta_i = (0,55 + 0,025L_e / b_{ei}) \leq 1,0 \quad (3.11)$$

3.5.2. Local buckling and cross-section classification

The plate elements of the cross-sections of a composite bridge are typically slender, which may leads to the development of a local instability phenomena, known as local buckling. This phenomena may be taken into account by classifying cross-sections of elements. (Lebet, Hirt, 2013)

On its turn, the classification of cross-section aims to examine whether the bending resistance of cross-section may be determined by elastic or plastic resistance. This

classification is defined according to the highest (least favourable) class of its compression parts, as described in detail in (EN 1994-2, 2005) (Chapter 5.5).

According to (Vayas & Iliopoulos, 2013), four classes of cross-sections (Figure 3-5) are defined, as follows:

- Class 1: Cross-sections develop their plastic bending resistance and have sufficient rotation capacity;
- Class 2: Cross-sections develop their plastic bending resistance but limited rotation capacity;
- Class 3: Cross-sections develop their elastic bending resistance;
- Class 4: Cross-sections are subjected to local buckling and have a resistance lower than the elastic resistance.

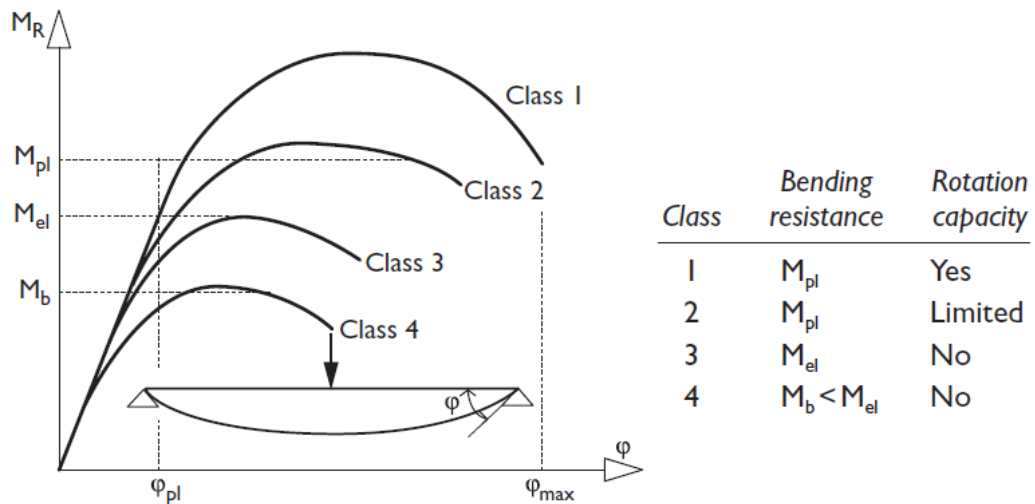


Figure 3-5 - Classes of cross sections (Vayas & Iliopoulos, 2013)

Furthermore, (EN 1993-1-1, 2005) adds that cross sections with class 1 or 2 flanges and class 3 web may be classified as class 2, when the web is represented by an effective web, in accordance with Figure 3-6.

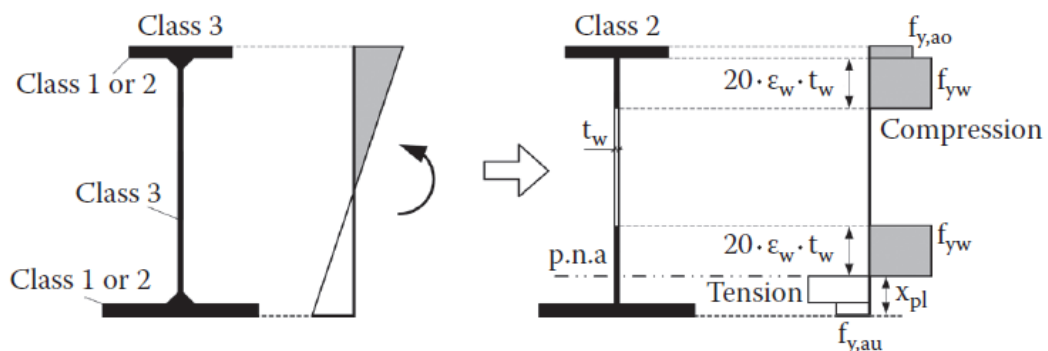


Figure 3-6 - Effective class 2 web that was initially class 3 (Vayas & Iliopoulos, 2013)

3.5.3. Effect of cracking of concrete

Cracking of concrete, in the negative moment regions should be taken into account when the tensile stresses are higher than the concrete's tensile strength (f_{ctm}). Standard (EN 1994-2, 2005), proposes two methods to consider the effect of cracking of concrete: "one is that first an un-cracked analysis may be carried out and the extent of concrete determined (when the concrete tensile stress exceeds a certain value), followed by another analysis cracked section properties in these regions; the second allows a simpler one-stage method". (Composite highway bridge design, 2014, p.37) The first method, called as "un-cracked analysis" and the second method known as "simplified method" should be determined in accordance with (EN 1994-2, 2005) (Chapter 5.4.2.3).

The simplified method may be used, when the ratio of the length of adjacent continuous spans (shorter/ longer) is greater than 0,6. It is a method in which the cracked flexural stiffness $E_a \cdot I_2$ is used over 15% of the span on each side of each internal support and the uncracked values $E_a \cdot I_1$ elsewhere. (Figure 3-7)

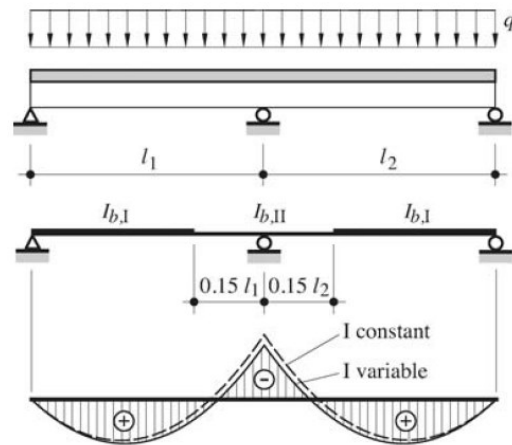


Figure 3-7 - Simplified method principle (Lebet & Hirt, 2013)

3.5.4. Effects of creep and shrinkage

The effects of creep are taken into account by determining an appropriate modular ratio for long-term effects. This modular ratio for creep is given by (EN 1994-2, 2005) (5.4.2.2(2)), which requires a creep coefficient according to (EN 1992-1-1, 2004) (Chapter 3.1.4). Thus, the modular ratios depending on the type of loading are given by:

$$n_L = n_0 (1 + \psi_L \varphi_t) \quad (3.12)$$

Where:

n_0 is the modular ratio E_a/E_{cm} for short-term loading;

E_{cm} is the secant modulus of elasticity of the concrete for short-term loading according to (EN 1992-1-1, 2004) (Table 3.1 or 11.3.1)

φ_t is the creep coefficient $\varphi(t, t_0)$ according to (EN 1992-1-1, 2004) (3.1.4 or 11.3.3)

ψ_L is the creep multiplier depending on the type of loading, which can be taken as 1,1 for permanent loads, 0,55 for primary effects of shrinkage and 1,5 for prestressing by imposed deformations.

On the other hand, the shrinkage strains is given by (EN 1992-1-1, 2004) (Annex B.2) and the modular ratio for shrinkage is given by (EN 1994-2, 2005) (Chapter 5.4.2.2(2)).

3.5.5. Stages and sequence of construction

(EN 1994-2, 2005) (Chapter 5.4.2.4), states that appropriate analysis should be made to cover the effects of staged construction, including where necessary separate effects of actions applied to structural steel and to wholly or partially composite members. However, adds that these effects may be neglected in analysis for ultimate limit states other than fatigue, for composite members where all cross-sections are in class 1 or 2 and in which no allowance for lateral buckling is needed.

3.6. Verification by Ultimate Limit States

In order to carry out a check according to (EN 1994-2, 2005) (6.1.1), the following parameters should be taken into account:

- Resistance of cross-sections;
- Resistance to lateral-torsional buckling;
- Resistance to shear buckling and in-plane forces applied to webs;
- Resistance to longitudinal shear;
- Resistance to fatigue.

3.6.1. Resistance of cross-sections

As it was already explained, depending on the classification of cross-section, the resistance of a composite cross-section may be determined either by using a plastic resistance model or an elastic resistance model. The resistance of cross sections of beams is described in detail in (EN 1994-2, 2005), where the (Clause 6.2.1.2) gives information related to the calculation of plastic resistance moment, and the (clause 6.2.1.5) gives information related to the elastic resistance to bending.

3.6.1.1. Plastic resistance moment of a composite cross-section

The calculation of plastic resistance moment is performed in accordance with Figure 3-8, taking into account the following assumptions:

- There is full interaction between structural steel, reinforcement, and concrete;
- The effective area of the structural steel member is stressed to its design yield strength f_{yd} in tension or compression;
- The effective areas of longitudinal reinforcement in tension and in compression are stressed to their design yield strength f_{sd} in tension or compression. Alternatively, reinforcement in compression in a concrete slab may be neglected;
- The effective area of concrete in compression resists a stress of $0,85f_{cd}$ (constant over the whole depth between the plastic neutral axis and the most compressed fibre of the concrete, where f_{cd} is the design cylinder compressive strength of concrete).

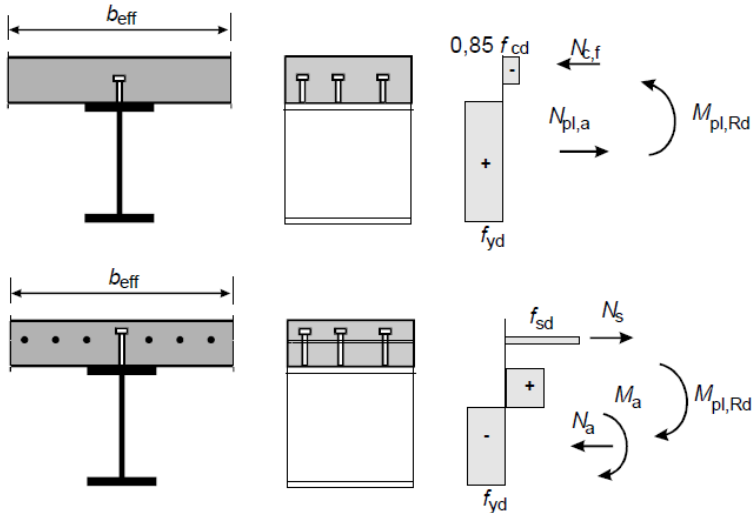


Figure 3-8 - Examples of plastic stress distributions for a composite beam with a solid slab and full shear connection in sagging and hogging bending (EN 1994-2, 2005)

3.6.1.2. Elastic resistance moment of a composite cross-section

The total stresses and strains of a composite cross-section that behaves essentially in an elastic manner, are determined by summation of the stress distributions for the bending moments at each stage of construction. Figure 3-9 shows diagrammatically this summation process, where some bending is carried on the bare steel beam, some is carried on a beam with long-term section properties (e.g. surfacing, mechanical components, etc.), and some is carried on a beam with short-term section properties (e.g. traffic loads and temperature). (Composite highway bridge design, 2010)

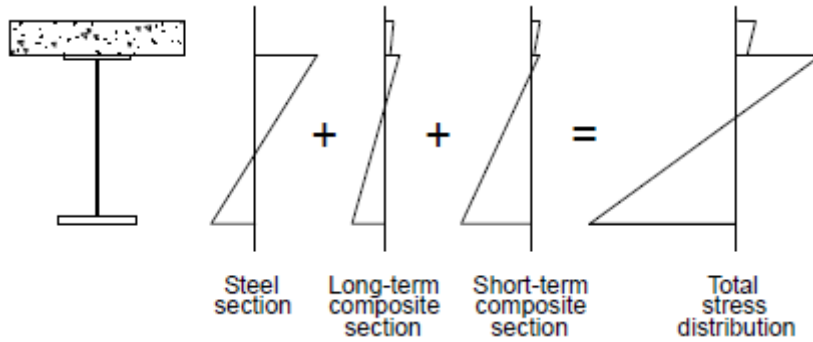


Figure 3-9 - Summation of stresses acting on different resisting cross sections (Composite highway bridge design, 2010)

Taking the aforementioned considerations, the elastic bending resistance can be determined using the following expression:

$$M_{El,Rd} = M_{a,Ed} + k \times M_{c,Ed} \quad (3.13)$$

Where:

$M_{a,Ed}$ is the design bending moment applied to structural steel section before composite behaviour;

$M_{c,Ed}$ is the part of the design bending moment acting on the composite section;

k is an amplifying factor that just causes the stress limit (determined using γ_{M1} for steel strength) to be reached in either the structural steel section or the reinforcement (whichever occurs first)

3.6.2. Resistance to lateral-torsional buckling

In a composite beam, the only regions of the main girders that are potentially susceptible to buckling are the bottom flanges where they are in compression (in regions adjacent to intermediate supports of continuous spans and adjacent to end supports). The steel top flanges are not susceptible to lateral buckling, because the concrete slab provides lateral restraint to the steel member. (Composite highway bridge design, 2010)

According to continuous U-frame model (Figure 3-10) from (EN 1994-2, 2005) (6.4.2), for beams with a uniform cross-section in class 1, 2, or 3, the design buckling resistance moment of a composite section can be expressed as:

$$M_{b,Rd} = \chi_{LT} \cdot M_{Rd} \quad (3.14)$$

In eq. (3.14), χ_{LT} is the reduction factor for lateral-torsional buckling corresponding to the relative slenderness determined by (EN 1994-2, 2005) (6.4.2 (4)), which in turn, depends of the elastic critical moment. This elastic critical moment (M_{cr}) is neither in EN

1993 nor in EN 1994, therefore, it must be determined either by an elastic buckling analysis or by reference to other sources. However, for hogging regions of composite bridges it is difficult to find suitable theoretical models that will give realistic values of M_{cr} . Additionally, (EN 1994-2, 2005) (Chapter 6.4.2) refers to (EN 1993-2, 2006) (Chapter 6.3.4), which does provide two general methods to determine the relative slenderness, one called ‘general method’ and one called ‘simplified method’. (Composite highway bridge design, 2010)

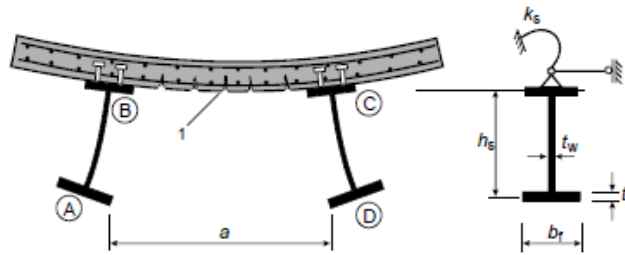


Figure 3-10 - U-frame model (EN 1994-2, 2005)

3.6.2.1. General method

The general method may be applicable to both lateral and lateral torsional buckling. The first step is to calculate an amplifier ($\alpha_{ult,k}$) of the design loads to reach the characteristic resistance of the most critical section neglecting any out-of-plane effects (second order bending moments should be included), followed by calculation of an amplifier of the in-plane design loads (α_{crit}) to reach the fundamental buckling mode for lateral or lateral torsional buckling. In order to obtain the critical load factor (α_{crit}), a 3D model should be used. (Vayas & Iliopoulos, 2013)

The non-dimensional slenderness is then given by:

$$\bar{\lambda}_{op} = \sqrt{\frac{\alpha_{ult,k}}{\alpha_{crit}}} \quad (3.15)$$

On its turn, the reduction factor χ_{op} is determined using the buckling curves of (EN 1993-1-1, 2005) (6.3.1.2). Thus, the final step corresponds to the buckling verification, which may be written as:

$$\frac{\chi_{op} \alpha_{ult,k}}{\gamma_{M1}} \geq 1,0 \quad (3.16)$$

3.6.2.2. Simplified method

The simplified method is valid only to verify the resistance to lateral torsional buckling of a compression flange and not for lateral buckling of full systems. It uses a Tee section comprising the bottom flange and one-third of the compression zone of the web (Figure 3-11), and treats it as a compression member subjected to out-of-plane flexural buckling.

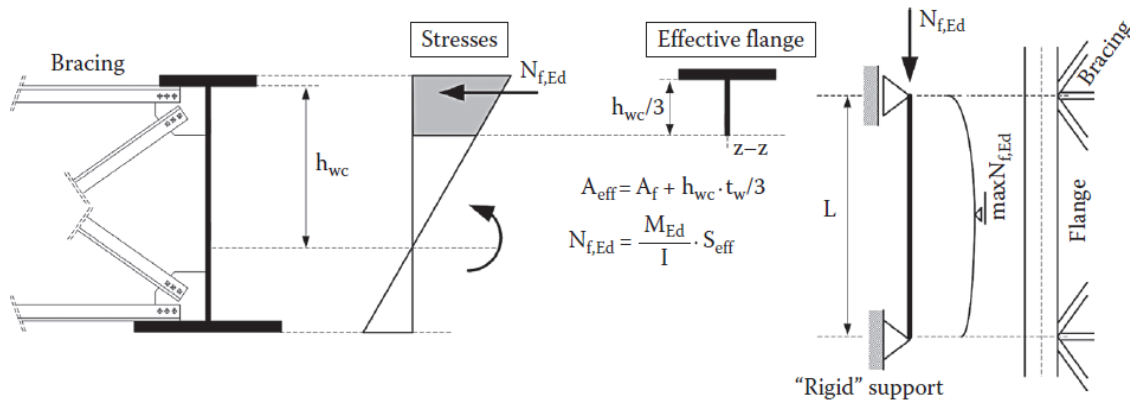


Figure 3-11 - Modelling of the compression flange as a T-section column on rigid supports (Vayas & Iliopoulos, 2013)

The steps to follow according to simplified method are listed on the following guidelines. In addition, Chapter 4 gives a detailed explanation of these steps.

- Calculation of N_{crit} , according to (EN 1993-2, 2006) (6.3.4.2 (6)) for the Tee section at the more highly stressed end of the length L between rigid restraints;
- Calculation of the restraint flexibility C_d for each intermediate restraint (EN 1993-2, 2006) (Annex D);
- Calculation of slenderness parameter $\bar{\lambda}_{LT}$ using equation 6.10 of (EN 1993-2, 2006) (6.3.4.2);
- Calculation of reduction factor for lateral torsional buckling χ_{LT} (EN 1993-1-1, 2005) (6.3.2.3);
- Verification of resistance to lateral torsional buckling.

3.6.3. Resistance to shear buckling and in-plane forces applied to webs

The webs of plate girders are usually slender, which makes them more susceptible to buckling under the effects of shear. In order to understand the behaviour of a panel in shear, there are two important phases to be known: (Lebet, Hirt, 2013)

- Pre-buckling behaviour, where the state of the in-plane stresses is a combination of tension and compression of equal intensity, which means that exists diagonals in tension and compression at 45° relative to the edges for a square panel (Figure 3-12 (a));
- Post-buckling behaviour, where the compression stresses will lead to the local buckling of the panel (Figure 3-12 (b)). This buckling occurs whenever the state in-plane stresses are bigger than the critical shear stresses.

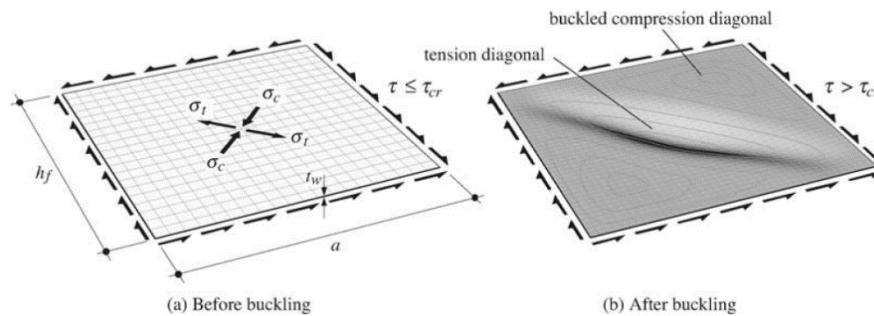


Figure 3-12 - Buckling of a panel in shear (Lebet & Hirt, 2013)

According to (EN 1993-1-5, 2006), the resistance to shear buckling of a plate girder should be checked when:

- For an unstiffened web:

$$\left(\frac{h_w}{t}\right) > \frac{72}{\eta} \varepsilon \quad (3.17)$$

- For a stiffened web:

$$\left(\frac{h_w}{t}\right) > \frac{31}{\eta} \varepsilon \sqrt{k_\tau} \quad (3.18)$$

Whenever it is necessary to check the shear resistance of webs, it should be determined according to (EN 1993-1-5, 2006). The rules presented on this standard leads to a long process that involves several variables and conditions. Taking this into account, a summary of the sequence considered for the resistance to shear buckling and in-plane forces applied to webs and respective reference in (EN1993-1-5) is listed on the following:

- Resistance to shear, from (EN 1993-1-5, 2006), (chapter 5);
- Resistance to transverse forces, from (EN 1993-1-5, 2006), (chapter 6);
- Interaction M-V, from (EN 1993-1-5, 2006), (chapter 7);
- Flange induced buckling, from (EN 1993-1-5, 2006), (chapter 8).

3.6.4. Resistance to longitudinal shear

The longitudinal shear at the concrete-steel interface is the means by which the loads are transferred from the girder into the slab. The longitudinal shear resistance is achieved by shear connectors, which are required on the top flanges of the girders, to provide the required transfer of composite action between the steel girder and concrete slab. (Composite highway bridge design, 2010) On the following, a brief description related to the design process of shear connectors, and the determination of longitudinal shear is presented.

3.6.4.1. Shear connectors

The design process of shear connectors is determined according to (EN 1994-2, 2005) (6.6.3.1), and consists of deriving the value of the longitudinal shear and the verification of the connectors, and of the resistance of the slab adjacent to the connectors. (Composite highway bridge design, 2010) Thus, the design value of the shear resistance may be defined by the following equation:

$$P_{Rd} = \min(P_{Rd,1}; P_{Rd,2}) \quad (3.19)$$

- Failure at stud shank

$$P_{Rd,1} = \frac{0,8 \times f_u \times \pi \times d^2 / 4}{\gamma_V} \quad (3.20)$$

- Crushing of concrete around the shank

$$P_{Rd,2} = \frac{0,29 \times \alpha_u \times d^2 \times \sqrt{f_{ck} \times E_{cm}}}{\gamma_V} \quad (3.21)$$

Figure 3-13 depicts a representation of the elements of the headed studs, as well as the dimension specific to these devices. Taking into consideration the procedure described on the above lines, Table 3-10 gives a synthesis of the design value of the shear resistance of headed studs with $h_{sc}/d \geq 4$ in solid slabs at ultimate limit states.

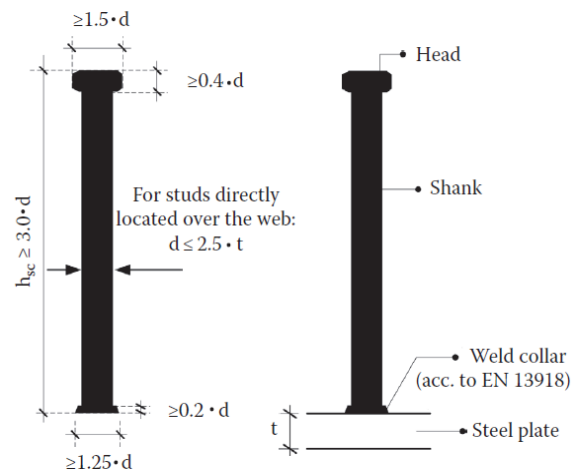


Figure 3-13 - Dimensions of headed studs (Vayas & Iliopoulos, 2013)

Shank diameter d (mm)	Minimum h _{sc} (mm)	f _u = 450 MPa and		
		C30/37 to C60/75 (Failure of shank)	C30/37 (Concrete crushing)	C35/45 to C60/75 (Failure of shank)
25	100	141,30	144,27	157,00
22	88	109,42	111,73	121,53
19	76	81,61	83,33	90,68
16	64	57,88	59,09	64,31

Table 3-10 - Shear resistance P_{Rd} (kN) of headed studs with h_{sc}/d ≥ 4 in solid slabs at ULS (Vayas & Iliopoulos, 2013)

3.6.4.2. Longitudinal shear for elastic behaviour

Where a uniform composite section is designed elastically, the longitudinal shear force may be determined from the simple relationship of mechanics:

$$V_{L,Ed} = \frac{V_{Ed} \times S}{I} \quad (3.22)$$

Where:

V_{Ed} is the design vertical shear force;

S is the static moment of the concrete slab in respect to the centre of gravity of the composite section;

I is the second moment of area of the composite section.

According to (Composite highway bridge design, 2010, p.65), “In hogging moment regions, where the slab is in tension, longitudinal shear may be calculated using uncracked section properties; this give a safe value without the need for more complex calculation, even when the plastic resistance of the cracked section is relied upon. Short term uncracked properties may be used for this purpose”.

3.6.4.3. Longitudinal shear for plastic behaviour

As indicated above, the Equation 3.22 is valid for elastic behaviour. However, at ULS and for cross sections of class 1 and 2, it is possible to exploit the plastic bending resistance (Figure 3-14), and then a slightly more complex evaluation is needed. (Vayas & Iliopoulos, 2013)

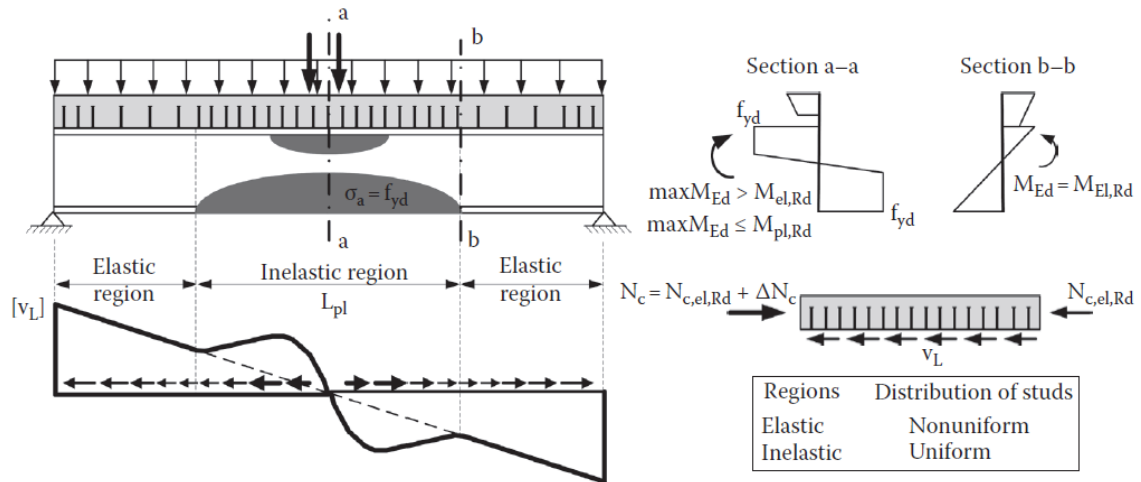


Figure 3-14 - Longitudinal shear in inelastic regions (Vayas & Iliopoulos, 2013)

Plastic behaviour is reached for regions where the design moment is larger than the elastic moment resistance, which is determined by consideration of the construction stages, as indicated on section 3.6.1.2. (Vayas & Iliopoulos, 2013) In such case, the design shear is then determined in accordance with (EN 1994-2, 2005) (6.6.2.2).

3.6.4.4. Longitudinal shear due to concentrated forces

Additionally, it is necessary to consider a more complex evaluation if there is a concentrated introduction of shear force, which can be due to a change of cross section, or where temperature and shrinkage effects (Figure 3-15) are introduced at the end of a beam. (Composite highway bridge design, 2010)

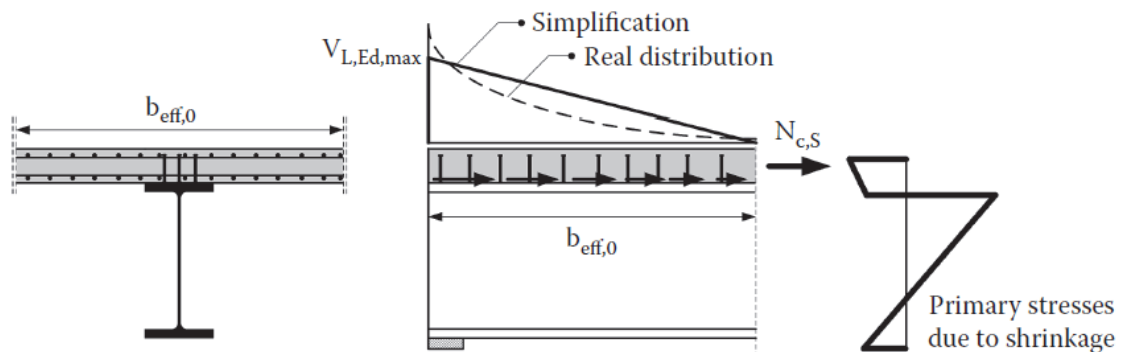


Figure 3-15 - Distribution of end shear due to shrinkage at an edge support (Vayas & Iliopoulos, 2013)

So, in this case, the shear flow (shear force per unit length) due to a concentrated introduction of force is approximated by a triangular distribution (Figure 3-15) with a maximum value given by:

$$V_{L,Ed,max} = \frac{2 \times N_{c,s}}{b_{eff,0}} \tag{3.23}$$

3.6.4.5. Longitudinal shear in concrete slabs

The slab must also be checked in order to verify its ability to transfer the longitudinal shear transmitted from the girder by shear connectors, on the potential failure surfaces (Figure 3-16). (Composite highway bridge design, 2014) The resistance to longitudinal shear in concrete slab should be determined in accordance with (EN 1994-2, 2005) (Chapter 6.6.6).

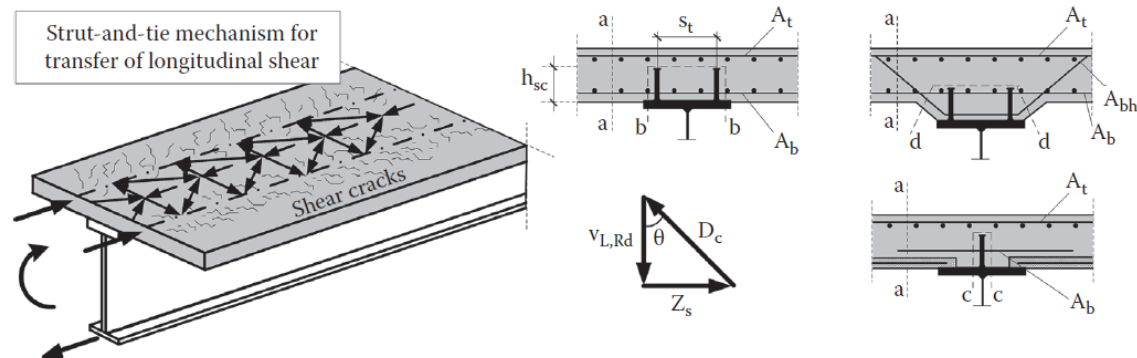


Figure 3-16- Failure mechanism and typical sections for checking shear failure (Vayas & Iliopoulos, 2013)

3.6.5. Resistance to fatigue

As defined by (Vayas, Iliopoulos, 2013, p.441): “Fatigue is a process in which damage is accumulated in the materials undergoing fluctuating loading”. According to (EN 1994-2, 2005) (Chapter 6.8.1), the resistance of composite structures to fatigue shall be verified where the structures are subjected to repeated fluctuations of stresses. This phenomenon is more likely to take place at regions of stress concentration such as rapid changes of cross sections, at section reductions due to bolted connections or in welding regions, where the material undergoes metallurgic changes. (Vayas, Iliopoulos, 2013)

Resistance to fatigue is covered generally in both (EN 1993-2, 2006) and (EN 1994-2, 2005), and detailed rules are given in: (Composite highway bridge design, 2010)

- (EN 1993-1-9, 2005), for structural steel;
- (EN 1992-1-1, 2004), for reinforcing steel;
- (EN 1994-2, 2005) (Chapter 6.8.7.2), for stud connectors.

3.7. Verifications by serviceability limit states

The verification of serviceability limit states should be performed for stress levels, deflections and cracking of concrete, which are calculated using an elastic global analysis and considering the effects of shear lag, creep and shrinkage of concrete. (Composite highway bridge design, 2010)

3.7.1. Stresses

Stress levels at SLS are verified for the characteristic combination of actions, to ensure that there is no inelastic behaviour. The stresses in the structural steel, in the concrete and the shear force per connector are limited by:

- (EN 1993-2, 2006) (Chapter 7.3(1)), for structural steel
- (EN 1994-2, 2005) (Chapter 7.2.2(2)), for concrete
- (EN 1993-2, 2006) (Chapter 6.8.1(3)), for shear force per connector

3.7.2. Deflections

According to (Vayas, Iliopoulos, 2013), there exist no limit deflection on Eurocodes for road bridges so that such limits must be agreed with the owner of the bridge. On its turn, the limit deflections may also be determined by reference to other sources. According to the Spanish standard (Recomendaciones para el proyecto de puentes mixtos para carreteras RPX - 95, 2003), the indicative limiting value for deflections related to the overload for frequent SLS combination of action, should not exceed the following values:

L/1000 : for roadway bridges;

L/1200 : for footway bridges and roadway bridges with footway tracks.

3.7.3. Cracking of concrete

In order to ensure that the crack widths will be limited and durability of concrete slab will not be substantially affected, some agreed limits should be taken into consideration. These limits are performed by (EN 1994-2, 2005) (7.4), which defines a minimum reinforcement area placed at hogging moment areas , as well as it gives some limiting spacing and diameters of the rebars.

Chapter 4 Numerical Example

The numerical example presented herein, together with the previous chapters aims to illustrate the different calculation steps of a twin composite girder bridge designing, according to the methodologies proposed by Eurocodes.

This example corresponds to a twin-girder bridge, commonly known as Ladder Deck Bridge, which, due to its simplicity has been a solution very implemented in many countries. The study carried out on this chapter is taken for a general situation, which does not corresponds to a real case, and covers only design of the superstructure.

Taking into account the above considerations, this chapter begins with a reference to the structural description of the bridge designing, and the normative standards used, followed by the classification and combination of actions to taken into consideration, distribution of effective width and methodology of global analysis, verification of Ultimate and Serviceability Limit States, until the design of shear connectors.¹

4.1. Structural description

In order to take an overall view of the composite bridge designing, a structural description is presented on this section, highlighting its type of use, and the structural arrangement.

The numerical example corresponds to a continuous three-span road bridge, of 37,5 m, 50 m, and 37,5 m (Figure 4-2), which is not designed to carry exceptional traffic. Moreover, the rolling surface has two traffic lanes of 3,5 m on either side, as well as it carries 0,75 m wide marginal strip, and 1,5 m wide footway on each side of the traffic lane, as represented in Figure 4-1.

As it can be seen by Figure 4-1, the steel beam depth, and the slab thickness are constant over the whole length of the bridge, at 2,12 m and 0,25 m respectively. However,

¹ References:

(Comprobación de un tablero mixto: Comisión 5 - Grupo de trabajo 5/3 "Puentes mixtos", 2006)
(Composite highway bridge design: Worked Examples, 2014)
(Davaine, Imbert, & Raoul, 2007)

the geometric properties of the web and flanges, namely the width and thickness vary along the length of the steel beams (Figure 4-2).

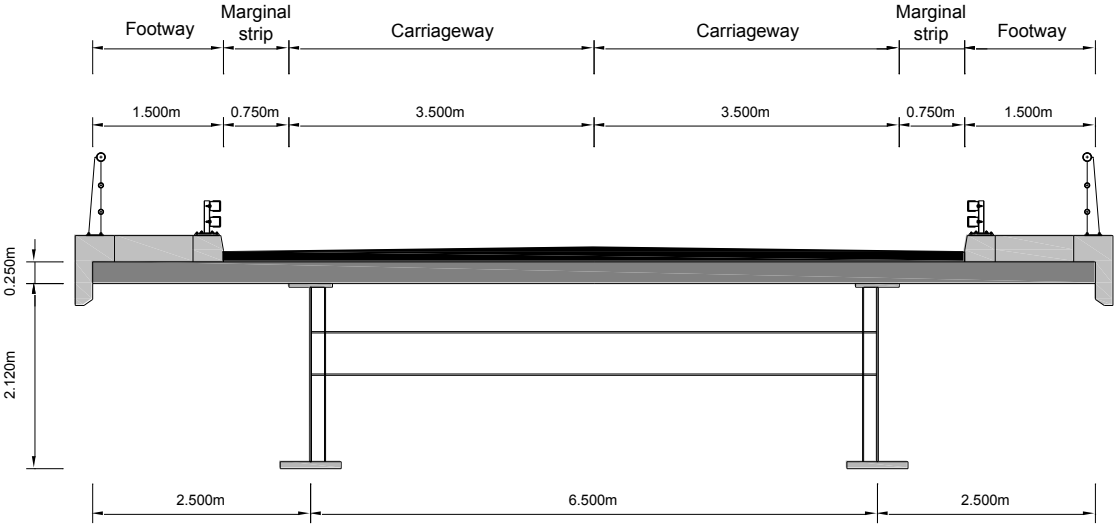


Figure 4-1 Cross section

In order to brief summarize the structural arrangement of the steel-concrete composite bridge, Figure 4-2 depicts a representation of the longitudinal view of the bridge, followed by the distribution of longitudinal and transverse stiffeners, as well as the cross bracings, until the final dimensions for the elements of the plate girders.

4.2. Materials

The following material properties are taken into account:

Structural Steel:

S355	$t \leq 40 \text{ mm}$	$f_y = 355 \text{ MPa}$	(EN 1993-1-1, 2005) (3.2)
S460	$40 < t \leq 80 \text{ mm}$	$f_y = 430 \text{ MPa}$	(EN 1993-1-1, 2005) (3.2)
		$E_a = 210 \text{ MPa}$	(EN 1993-1-1, 2005) (3.2)

Concrete:

C35/45	$F_{ck} = 35 \text{ MPa}$	(EN 1992-1-1, 2004) (Table 3.1)
	$E_{cm} = 34 \text{ GPa}$	(EN 1992-1-1, 2004) (Table 3.1)

Reinforcement:

A500NR	$f_{sk} = 500 \text{ MPa}$	(EN 1991-1-1, 2002) (3.2)
	$E_s = 210 \text{ GPa}$	(EN 1992-2, 2005) (3.2.2)

* The modulus of elasticity of both structural steel and reinforcing steel is taken as 210 GPa, as permitted by EN 1994-2.

In addition to the steel grades defined above, the steel subgrades should be chosen to avoid the brittle fracture at low temperatures. This subgrade depends mainly on the plate thickness, on the tensile stress level σ_{Ed} in the section and on the service temperature T_{Ed} .

Standard	Grade	Quality	T_{Ed} (20°C)		
			$\sigma_{Ed}=0,75 f_y(t)$	$\sigma_{Ed}=0,50 f_y(t)$	$\sigma_{Ed}=0,25 f_y(t)$
EN 10025-2 Non-alloy steels	S355	JR	20	40	70
		J0	35	55	95
		J2	50	80	130
		K2	60	95	150
EN 10025-3 and 4 Fine grain steels N (normalized) M (thermomechanical)	S355	N, M	60	95	150
		NL, ML	90	135	200
	S460	N, M	50	75	130
		NL, ML	70	110	175

Table 4-1 - Maximum permissible thickness t [mm] according to EN 10025, as a function of the temperature and the Stress in the plate

The combination of actions to be considered to calculate σ_{Ed} is the accidental one where the thermal action is the accidental load, however, in practice it can be assumed equal to the value for the frequent actions.

The service temperature T_{Ed} can be taken as equal to the characteristic value of the minimum shade air temperature T_{min} defined in Annex A of EN 1991-1-5. A value of T_{min} equal to -20°C have been assumed in this numerical example.

Thus, for the structural steel of the deck, grade S355 and S460 are used with the subgrades indicated on the following:

Structural Steel:

S355 J0 $t \leq 40$ mm

S460 N $40 < t \leq 80$ mm

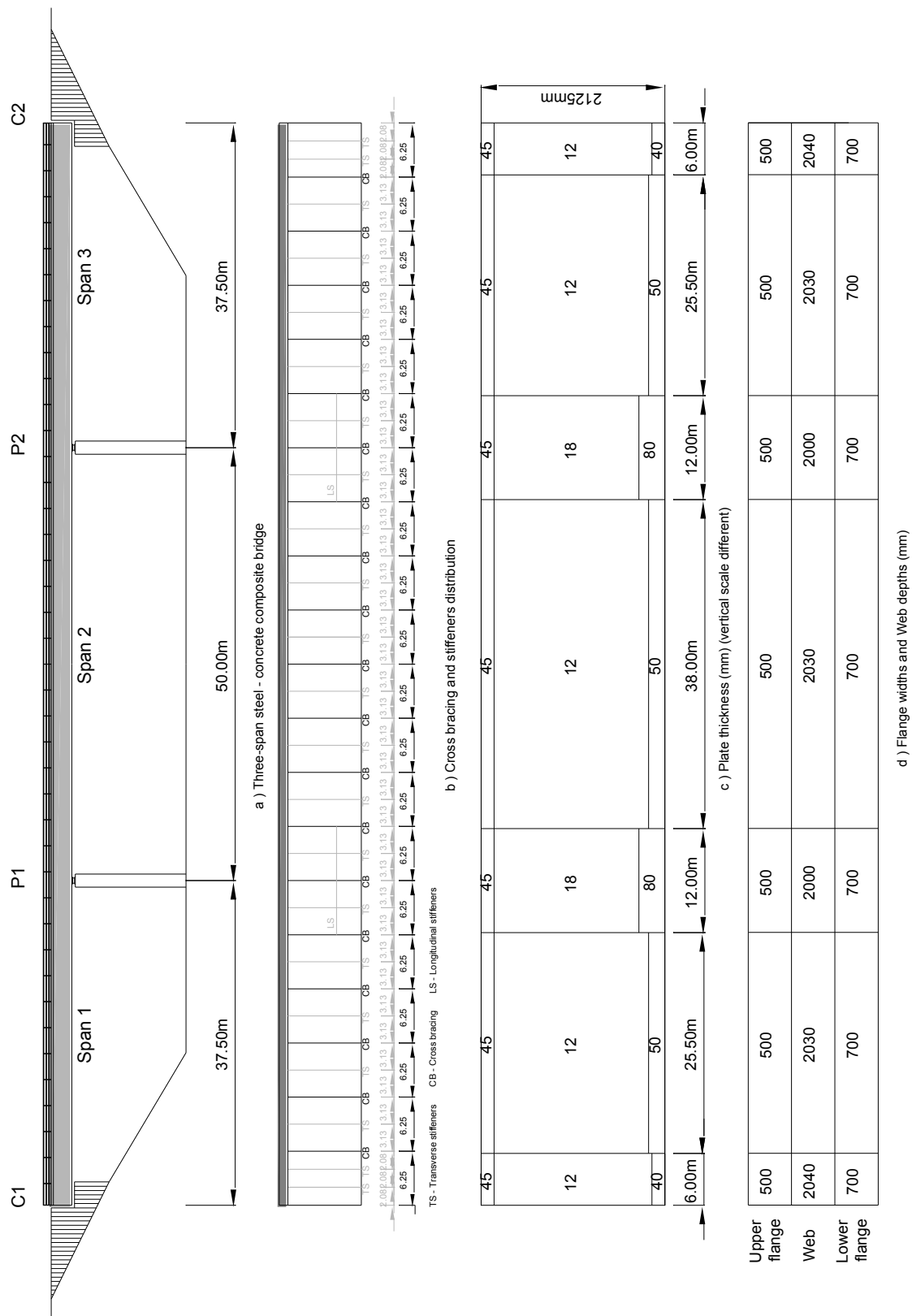


Figure 4-2 - Structural arrangement of the steel-concrete composite bridge

4.3. Fabrication and erection

The following constructive process is assumed:

1. Erection of steelwork for road bridge;
2. The slab is cast-in-situ, over the steelwork at once, and without stop;
3. Dead load at once, 15 days after the concreting slab.

4.4. Normative standard used

As it was already mentioned, this thesis aims to illustrate the different calculation steps of a twin composite girder bridge design, according to the methodologies proposed by Eurocodes. Taking this into account, the following standards are used:

Eurocode 0	Basis of structural design	(EN 1990, 2002)
Eurocode 1	Actions on structures	
EN 1991-1-1	Actions: General Actions	(EN 1991-1-1, 2002)
EN 1991-1-5	Thermal Action	(EN 1993-1-5, 2006)
EN 1991-2	Traffic loads on bridges	(EN 1991-2, 2003)
Eurocode 2	Design of concrete structures	
EN 1992-1-1	General rules, and rules for buildings	(EN 1992-1-1, 2004)
EN 1992-2	Concrete bridges	(EN 1992-2, 2005)
Eurocode 3	Design of steel structures	
EN 1993-1-1	General rules and rules for buildings	(EN 1993-1-1, 2005)
EN 1993-1-5	Plated structural Elements	(EN 1993-1-5, 2006)
EN 1993-2	Steel bridges	(EN 1993-2, 2006)
Eurocode 4	Design of composite steel and concrete structures	
EN 1994-1-1	General rules, and rules for buildings	(EN 1994-1-1, 2004)
EN 1994-2	Composite structures: Rules for bridges	(EN 1994-2, 2005)

4.5. Actions

As it can be noted on section 3.3, the actions are classified in relation to their duration, magnitude, and probability of occurrence, as permanent, variable, accidental and seismic actions. Taking into account the scope of this numerical example, as well as the characteristics of the bridge, the actions to take in consideration for this numerical example, are described on the following sections.

4.5.1. Permanent actions

- Self-weight of structural elements

The density of structural steel (main girders, cross bracing and stiffeners) is taken as 77 kN/m³, on its turn, the density of reinforced concrete and wet concrete (slab) is taken as 25 and 26 kN/m³, respectively. Thus:

a) Steel structure	7,2 kN/m
b) Concrete slab	35,94 kN/m
c) Wet concrete	37,38 kN/m
(during construction)		<hr style="width: 50%; margin-left: auto; margin-right: 0;"/> (each beam)

- Self-weight of the non-structural elements (Dead loads)

a) Asphalt layer	0,08 x 24 = 1,9 kN/m ²
b) Waterproofing layer	0,03 x 24 = 0.7 kN/m ²
c) pedestrian footway*	6.75 kN/m
d) Parapets *	0,5 kN/m
e) safety barriers*	0,5 kN/m
f) kerbs *	2,2 kN/m
g) edge beam*	4,25 kN/m

* (on either side)

 25,25 kN/m
(each beam)

4.5.2. Variable actions

- Traffic loads

Traffic loads on road bridges, include vertical and horizontal forces on the carriageway, which are determined by chapter 4 of (EN 1991-2, 2003). According to this standard, the vertical loads on the carriageway are represented by four load models, as stated in 3.3.1.2. Taking into consideration that the road bridge of this numerical example is not open to exceptional traffic, the load model 3 (special traffic) does not need to be checked. Furthermore, the horizontal actions due to acceleration and backing are not studied when checking the superstructure. Thus, the traffic loads on the present road bridge are represented by Load Model 1.

Load Model 1 consists of two partial systems; a double axle concentrated loads, and uniformly distributed loads, as represented bellow (Figure 4-3). The first step to determine these two partial systems, is to define the number of notional lanes. For this example, the number of notional lanes is determined by the following:

- Carriageway width, w

$$w = (2 \times 3,5) + (2 \times 0,75)$$

$$w = 8,5m > 6m$$

- Number of notional lanes

$$n_1 = \text{Int}\left(\frac{w}{3}\right) = \frac{8,5}{3} = 2,83 \rightarrow 2$$

- Width of a notional lane, w_l

$$w_l = 3m$$

- Width of the remaining area

$$w - (3 \times n_1) = 8,5 - (3 \times 2) = 2,5m$$

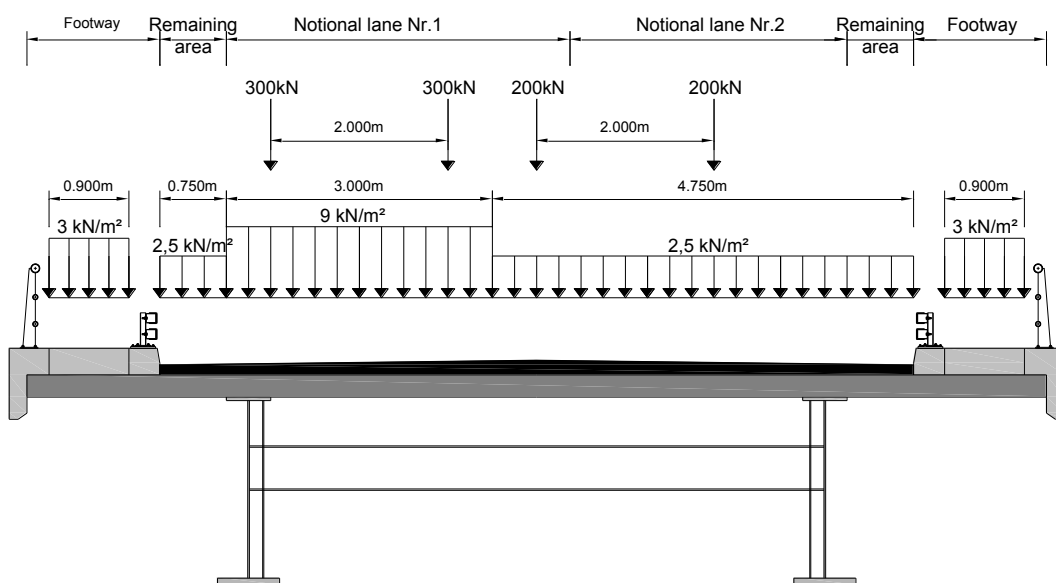


Figure 4-3 - Positioning of the traffic loads in transverse position

- Pedestrian loads

Pedestrian traffic load is represented by a distributed load of $q_{fk}=5\text{kN/m}^2$, given by (EN 1991-2, 2003) (5.3.2.1) that acts on the unfavourable parts of the influence line in longitudinal and transverse directions. For road bridges, a vertical load represented by the reduced value in combination with the traffic loads is taken into account. Thus, $0,6 q_{fk}$ is applied ($q_{fk} = 0,6 \times 5,0 = 3,0 \text{ kN/m}^2$), as displayed in Figure 4-3.

- Thermal loads

Temperature effects are defined by (EN 1991-1-5, 2003). According to the mentioned standard, the real temperature distribution within an individual structural element may be divided into four independent components; a uniform temperature component, a linear varying temperature component about y-y axis, a uniform temperature component, a linear varying temperature component about z-z axis, and a non-linear temperature component. However, for the majority of the plate girder bridges, the consideration of a uniform temperature component, and a linear varying temperature component about y-y axis, is considered adequate. Thus, for calculation of internal forces and moments due to temperature in the numerical example, a linear varying temperature component is assumed.

Table 6.1 by (EN 1991-1-5, 2003) (6.1.4.1), allows the recommended values of linear temperature difference component for different types of bridge decks, which on its turn, is modified by Portuguese National Annex. Thus, for a road bridge with a type 2 deck (composite deck), the following values are given:

	Top Warmer than bottom $\Delta T_{M,heat} (^{\circ}C)$	Bottom warmer than top $\Delta T_{M,cool} (^{\circ}C)$
Type 2: Composite deck	15	15

- Wind

The wind actions are not taking into consideration in this numerical example as they have no impact on the longitudinal global bending analysis of the bridge geometry.

- Shrinkage

The shrinkage strain has two components, the drying shrinkage and the autogenous shrinkage. However, in composite bridges, only drying shrinkage is considered directly for the calculation of stresses and deformations.

Taking into account the procedure outlined in clause 3.1(2) of (EN 1994-2, 2005), as well as in clause 3.1.4(5) and in Annex B.2) of (EN 1992-1-1, 2004), the calculation of the drying shrinkage is performed, as presented on the following lines.

$$\varepsilon_{cd}(t) = \beta_{ds}(t, t_s) \times k_h \times \varepsilon_{cd,0}$$

Where:

k_h is a coefficient depending on the notional size of the cross-section, obtained according to Table 3.3 of (EN 1992-1-1, 2004). For this case, it is taken equal to 0,805;

$\beta_{ds}(t, t_s)$ is a function describing the time-dependent development of the drying shrinkage, equal to:

$$\beta_{ds}(t, t_s) = \frac{t - t_s}{t - t_s + 0,04\sqrt[3]{h_0^3}}$$

For $t = \infty \rightarrow \beta_{ds} = 1$:

$\varepsilon_{cd,0}$ is the basic drying shrinkage, given by:

$$\varepsilon_{cd,0} = 0,85 \times [220 + 110 \times \alpha_{ds1} \times \exp(-\alpha_{ds2} f_{cm} / f_{cm0}) \times \beta_{RH}] \times 10^{-6}$$

For 70% relative humidity, $f_{ck} = 35 \text{ MPa}$ and class N cement:

$$f_{cm0} = 10, \quad \alpha_{ds1} = 4 \quad \alpha_{ds2} = 0,12$$

$$\beta_{RH} = 1,55 [1 - (RH / 100)^3] = 1,55 [1 - 0,7^3] = 1,018$$

$$\varepsilon_{cd,0} = 0,85 \times [220 + 110 \times 4 \times \exp(-0,12 \times 43 / 10) \times 1,018] \times 10^{-6} = 41,4 \times 10^{-5}$$

Then:

$$\varepsilon_{cd}(\infty) = 1,0 \times 0,805 \times 41,4 \times 10^{-5} = 33,3 \times 10^{-5}$$

- Creep

The effect of creep is covered by (EN 1994-2, 2005), (5.4.2.2 (4)) and (EN 1992-1-1, 2004), (B.1). The creep factor is calculated for long term loading but the age at first loading is assumed to be 15 days, after concreting stage.

$$\varphi(t, t_0) = \varphi_0 \times \beta_c(t, t_0)$$

Where:

φ_0 is the notional creep coefficient, given by:

$$\varphi_0 = \varphi_{RH} \times \beta_{(fcm)} \times \beta_{(t_0)}$$

$$\varphi_{RH} = \left[1 + \frac{1 - RH / 100}{0,1 \times \sqrt[3]{h_0}} \alpha_1 \right] \alpha_2 = \left[1 + \frac{1 - 70 / 100}{0,1 \times \sqrt[3]{243,90}} \times 0,87 \right] \times 0,96 = 1,36$$

$$\beta_{(fcm)} = \frac{16,8}{\sqrt{fcm}} = \frac{16,8}{\sqrt{43}} = 2,56$$

$$\beta_{(t_0)} = \frac{1}{0,1 \times t_0^{0,20}} = \frac{1}{0,1 + 15^{0,20}} = 0,55$$

Then:

$$\varphi_0 = 1.36 \times 2.56 \times 0.55 = 1,91;$$

$\beta_c(t, t_0)$ is the coefficient to describe the development of creep with time after loading, given by:

$$\beta_c(t, t_0) = \left[\frac{(t - t_0)}{\beta H + t - t_0} \right]^{0,3}$$

Thus:

$$\beta_c(t, t_0) = \left[\frac{10000}{608,48 + 10000} \right]^{0,3} = 0,982$$

Thus:

$$\varphi(t, t_0) = 1,91 \times 0,982 = 1,88$$

- Construction loads

Construction loads are classed as variable loads, which comes from six different sources, Q_{ca} , Q_{cb} , Q_{cc} , Q_{cd} , Q_{ce} , and Q_{cf} , according to Table 4.1 of (EN 1991-1-6, 2005). For global analysis of steel structure during the casting of concrete, the following actions are taken into account simultaneously (wet concrete is assumed to have a density of 1 kN/m^3 higher than that of hardened concrete):

a) Personal and hand tools (Q_{ca})	1 kN/m^2
b) Formwork and load bearing members (Q_{cb})	0,5 kN/m^2
c) Weight of fresh concrete (Q_{cf})	0,25 kN/m^2
	1,75 kN/m^2

4.6. Effective width

As it was already explained on section 3.5.1, the verification of cross-section should be determined taking into account the distribution of effective width between supports and mid span regions, due to non-uniform distribution of stresses over the total width of the slab, as a result of an effect known as shear lag. The effective width b_{eff} , at mid span or an internal support, as well as at an end support, is determined according to (EN1994-2, 5.4.1.2), as presented on the following lines.

$$b_{eff} = b_0 + \sum b_{ei}$$

$$b_{ei} = L_e / 8 \quad (\text{but no more than geometric width})$$

At the abutments:

$$b_{eff} = b_0 + \sum \beta_i b_{ei}$$

$$\beta_i = (0,55 + 0,025 \times L_e / b_{ei}) \leq 1$$

Where:

L_e is the distance between points of zero-bending moment (Figure 4-4), provided that the adjacent internal spans do not differ more than 50% and any cantilever is not larger than $\frac{1}{2}$ the adjacent span;

- Abutment and midspan section (Span 1 and Span 3)

$$L_e = 0,85L_1 = 0,85 \times 37,50 = 31,875m$$

- Hogging section

$$L_e = 0,25(L_1 + L_2) = 0,25 \times (37,5 + 50) = 21,875m$$

- Midspan section (Span 2)

$$L_e = 0,70 \times L_2 = 0,70 \times 50 = 35m$$

β_i is a reduction factor, taken as:

- Abutment section (Span 1 and Span 3)

$$\beta_i = \left(0,55 + 0,025 \times \frac{L_e}{b_{ei}} \right) \leq 1$$

$$\beta_i = \left(0,55 + 0,025 \times \frac{31,875}{2,4} \right) = 0,882$$

$$\beta_i = \left(0,55 + 0,025 \times \frac{31,875}{3,15} \right) = 0,803$$

Thus:

- Midspan section (Span 1 and Span 3)

$$b_{eff} = b_0 + \sum b_{ei}$$

$$b_{eff} = 0,2 + (2,40 + 3,15) = 5,75$$

- Midspan section (Span 2)

$$b_{eff} = b_0 + \sum b_{ei}$$

$$b_{eff} = 0,2 + (2,40 + 3,15) = 5,75$$

- Abutment section (Span 1 and Span 3)

$$b_{eff} = b_0 + \sum \beta_i \times b_{ei}$$

$$b_{eff} = 0,2 + (0,882 \times 2,4) + (0,803 \times 3,15)$$

$$b_{eff} = 4,85$$

- Hogging section

$$b_{eff} = b_0 + \sum b_{ei}$$

$$b_{eff} = 0,2 + (2,4 + 2,73) = 5,33$$

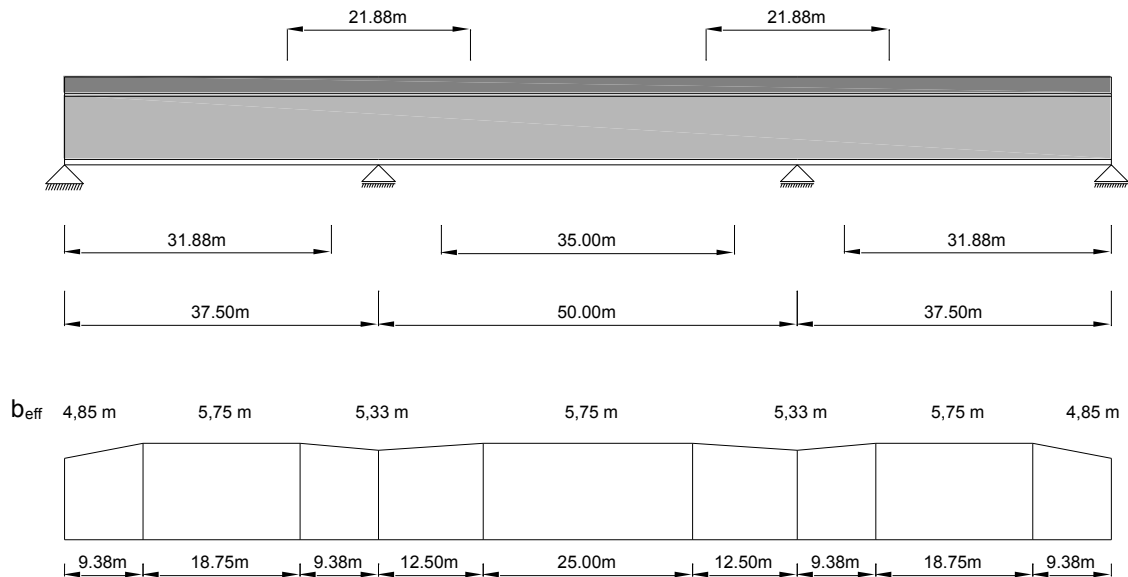


Figure 4-4 - Effective width of the concrete flange

4.7. Global analysis

The global analysis of the bridge is valid for Ultimate and Serviceability Limit States, and aims the calculation of the whole structure in order to determine the internal forces and moments, as well as the corresponding stresses on its various sections. This global analysis is calculated by respecting the stages of construction, the effects of creep and shrinkage, as well as the effect of cracking of concrete.

4.7.1. Stages of construction

As it can be inferred by (EN 1994-2, 2005) (5.4.2.4), an appropriate analysis should be made to cover the effects of staged construction, including separate effects of actions applied to structural steel and to wholly or partially composite members. For this numerical example, the sequence of construction listed on section 4.3, is considered.

4.7.2. Effect of creep

The effects of creep are taken into account by using modular ratios n_L for the concrete, as indicated by (EN 1994-2, 2005) (5.4.2.2). The modular ratios to consider, depending on the type of loading, are displayed on the following guidelines:

- To calculate the structure subjected to overload and temperature:

$$n_0 = E_a / E_{cm} = 210 / 34 = 6,2$$

- To calculate the structure subjected to permanent loads:

$$n = n_0(1 + 1,1 \times 1,88) = 19$$

- To calculate the isostatics and hyperstatic effects of shrinkage:

$$n = n_0(1 + 0,55 \times 1,88) = 13$$

4.7.3. Effect of cracking of concrete

Since the ratio of the length of adjacent continuous spans (shorter/ longer) between supports is greater than 0,6 ($37,5/50 = 0,75$), the effect of cracking of concrete may be taken into account by using cracked section properties over 15% of the span on each side of each internal supports, and as uncracked section elsewhere. (EN 1994-2, 2005) (5.4.2.3)

Thus, the cracked section properties may be considered at 5,6m ($0,15 \times 37,5 = 5,6$ m) over span 1 and span 3, and 7,5m ($0,15 \times 50 = 7,5$ m) over the span 2, adjacent to each pillar. However, since the variation of cross-section (Section Type 1 to Section Type 3) occurs at 6 m adjacent to each pillar, for simplification, this length is assumed as the cracked zone.

4.7.4. Mechanical characteristics of sections

As it can be observed by Figure 4-2, the effective widths and consequently the properties of the cross section vary along the bridge. However, according to (EN 1994-2, 2005) (5.4.1.2 (4)), since an elastic global analysis is used, a uniform effective width may be considered. Thus, the mechanical properties of sections, for global analysis of this numerical example, are to be determined considering a uniform effective width equal to 5,75 m, along the whole structure.

- Section Type 1: Section over pillar

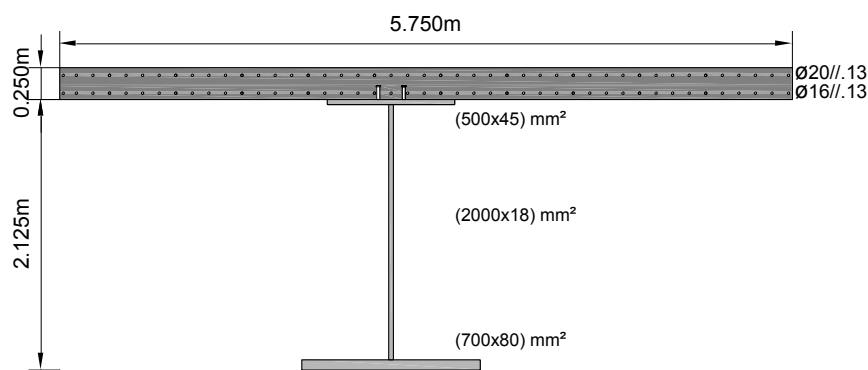


Figure 4-5 - Section Type 1 properties

	Steel	Homogenised section			Cracked
	Section	n = 6,2	n = 13	n = 19	Section
Area (m ²)	0,115	0,347	0,229	0,190	0,138
Inertia (m ⁴)	0,085	0,253	0,210	0,185	0,129
v (m)	1,353	0,612	0,864	1,014	1,351
v' (m)	0,772	1,763	1,511	1,361	1,024

Table 4-2 - Mechanical properties of section type 1

Notes:

v is the distance between the centre of gravity and the top fibre of steel section;

v' is the distance between the centre of gravity and the bottom fibre of steel section;

For cracked section, the top fibre of slab thickness is considered the highest fibre.

- Section Type 2: Section over abutments

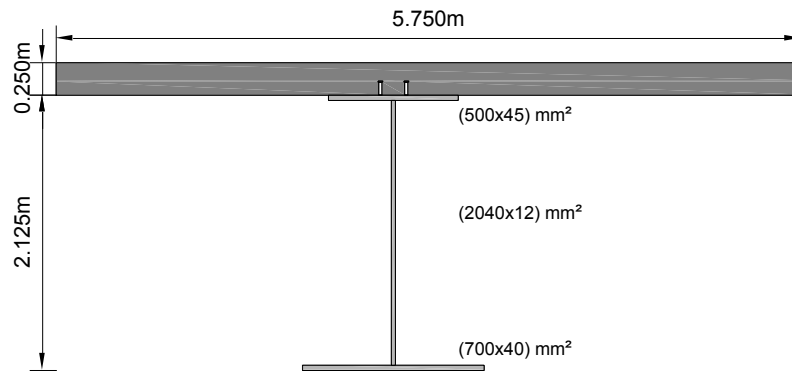


Figure 4-6 - Section Type 2 properties

	Steel	Homogenised section		
	Section	n = 6,2	n = 13	n = 19
Area (m ²)	0,075	0,308	0,189	0,151
Inertia (m ⁴)	0,063	0,154	0,135	0,123
v (m)	1,141	0,433	0,626	0,754
v' (m)	0,984	1,942	1,749	1,621

Table 4-3 - Mechanical properties of section type 2

- Section Type 3: Section of span

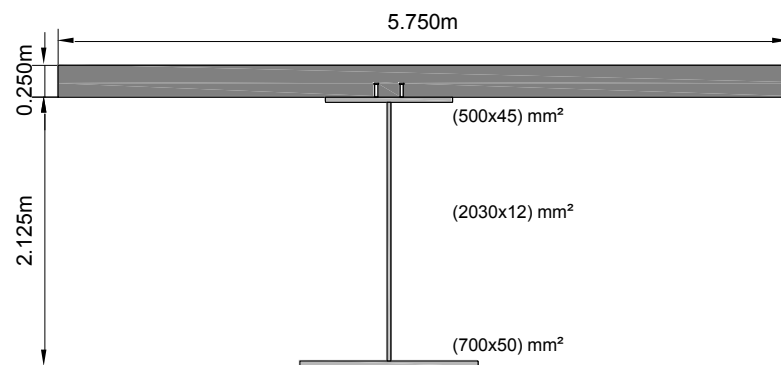


Figure 4-7 - Section Type 3 properties

	Steel	Homogenised section		
	Section	n = 6,2	n = 13	n = 19
Area (m ²)	0,082	0,314	0,196	0,158
Inertia (m ⁴)	0,068	0,192	0,155	0,140
v (m)	1,219	0,475	0,686	0,823
v' (m)	0,906	1,900	1,689	1,552

Table 4-4 - Mechanical properties of section type 3

4.7.5. Model calculation

In order to analyse the global longitudinal bending, the deck is modelled as a continuous beam, which is divided longitudinally by different section types, as show in Figure 4-8. This division is intended to give a realistic representation of slab, taking into consideration the mechanical properties of cross-sections determined on the previously section.

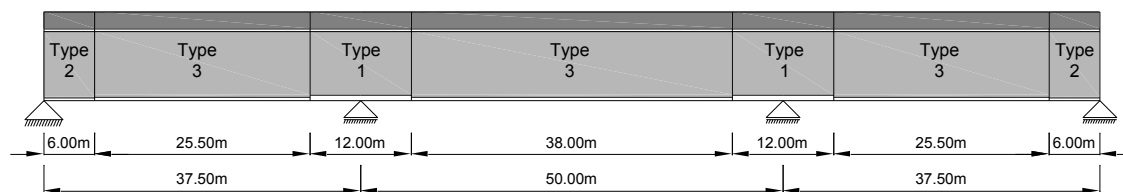


Figure 4-8 - Model calculation

As it can be inferred by 3.5, an appropriate allowance should be made for the effects of cracking of concrete, creep and shrinkage, and sequences of construction. Taking this into account, Table 4-5 summarises the properties of section types depending on the type of loading.

		Section Type 1	Section Type 2	Section Type 3
Self-weight of steel		Steel section	Steel section	Steel section
Self-weight of concrete		Steel section	Steel section	Steel section
S-w of wet concrete		Steel section	Steel section	Steel section
Dead Load	t = 0	Cracked Section	n = 6,2	n = 6,2
	t = ∞	Cracked Section	n = 19	n = 19
Traffic loads		Cracked Section	n = 6,2	n = 6,2
Pedestrian traffic		Cracked Section	n = 6,2	n = 6,2
Thermal loads		Cracked Section	n = 6,2	n = 6,2
Shrinkage		Cracked Section	n = 13	n = 13
Construction loads		Steel section	Steel section	Steel section

Table 4-5 - Properties for steel and composite cross sections

4.7.6. Analysis results

The results of action effects based on elastic theory, namely the bending moments, as well as the shear forces obtained for cross-sections over piers and at mid span, are summarised on Table 4-6. In addition, a brief description about determination of actions due to shrinkage is given on this section. Table 4-7, gives the deflection values obtained for the cross section at mid span.

- Action effects

		Cross section over Pier		Cross section at mid span	
		M (kN.m)	V (kN)	M (kN.m)	V (kN)
Self-weight of steel		- 1484	180	766	0
Self-weight of concrete		- 7405	899	3826	0
S-w of wet concrete		-7702	906	3979	0
Dead Load	t = 0	- 4555	631	3335	0
	t = ∞	- 4902	631	2988	0
Distributed traffic load		- 5988	808	5618	0
Heavy vehicle		$M_{\max} = - 3217$	$V_{\text{conc}} = 516$	7007	400
		$M_{\text{con}} = 0$	$V_{\max} = 800$		
Pedestrian traffic		- 536	72	504	0
Thermal action	Heat	3102	0	3102	0
	Cool	- 3102	0	- 3102	0
Shrinkage		- 4681	0	- 645	- 4681
Construction loads		-2072	244	1071	0

Table 4-6 - Results of action effects

- Action effects due to shrinkage

Taking into account the slab is connected with steel girder due to its shear connection, the shortening of the concrete due to shrinkage, leads to the development of a tension force N_{sh} , acting at the centre of the concrete flange. To re-establish the equilibrium, an equal compression force, as well as a bending moment M_{sh} , are applied to the composite section.

Thus, the actions due to shrinkage are calculated for mechanical characteristic sections with $n = 13$, considering a restraint force and a moment at the end spans girder (Figure 4-9), determined by the following:

- Compression force (N_{sh})

$$N_{sh} = A_c \times \varepsilon_{cm} \times \left(\frac{E_{cm}}{1 + 0,55 \times \varphi(\infty, t_0)} \right)$$

$$N_{sh} = (5,75 \times 0,25) \times 33,3 \times 10^{-5} \times \left(\frac{33 \times 10^6}{1 + 0,55 \times 1,88} \right)$$

$$= 8002kN$$

- Moment (M_{sh})

$$M_{sh} = N \times \left(v - \frac{0,25}{2} \right)$$

$$M_{sh} = 8002 \times \left(0,626 - \frac{0,25}{2} \right)$$

$$= 4009kNm$$

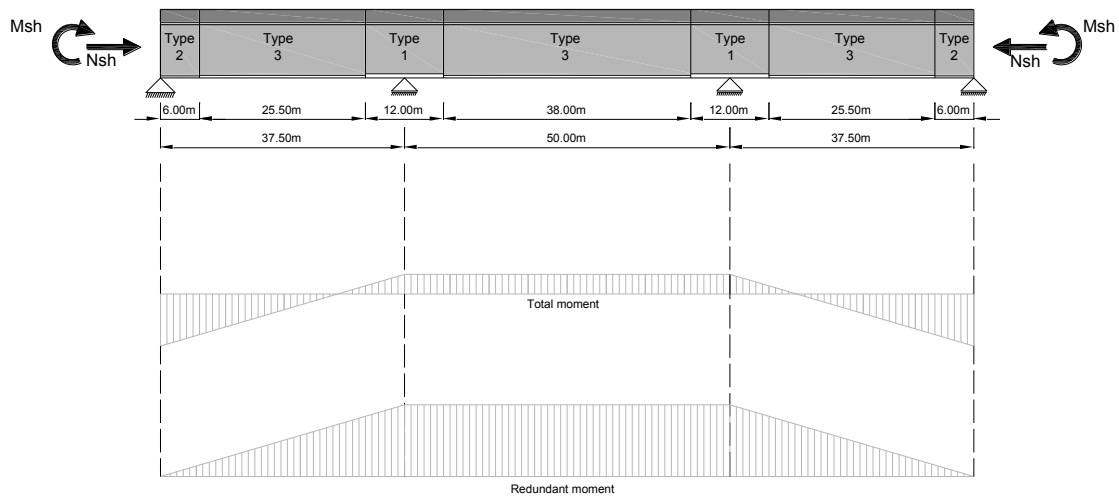


Figure 4-9 - Shrinkage loads model

- Deflection values

	$t = 0$ (mm)	$t = \infty$ (mm)
Self-weight of steel	8,8	8,8
Self-weight of concrete	43,9	43,9
Deal load	15,3	17,7
UDL Traffic load	31,3	31,3
Tsk Traffic load	28,3	28,3
Pedestrian traffic	2,8	2,8

Table 4-7 - Deflection values at mid span

4.7.7. Safety factors and combination values

The partial factors γ for actions and materials, as well as the combination factors ψ , to taken under consideration are given on the following tables:

- Partial factors for actions

Action Situation	Symbol	ULS	SLS	Reference
Permanent Loads	γ_G	1,35	1,0	(EN 1990, 2002) (A2) and (Table A.2.4(B))
Traffic Loads gr1a (LM1)	γ_Q	1,35	1,0	
Shrinkage	γ_{sh}	1,5	1,0	
Thermal Loads	γ_Q	1,0	1,0	

Table 4-8 - Partial factors for actions

- Partial factors for materials

Material	Symbol	ULS	SLS	Reference
Concrete	γ_Q	1,5	1,0	(EN 1992-1-1, 2004) (2.4.2.4)
Reinforcement	γ_S	1,15	1,0	
Structural Steel	γ_{M0}	1,0	1,0	(EN 1993-2, 2006) (6.1) and (Table 6.2)
	γ_{M1}	1,1		
Studs	γ_V	1,25	1,25	(EN 1994-2, 2005) (2.4.1.2)

Table 4-9 - Partial factors for materials

- Factors for combination values

Load Action		ψ_0	ψ_1	ψ_2	Reference
gr1a (LM1 + pedestrian loads)	TS	0,75	0,75	0	(EN 1990, 2002) (A.2) and (Table (A2.1))
	UDL	0,40	0,40	0	
	Pedestrian	0,40	0,40	0	
Thermal Load		0,60	0,60	0,50	

Table 4-10 - Factors for combination values

4.7.8. Design value of the combined actions

Taking into consideration the earlier considerations, the load combination of actions to be considered for Ultimate Limit States (ULS) and Serviceability Limit States (SLS) verifications in this numerical example are summarized on the following.

4.7.8.1. Ultimate Limit States (ULS)

The combined values of actions for ULS are performed for the cross sections at mid span and over pier, taking the group load model gr1a and the temperature, as leading variable actions. In addition, for the cross-section over pier two hypothesis are assumed, a hypothesis considering the values of the maximum moment and the concomitant shear, and other considering the concomitant moment and the maximum shear.

a) Leading variable action: gr1a

$$1,35 \times G_{K,\text{sup}} + 1,00 \times S + 1,35 \times (UDL_k + TS_k + q_{fk,\text{comb}})$$

b) Leading variable action: Temperature

$$1,35 \times G_{K,\text{sup}} + 1,00 \times S + 1,50 \times T_k + 1,35 \times (0,4 \times UDL_k + 0,75 \times TS_k + 0,4 \times q_{fk,\text{comb}})$$

- **Cross section at mid span**

a) Leading variable action: gr1a

$$\begin{aligned} M_{sd} &= 1,35 \times (766 + 3826 + 2988) \\ &\quad - (1,00 \times 4681) \\ &\quad + 1,35 \times (5618 + 7007 + 504) \\ &\quad + 1,5 \times 0,6 \times 3102 \\ &= 26068 \text{ kNm} \end{aligned}$$

$$V_{sd} = 1,35 \times (400) = 540 \text{ kN}$$

b) Leading variable action: Temperature

$$\begin{aligned} M_{sd} &= 1,35 \times (766 + 3826 + 2988) \\ &\quad - (1,00 \times 4681) + (1,50 \times 3102) \\ &\quad + 1,35 \times (0,4 \times 5618 + 0,75 \times 7007 + 0,4 \times 504) \\ &= 20606 \text{ kNm} \end{aligned}$$

$$V_{sd} = 1,35 \times (0,75 \times 400) = 405 \text{ kN}$$

- **Cross section over Pier**

- 1^a hypothesis: $M_{\max} - V_{\text{con}}$

a) Leading variable action: gr1a

b) Leading variable action: Temperature

$$\begin{aligned} M_{sd} &= 1,35 \times (-1484 - 7405 - 4902) \\ &\quad - (1,00 \times 4681) \\ &\quad + 1,35 \times (-5988 - 3217 - 536) \\ &\quad - 1,5 \times 0,6 \times 3102 \\ &= -3924 \text{ kNm} \end{aligned}$$

$$\begin{aligned} M_{sd} &= 1,35 \times (-1484 - 7405 - 4902) \\ &\quad - (1,00 \times 4681) + (1,50 \times (-3102)) \\ &\quad + 1,35 \times \left(\begin{array}{l} 0,4 \times (-5988) + 0,75 \times (-3217) \\ + 0,4 \times (-536) \end{array} \right) \\ &= -34732 \text{ kNm} \end{aligned}$$

$$\begin{aligned} V_{sd} &= 1,35 \times (180 + 899 + 631) \\ &\quad + 1,35 \times (808 + 516 + 72) \\ &= 4193 \text{ kN} \end{aligned}$$

$$\begin{aligned} V_{sd} &= 1,35 \times (180 + 899 + 631) \\ &\quad + 1,35 \times (0,75 \times 516 + 0,40 \times 808 + 0,4 \times 72) \\ &= 3306 \text{ kN} \end{aligned}$$

- 2^a hypothesis: $M_{\text{con}} - V_{\text{max}}$

a) Leading variable action: gr1a

b) Leading variable action: Temperature

$$\begin{aligned} M_{sd} &= 1,35 \times (-1484 - 7405 - 4902) \\ &\quad - (1,00 \times 4681) \\ &\quad + 1,35 \times (-5988 - 0 - 536) \\ &\quad - 1,5 \times 0,6 \times 3102 \\ &= -34898 \text{ kNm} \end{aligned}$$

$$\begin{aligned} M_{sd} &= 1,35 \times (-1484 - 7405 - 4902) \\ &\quad - (1,00 \times 4681) + (1,50 \times (-3102)) \\ &\quad + 1,35 \times (0,4 \times (-5988) + 0,4 \times (-536)) \\ &= -31475 \text{ kNm} \end{aligned}$$

$$\begin{aligned} V_{sd} &= 1,35 \times (180 + 899 + 631) \\ &\quad + 1,35 \times (808 + 800 + 72) \\ &= 4577 \text{ kN} \end{aligned}$$

$$\begin{aligned} V_{sd} &= 1,35 \times (180 + 899 + 631) \\ &\quad + 1,35 \times (0,75 \times 800 + 0,40 \times 808 + 0,4 \times 72) \\ &= 3594 \text{ kN} \end{aligned}$$

- Synthesis

Section	Actions	M (kNm)	V (kN)
Mid-span	M - V	26068	540
Over-Pier	$M_{\max} - V_{\text{con}}$	- 39241	4193
	$M_{\text{con}} - V_{\text{max}}$	- 34898	4577

Table 4-11 - Combined values at ULS

4.7.8.2. Serviceability Limit States (SLS)

Analogously to ULS, the combined values of actions for Serviceability Limit States are performed for the cross sections at mid span and over pier, which on its turn are divided into Characteristic SLS combination, Frequent SLS combination, and Quasi-permanent SLS combination.

- Characteristic SLS combination

a) Leading variable action: gr1a

$$G_{K,sup} + 1,00 \times S + (UDL_k + TS_k + q_{fk,comb}) + (0,6 \times T_k)$$

b) Leading variable action: Temperature

$$G_{K,sup} + 1,00 \times S + T_k + (0,4 \times UDL_k + 0,75 \times TS_k + 0,4 \times q_{fk,comb})$$

- Frequent SLS combination

a) Leading variable action: gr1a

$$G_{K,sup} + 1,00 \times S + 0,4 \times UDL + 0,75 \times TS_k + (0,5 \times T_k)$$

b) Leading variable action: Temperature

$$G_{K,sup} + 1,00 \times S + 0,6 \times T_k$$

- Quasi-permanent SLS Combination

$$G_{K,sup} + 1,00 \times S + 0,5 \times T_k$$

- Synthesis

	Section	Actions	M (kNm)	V (kN)
Characteristic Combination	Mid-span	M - V	17889	400
	Over-Pier	$M_{max} - V_{con}$	- 30074	3106
		$M_{con} - V_{max}$	- 26857	3390
Frequent Combination	Mid-span	M - V	11952,45	300
	Over-Pier	$M_{max} - V_{con}$	- 24831	- 2420
		$M_{con} - V_{max}$	- 22418	2633
Quasi – Permanent	Mid-span	M - V	4450	- 2023
	Over-Pier	M- V	0	1710

Table 4-12 - Combined values at SLS

4.8. Verification by Ultimate Limit States (ULS)

The verification of structural safety of the bridge for Ultimate Limit States, should be carried out, taking the clauses of Chapter 6 of (EN 1994-2, 2005) into account. Considering the values of combined loads determined on 4.7.8.1, the following parameters are checked on this section:

- Verification of structural safety in bending, which is preceded by determination of the class of cross section, in order to examine whether the bending resistance of cross section may be determined by an elastic or plastic analysis;
- Verification of structural safety in shear;
- Verification of bending moment and shear force (M-V) interaction.

4.8.1. Cross section at Mid-span

4.8.1.1. Verification of structural safety in bending

- Classification of cross section
 - Top flange (compression)

Considering that after concrete casting, the top flanges are rigidly connected to the concrete slab through the shear connectors (providing the spacing of connectors is appropriately selected), the steel top flange, which is attached to the slab may be classified as class 1, since concrete prevents its local buckling.

- Web

- Design resistance of concrete slab

$$\begin{aligned} N_c &= h_c \times b_{eff} \times f_{cd} \\ &= 0,25 \times 5,75 \times \left(0,85 \times \frac{35 \times 10^3}{1,5} \right) \\ &= 28510,42 \text{ kN} \end{aligned}$$

- Design resistance of structural steel

$$\begin{aligned} N_s &= A_s \times f_{yd} \\ &= [(0,5 \times 0,045) + (0,7 \times 0,05)] \times \left(\frac{430 \times 10^3}{1,0} \right) \\ &\quad + (2,03 \times 0,012) \times \left(\frac{355 \times 10^3}{1,0} \right) = 33373 \text{ kN} \end{aligned}$$

- Location of the neutral plastic axis

$$\begin{aligned} &2 \times b_f \times t_f \times \frac{f_y}{\gamma_a} \\ &= 2 \times 0,5 \times 0,045 \times \frac{355 \times 10^3}{1,0} = 15975 \text{ kN} \end{aligned}$$

$$N_c < N_s \rightarrow 28510 < 33373$$

$$N_s - N_c < 2 \times b_f \times t_f \times f_y / \gamma_a \rightarrow 4863 < 19350$$

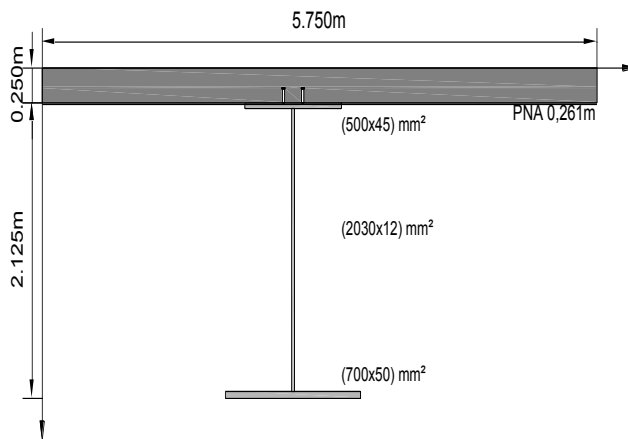
From the above conditions, it can be inferred that the plastic neutral axis is located in the thickness of the upper steel flange, which means that the web is subjected only to tensile stress, and therefore is class 1.

Thus, the cross section at mid-span can be classified as class 1.

- Bending resistance of section

- Location of the neutral plastic axis

Taking into consideration that the neutral plastic axis is located in the thickness of the steel flange, the distance at which plastic neutral axis lies below the top of concrete flange is determined by the following:



$$N_c = 28510,42kN$$

$$N_{fl} = 0,5 \times 0,045 \times \frac{430 \times 10^3}{1,0} = 9675kN$$

$$N_w = 0,012 \times 2,03 \times \frac{355 \times 10^3}{1,0} = 8647,8kN$$

$$N_{bfl} = 0,7 \times 0,05 \times \frac{430 \times 10^3}{1,0} = 15050kN$$

Figure 4-10 – Location of plastic neutral axis

$$28510,42 + (9675 \times x) = (1 - x) \times 9675 + 8647,8 + 15050 \Leftrightarrow x = 0,251$$

$$PNA = 0,25 + (0,045 \times 0,251) = 0,261m \text{ (Below the top flange)}$$

- Design plastic resistance moment (relative to the centre of lower flange)

$$M_{pl,Rd} = (28510,42 \times 0,136) + (9675 \times 0,251 \times 0,0055) + ((1 - 0,251) \times 9675 \times 0,017) + (8647,8 \times 1,049) + (15050 \times 2,089) = 44525kN$$

- Bending resistance check

Since $M_{Ed} = 26068 \text{ kN} < M_{pl,Rd} = 44525 \text{ kN}$, the bending resistance of section at mid-span is verified.

4.8.1.2. Verification of structural safety in shear

According to clause 5.1 (2) of (EN 1993-1-5, 2006), the web (provided by stiffeners) should be checked in terms of shear buckling, if the width to thickness ratio of the web is higher than the following value:

$$\left(\frac{h_w}{t}\right) > \frac{31}{\eta} \varepsilon \sqrt{k_\tau}$$

For the section at mid-span:

$$\begin{aligned} a_w &= 3125 \text{ mm} & a_w / h_w &= 1,539 \\ t_w &= 12 \text{ mm} & \eta &= 1,20 \text{ (recommended value)} \\ h_w &= 2030 \text{ mm} & \varepsilon &= \sqrt{\frac{235}{355}} = 0,814 \\ f_y &= 355 \text{ MPa} \end{aligned}$$

Since $a_w / h_w > 1$ and there are no longitudinal stiffeners:

$$\begin{aligned} k_\tau &= 5,34 + 4,00(h_w / a)^2 \\ k_\tau &= 5,34 + 4,00(2030/3125)^2 = 7,028 \end{aligned}$$

Thus:

$$\frac{h_w}{t} = \frac{2300}{12} = 169,2 \qquad \frac{31}{\eta} \varepsilon \sqrt{k_\tau} = \frac{31}{1,2} \times 0,814 \times \sqrt{7,028} = 55,7$$

Since $169,2 > 55,7$, the shear buckling resistance of the web needs to be verified. According to clause 5.2 of (EN 1993-1-5, 2006) the design shear resistance is obtained considering the contribution of the web and the contribution of the flanges, as follows:

$$V_{b,Rd} = V_{bw,Rd} + V_{bf,Rd} \leq \frac{\eta \times f_{yw} \times h_w \times t}{\sqrt{3} \times \gamma_{M1}}$$

- Web contribution

The procedure to determine the contribution of the web is performed below. It is determined by clause 5.2 of (EN 1993-1-5, 2006), which on its turn, makes reference to Annex A.1 (2), Table 5.1 and clause 5.3 (3) of (EN 1993-1-5, 2006), as represented on the following:

$$V_{bw,Rd} = \frac{\chi_w \times f_{yw} \times h_w \times t_w}{\sqrt{3} \times \gamma_{M1}}$$

Where:

χ_w is the reduction factor for shear, which depends of the nondimensional slenderness for shear $\bar{\lambda}_w$;

- Elastic critical shear buckling stress (EN 1993-1-5, A.1(2)):

$$\tau_{cr} = k_\tau \times \sigma_E$$

$$\sigma_E = \frac{\pi^2 \times E \times t_w^2}{12 \times (1 - \nu^2) \times h_w^2} = \frac{\pi^2 \times 210 \times 10^3 \times 12^2}{12 \times (1 - 0,3^2) \times 2030^2} = 6,63 \text{ N/mm}^2$$

Then:

$$\tau_{cr} = k_\tau \times \sigma_E = 7,028 \times 6,63 = 46,6 \text{ N/mm}^2$$

- Nondimensional slenderness parameter (EN 1993-1-5, 5.3(3)):

$$\bar{\lambda}_w = 0,76 \times \sqrt{\frac{f_y}{\tau_{cr}}} = 0,76 \times \sqrt{\frac{355}{46,6}} = 2,10 > 1,08$$

Since the slenderness parameter $\bar{\lambda}_w > 1,08$ the contribution to shear buckling resistance is given by:

$$\chi_w = \frac{1,37}{0,7 + \bar{\lambda}_w} = \frac{1,37}{0,7 + 2,10} = 0,49$$

γ_{M1} is a partial factor equal to 1,1

Thus:

$$V_{bw,Rd} = \frac{0,49 \times 355 \times 2030 \times 12}{\sqrt{3} \times 1,1} \times 10^{-3} = 2224 \text{ kN}$$

- Flange contribution

Analogously to the determination of the web contribution, on the following lines, the flange contribution is to be performed.

It is determined by clause 5.4 of (EN 1993-1-5, 2006), as described on the following:

$$V_{bf,Rd} = \frac{b_f \times t_f^2 \times f_{yf}}{c \times \gamma_{M1}} \times \left(1 - \left(\frac{M_{Ed}}{M_{f,Rd}} \right)^2 \right)$$

Where:

$M_{f,Rd}$ is the moment of resistance of the cross section consisting of the effective area of the flanges only;

- The axial resistance of the composite flange taking into account the modular ratio for short-term loading is:

$$N_{Rd} = \left(\frac{5,75 \times 0,25}{6,2} \times \frac{35 \times 10^3}{1,5} \right) + \left(0,5 \times 0,045 \times \frac{430 \times 10^3}{1,0} \right) = 15084,9 \text{ kN}$$

- And the axial resistance of the bottom flange is:

$$N_{Rd} = \left(0,7 \times 0,05 \times \frac{430 \times 10^3}{1,0} \right) = 15050 \text{ kN}$$

- The lever arm between top and bottom is determined by:

$$y_G = \frac{\frac{5,75 \times 0,25 \times 0,125}{6,2} + 0,5 \times 0,045 \times 0,2725}{\frac{5,75 \times 0,25}{6,2} + 0,5 \times 0,04} = 0,139 \text{ m}$$

$$h = 0,25 + 2,12 - 0,139 - (0,05/2) = 2,206 \text{ m}$$

Thus, according to (EN 1994-2, 2005) (5.2), the moment of resistance of the effective area of the flanges, is obtained taking into account the bottom flange, since it corresponds to a smaller resistant moment.

$$M_{f,Rd} = 15050 \times 2,206 = 33200 \text{ kN}$$

c is obtained by (EN 1993-1-5, 2006), (5.4), as follow:

$$c = a \times \left(0,25 + \frac{1,6 \times b_f \times t_f^2 \times f_{yf}}{t \times h_w^2 \times f_{yw}} \right)$$

$$c = 3,125 \times \left(0,25 + \frac{1,6 \times 700 \times 50^2 \times 430}{12 \times 2030^2 \times 355} \right) = 996 \text{ mm}$$

Then:

$$V_{bf,Rd} = \frac{700 \times 50^2 \times 430}{996 \times 1,1} \times \left(1 - \left(\frac{26068}{33200} \right)^2 \right) = 263 \text{ kN}$$

- Shear resistance

As it can be inferred by the above lines, the shear resistance is equal to:

$$V_{b,Rd} = 2224 + 263 \leq \frac{1,2 \times 355 \times 2030 \times 12}{\sqrt{3} \times 1,1}$$

$$V_{b,Rd} = 2487 \leq 5446,7$$

Since $V_{Ed} = 540 \text{ kN} < V_{b,Rd} = 2487 \text{ kN}$, the shear resistance of section at mid-span is verified.

4.8.1.3. Verification of M-V interaction

The interaction between shear force and bending moment is performed by Clause 7.1 of (EN 1993-1-5, 2006).

$$\bar{\eta}_3 = \frac{V_{Ed}}{V_{Rd}} = \frac{540}{2487} = 0,22$$

Since the above condition does not exceed 0,5, the design resistance to bending does not need to be reduced.

4.8.2. Cross section over pier

4.8.2.1. Verification of structural safety in bending

- Classification of cross section
 - Bottom flange (compression)

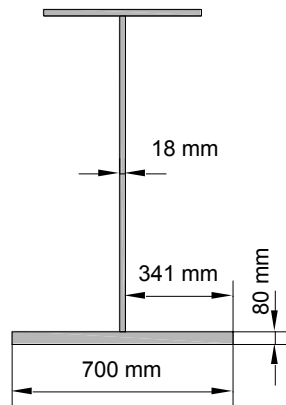


Figure 4-11 - Bottom flange geometry

$$t_f = 80 \text{ mm}$$

$$c = \left(\frac{700 - 18}{2} \right) = 341 \text{ mm}$$

$$\varepsilon = \sqrt{\frac{235}{430}} = 0,739$$

$$\frac{c}{t_f} = \frac{341}{80} = 4,26$$

$$10 \times \varepsilon = 73,9$$

Since the following condition is satisfied, ($c/t = 4,26 < 10\varepsilon = 73,9$) the bottom flange is classified as class 1.

- Web

For $t_f = 18$ mm, the yield strength is $f_y = 355$ N/mm². Thus the width to thickness ratio, and the coefficient ε , are:

$$\frac{h_w}{t_w} = \frac{2000}{18} = 111,1$$

$$\varepsilon = \sqrt{\frac{235}{355}} = 0,81$$

The web of the section over pier is in tension on its upper part and in compression on its lower part. Therefore, it is necessary to determine the position of the Plastic Neutral Axis (PNA), which is deduced by equalizing the axial forces from tension and compression zones.

Since the concrete slab is cracked, it is necessary to consider the design resistance of the reinforcing steel bars, for an effective section equal to 5,3 m, as defined on section 4.6.

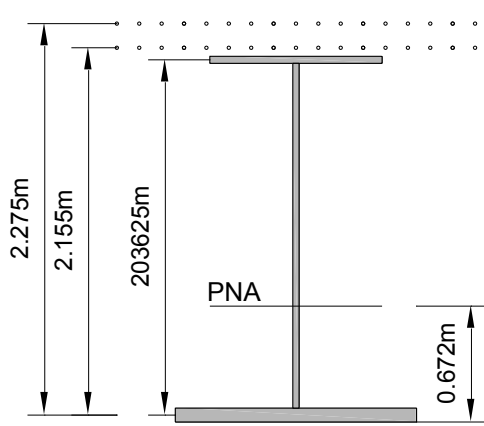


Figure 4-12 - Location of plastic neutral axis

$$N_{\phi Top} = 41 \times 314,16 \times \frac{500}{1,15} \times 10^{-3} = 5600 \text{ kN}$$

$$N_{\phi Bottom} = 41 \times 201,06 \times \frac{500}{1,15} \times 10^{-3} = 3584 \text{ kN}$$

$$N_{TopFl} = 500 \times 45 \times \frac{430}{1,0} \times 10^{-3} = 9675 \text{ kN}$$

$$N_{Web} = 2000 \times 18 \times \frac{355}{1,0} \times 10^{-3} = 12780 \text{ kN}$$

$$N_{BottomFl} = 700 \times 80 \times \frac{430}{1,0} \times 10^{-3} = 24080 \text{ kN}$$

$$5600 + 3584 + 9675 + (12780 \times x) = (1 - x) \times 12780 + 24080 \Leftrightarrow x = 0,704$$

$$PNA = 80 + 2000 \times (1 - 0,704) = 672 \text{ mm (Above the bottom flange)}$$

According to Table 5.2 of (EN 1993-1-1, 2005), for $\alpha = 1 - 0,704 = 0,296$, and taking into consideration the following condition, the web is classified as Class 2.

$$\frac{h_w}{t_w} = 111,1 \leq 41,5 \times \frac{\epsilon}{\alpha} = 41,5 \times \frac{0,81}{0,296} = 114$$

Therefore, the cross-section is Class 2.

- Bending resistance of section

- Design resistance moment

$$M_{pl,Rd} = -(5600 \times 2,275) - (3584 \times 2,155) - (9675 \times 2,063) - (12780 \times 1,336 \times 0,704) + (12780 \times (1 - 0,704) \times 0,336)$$

$$M_{pl,Rd} = -51172 \text{ kNm}$$

- Bending resistance check

Since $M_{Ed} = -39241 \text{ kN} < M_{pl,Rd} = -51172 \text{ kN}$, the bending resistance of the pier section is verified.

4.8.2.2. Verification of structural safety in shear

According to clause 5.1 (2) of (EN 1993-1-5, 2006), the web (provided by stiffeners) should be checked in terms of shear buckling, if the width to thickness ratio of the web is higher than the following value:

$$\left(\frac{h_w}{t}\right) > \frac{31}{\eta} \varepsilon \sqrt{k_\tau}$$

For the section at support:

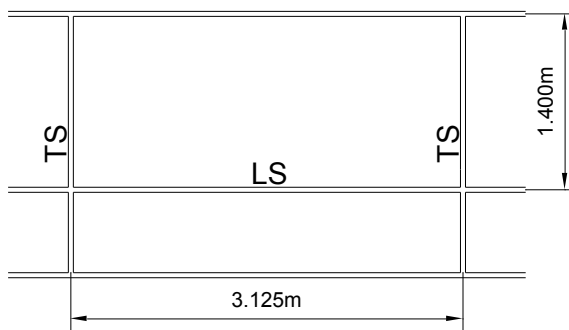


Figure 4-13 -Transverse and longitudinal stiffeners spacing

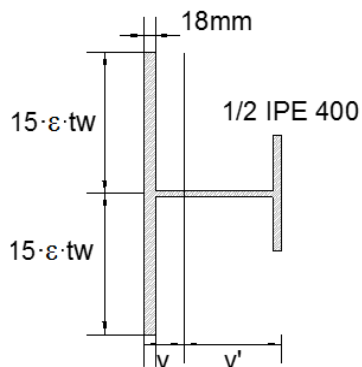
$$\begin{aligned} a &= 3125 \text{ mm} \\ t_w &= 18 \text{ mm} \\ h_w &= 2000 \text{ mm} \\ f_y &= 355 \text{ MPa} \\ a_w/t_w &= 1,56 \\ \eta &= 1,20 \text{ (recommended value)} \end{aligned}$$

$$\varepsilon = \sqrt{\frac{235}{355}} = 0,814$$

Since $a_w / h_w > 1$ and there is a longitudinal stiffener:

$$k_\tau = 5,34 + 4,00 \times (h_w / a)^2 + k_{sl}$$

Where:



$$I_{sl} = 8509 \text{ cm}^4$$

$$A = 119 \text{ cm}^2$$

$$v = 6,4 \text{ cm}$$

$$v' = 15,4 \text{ cm}$$

$$k_{sl} = \max \left(9 \times \left(\frac{h_w}{a}\right)^2 \times \sqrt[4]{\left(\frac{I_{sl}}{t^3 \times h_w}\right)^3}; \frac{2,1}{t} \times \sqrt[3]{\frac{I_{sl}}{h_w}} \right)$$

$$k_{sl} = \max \left(9 \times \left(\frac{2000}{3125}\right)^2 \times \sqrt[4]{\left(\frac{8509 \times 10^4}{18^3 \times 2000}\right)^3}; \frac{2,1}{18} \times \sqrt[3]{\frac{8509 \times 10^4}{2000}} \right)$$

$$k_{sl} = \max(16,4; 4,1) = 16,4$$

Thus:

$$k_{\tau} = 5,34 + 4,00(2000/3125)^2 + 16,4 = 23,4$$

Then:

$$\frac{h_w}{t} = \frac{2000}{18} = 111,1 \qquad \frac{31}{\eta} \varepsilon \sqrt{k_{\tau}} = \frac{31}{1,2} \times 0,814 \times \sqrt{23,4} = 101,7$$

Since $111,1 > 101,7$ the shear buckling resistance of the web needs to be verified. According to clause 5.2 from (EN 1993-1-5, 2006) the design shear resistance is obtained considering the contribution of the web and the contribution of the flanges, as follows:

$$V_{b,Rd} = V_{bw,Rd} + V_{bf,Rd} \leq \frac{\eta \times f_{yw} \times h_w \times t}{\sqrt{3} \times \gamma_{M1}}$$

- Web contribution

The procedure to performer the contribution of the web is described by clause 5.2, of (EN 1993-1-5, 2006), as represented in the following:

$$V_{bw,Rd} = \frac{\chi_w \times f_{yw} \times h_w \times t_w}{\sqrt{3} \times \gamma_{M1}}$$

Where:

χ_w is the reduction factor for shear, which depends of the nondimensional slenderness for shear $\bar{\lambda}_w$;

- Shear buckling coefficient for intermediate section h_{w1} (EN 1993-1-5, 2006), (A.3):

$$\frac{a}{h_{w1}} = \frac{3125}{1400} = 2,23$$

Since the above condition is higher than 1:

$$k_{\tau} = 5,34 + 4,00 \left(\frac{1400}{3125} \right)^2 = 6,14$$

- Nondimensional slenderness parameter for web with longitudinal stiffeners (EN 1993-1-5, 5.3(3)):

$$\bar{\lambda}_w = \frac{h_{wi}}{37,4 \times t \times \varepsilon \times \sqrt{k_{\tau i}}}$$

$$\bar{\lambda}_w = \max\left(\frac{2000}{37,4 \times 18 \times 0,81 \times \sqrt{23,4}}; \frac{1400}{37,4 \times 18 \times 0,81 \times \sqrt{6,14}}\right)$$

$$\bar{\lambda}_w = \max(0,76; 1,04) = 1,04$$

Since $0,83/\eta \leq \bar{\lambda}_w < 1,08$, according to Table 5.1, from (EN 1993-1-5, 2006),

the contribution from the web χ_w is given by:

$$\chi_w = \frac{0,83}{\bar{\lambda}_w} = \frac{0,83}{1,04} = 0,80$$

Thus:

$$V_{bw,Rd} = \frac{\chi_w \times f_{yw} \times h_w \times t_w}{\sqrt{3} \times \gamma_{M1}} = \frac{0,80 \times 355 \times 2000 \times 18}{\sqrt{3} \times 1,1} \times 10^{-3} = 5366 \text{ kN}$$

- Flange contribution

Analogously to the determination of the web contribution, on the following lines, it is performed the flange contribution, which is determined by clause 5.4 of (EN 1993-1-5, 2006), as represented on the following:

$$V_{bf,Rd} = \frac{b_f \times t_f^2 \times f_{yf}}{c \times \gamma_{M1}} \times \left(1 - \left(\frac{M_{Ed}}{M_{f,Rd}}\right)^2\right)$$

Where:

$M_{f,Rd}$ is the moment of resistance of the cross section consisting of the effective area of the flanges only;

- The axial resistance of the top bars and top flange is:

$$N_{Rd} = \left((12881 + 8244) \times 10^{-6} \times \frac{500 \times 10^3}{1,15} \right) + \left((500 \times 45) \times 10^{-6} \times \frac{430 \times 10^3}{1,0} \right)$$

$$= 18860 \text{ kN}$$

- And the axial resistance of the bottom flange is:

$$N_{Rd} = \left((700 \times 80) \times 10^{-6} \times \frac{430 \times 10^3}{1,0} \right) = 24080 \text{ kN}$$

- The lever arm between top and bottom is determined by:

$$y_G = \frac{(12881 \times 60) + (8244 \times 177) + (500 \times 45 \times 272,5)}{12881 + 8244 + (500 \times 45)} = 0,192 \text{ m}$$

$$h = 0,25 + 2,125 - 0,192 - (0,08/2) = 2,143 \text{ m}$$

Thus, according to (EN 1993-1-5, 2006) (6.5.2), the moment of resistance of the effective area of the flanges, is obtained taking into account the top flange considering the top bars and top steel flange, since it corresponds to a smaller resistant moment.

$$M_{f,Rd} = 18860 \times 2,143 = 40417 \text{ kN}$$

c is obtained by (EN 1993-1-5, 2006) (5.4). Since the upper flange is a composite flange (steel reinforcement and steel upper flange), the lower steel flange is taken in consideration, in order to evaluate the contribution of the flange to the shear resistance. Thus:

$$c = a \times \left(0,25 + \frac{1,6 \times b_f \times t_f^2 \times f_{yf}}{t \times h_w^2 \times f_{yw}} \right)$$

$$c = 3125 \times \left(0,25 + \frac{1,6 \times 700 \times 80^2 \times 430}{18 \times 2000^2 \times 355} \right) = 1158 \text{ mm}$$

Then:

$$V_{bf,Rd} = \frac{700 \times 80^2 \times 430}{1158 \times 1,1} \times \left(1 - \left(\frac{39241}{40417} \right)^2 \right) = 87 \text{ kN}$$

- Shear resistance

As noted by the above lines, the shear resistance is equal to:

$$V_{b,Rd} = 5366 + 87 \leq \frac{1,2 \times 355 \times 2000 \times 18}{\sqrt{3} \times 1,1}$$

$$V_{b,Rd} = 5453 \leq 8049,3$$

Since $V_{Ed} = 4577 \text{ kN} < V_{b,Rd} = 5453 \text{ kN}$, the shear resistance of section at mid-span is verified.

4.8.2.3. Verification of M-V interaction

The interaction between shear force and bending moment is performed by Clause 7.1 of (EN 1993-1-5, 2006). Thus:

$$\bar{\eta}_3 = \frac{V_{Ed}}{V_{Rd}} = \frac{4577}{5453} = 0,84$$

Since the above condition exceeds 0,5, the combined effects of bending and shear in the web of the cross section should satisfy the following condition:

$$\bar{\eta}_1 + \left(1 - \frac{M_{f,Rd}}{M_{pl,Rd}}\right) (2\bar{\eta}_3 - 1)^2 \leq 1,0$$

Where:

$M_{f,Rd}$ is the design plastic moment of resistance of the section consisting of the effective area of the flanges;

$M_{pl,Rd}$ is the design plastic resistance of the cross section consisting of the effective area of the flanges and the fully effective web irrespective of its section class;

$$\bar{\eta}_1 = \frac{M_{Ed}}{M_{pl,Rd}};$$

$$\bar{\eta}_3 = \frac{V_{Ed}}{V_{b,Rd}}.$$

- Maximum moment with concomitant shear

$$\bar{\eta}_1 = \frac{39241}{51172} = 0,77 \qquad \bar{\eta}_3 = \frac{4193}{5453} = 0,77$$

$$0,77 + \left(1 - \frac{40417}{51172}\right) (2 \times 0,77 - 1)^2 = 0,83 < 1,0$$

- Maximum shear with concomitant moment

$$\bar{\eta}_1 = \frac{34898}{51172} = 0,68 \qquad \bar{\eta}_3 = \frac{4577}{5453} = 0,84$$

$$0,68 + \left(1 - \frac{40417}{51172}\right) (2 \times 0,84 - 1)^2 = 0,77 < 1,0$$

Since the above conditions does not exceed 1,0, the design resistance to bending does not need to be reduced.

4.8.3. Lateral torsional buckling

The resistance to the lateral torsional buckling of the compression flanges of in-plane loaded girders is carried out according to clause 6.4 of (EN 1994-2, 2005). Since the top flanges are connected to concrete slab, which provides lateral restraint, this element is not susceptible to lateral torsional buckling. Taking this into consideration, only bottom flanges at internal supports are susceptible to lateral deformations. The only exception may occur before concrete casting, where the top flange is not connected with concrete slab, and this element may deform laterally.

(EN 1993-2, 2006), proposes two approaches to calculate the lateral torsional buckling, a simplified method, and a general method. Since the general method requires a software which performs critical load calculations, and bearing in mind the purpose of this numerical example, on the following, the simplified method during construction is performed.

4.8.3.1. Rigidity C_d of bracing transverse frames

Figure 4-14 shows the structural form of cross section with cross bracing, including the notations defining the modelled transverse frame, for the present numerical example.

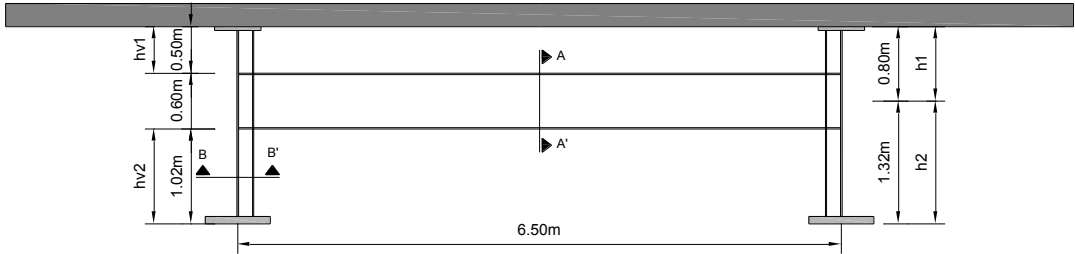


Figure 4-14 - Notations defining the modelled transverse frame

The rigidity C_d of bracing transverse frames may be determined by application of a transverse force ($H = 1$) at the ends of the cross frames, which can lead to a symmetric or antisymmetric loaded cross bracing, as illustrated in Figure 4-15.

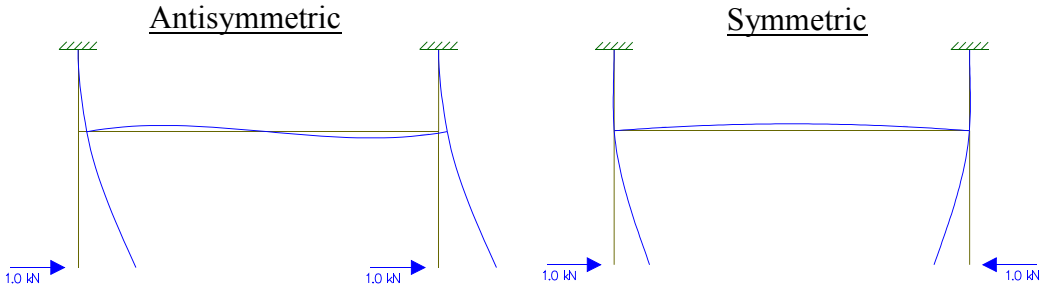


Figure 4-15 - Load cases modelling for the rigidity C_d calculation

On its turn, the rigidity C_d , is performed by the following equation:

$$C_d = \frac{H}{\delta} = \frac{1}{\delta}$$

Taking this into account, and as it can be observed by Figure 4-15, the symmetric loaded cross bracing corresponds to the most unfavourable load case for the rigidity C_d calculation. Thus, and in accordance with Annex D of EN 1993-2, this rigidity is determined by:

$$C_d = \frac{E \times I_v}{\frac{h_v^3}{3} + \frac{h^2 \times b_q \times I_v}{2 \times I_q}}$$

- Cross section properties

- Section AA'

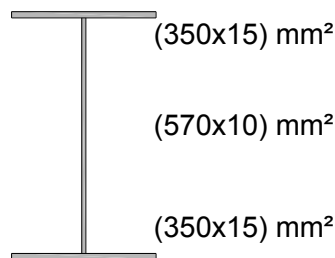


Figure 4-16 - Geometric properties of section AA'

$$A_q = 16200 \text{ mm}^2$$

$$I_q = 1053 \times 10^6 \text{ mm}^4$$

$$EI_q = 221102 \text{ kNm}^2$$

- Section BB'

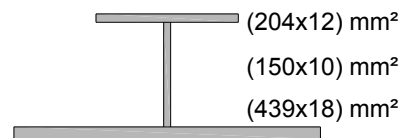


Figure 4-17 - Geometric properties of section BB'

$$A_v = 11856 \text{ mm}^2$$

$$I_q = 57 \times 10^6 \text{ mm}^4$$

$$EI_q = 11886 \text{ kNm}^2$$

- Upper chord (only during construction)

$$C_d = \frac{11886}{\frac{0,8^3}{3} + \frac{0,8^2 \times 6,50 \times 57 \times 10^6}{2 \times 1053 \times 10^6}} = 41962 \text{ kN/m}$$

- Lower chord

$$C_d = \frac{11886}{\frac{1,325^3}{3} + \frac{1,325^2 \times 6,50 \times 57 \times 10^6}{2 \times 1053 \times 10^6}} = 10962 \text{ kN/m}$$

4.8.3.2. Simplified method

The simplified method is performed by clause 6.3.4.2 and Annex D2.4 of (EN 1993-2, 2006). This method may be used to verify the resistance to lateral torsional buckling, assuming a uniform cross-section and a uniform load over the whole length of the deck, as well as a uniformly distributed lateral spring support in span.

Taking this into account, as well as the geometric properties of the sections (section 4.7.4), this method is implemented to check the lateral torsional buckling resistance of the upper chord, which corresponds to a plate with constant geometric properties (500 x 450 mm). It is performed for the principal span, treating this one as a uniform compressed member. This assumptions is thus safe-side.

The resistance to lateral torsional buckling of the lower chord is not checked with simplified method, since the flange cross-section geometry is not constant, and the compressed part is limited to the zones around the piers.

Thus, for the principal span:

$L = 50 \text{ m}$ span length between the rigid supports;

$l = 6,25 \text{ m}$ distance between the springs.

The critical axial load N_{crit} , considering the compressive force N_{Ed} constant over the length of the chord, is calculated by EN 1993-2, 6.3.4.2 (6) as described on the following:

$$N_{crit} = m \times N_E$$

Where:

m is given by EN 1993-2, 6.3.4.2(6), as represented in the following:

$$c = \frac{C_d}{l} = \frac{41962}{6,25} = 6714$$

$$I = \frac{0,045 \times 0,5^3}{12} = 468,8 \times 10^{-6}$$

$$\gamma = \frac{c \times L^4}{E \times I} = \frac{6714 \times 50^4}{210 \times 10^6 \times 468,8 \times 10^{-6}} = 426240$$

$$m = \frac{2}{\pi^2} \sqrt{\gamma} = \frac{2}{\pi^2} \sqrt{426240} = 132,30$$

N_E is determined by EN 1993-2, 6.3.4.2(6), as described in the following:

$$N_E = \pi^2 \times \frac{E \times I}{L^2} = \pi^2 \times \frac{210 \times 10^6 \times 468,8 \times 10^{-6}}{50^2} = 388,6 \text{ kN}$$

Thus:

$$N_{crit} = 132,30 \times 388,6 = 51412 \text{ kN}$$

The critical buckling length of the system on elastic supports is given by:

$$l_k = \pi \times \sqrt{\frac{E \times I}{N_{crit}}} = \pi \times \sqrt{\frac{210 \times 10^6 \times 416,7 \times 10^{-6}}{48484}} = 4,35m < l$$

Since the critical buckling length cannot be less than the distance between the sprigs, for $L = l = 6,25$ m, N_{crit} is assumed to be equal to:

$$N_{crit} = \pi^2 \times \frac{210 \times 10^6 \times 468,8 \times 10^{-6}}{6,25^2} = 24874kN$$

In addition, the effect of initial imperfections and second order effects on a support spring, are taken into account by applying an additional lateral force F_{Ed} at the connection of the chord to the spring equal to:

$$F_{sd} = \frac{N_{sd}}{100}, \text{ (since } l_k \leq 1,20 \times l \text{)}$$

Thus:

- Pier section (Tension zone)

$$M_d = -1,35 \times (1484 + 7405 + 2072) = -14797,4kNm$$

$$\sigma_{top} = \frac{14797,4 \times 1,353}{0,085} \times 10^{-3} = 235,5MPa$$

- Mid-span section (Compressed zone)

$$M_d = -1,35 \times (766 + 3826 + 1071) = 7646,4kNm$$

$$\sigma_{top} = -\frac{7646,4 \times 1,219}{0,068} \times 10^{-3} = -137,1MPa$$

Taking into consideration the compression zone in mid-span:

$$N_{sd} = \sigma_{Top} \times A_f = -137,1 \times (500 \times 45) \times 10^{-3} = -3085kN$$

$$F_{sd} = \frac{N_{sd}}{100} = \frac{-3085}{100} = -30,85kN$$

On its turn, the safety verification may be carried out, considering the slenderness parameter defined by the following:

$$\bar{\lambda}_{LT} = \sqrt{\frac{A_{eff} \times f_y}{N_{crit}}}$$

Where:

A_{eff} is the effective area of the chord, given by EN 1993-2, 6.3.4.2 (7):

$$A_{eff} = A_f + \frac{A_{wc}}{3}$$

$$A_{eff} = (500 \times 45) + \frac{(12 \times (1219 - 45))}{3} \times 10^{-6} = 0,027 m^2$$

N_{crit} is the elastic critical load of the column for out-of-plane buckling:

Thus:

$$\bar{\lambda}_{LT} = \sqrt{\frac{0,027 \times 430 \times 10^3}{24874}} = 0,68$$

The reduction factor for lateral torsional buckling may be determined from clause 6.3.2.3 of (EN 1993-1-1, 2005), as presented in the following:

$$\chi_{LT} = \frac{1}{\phi_{LT} + \sqrt{\phi_{LT}^2 - \bar{\lambda}_{LT}^2}} \leq 1$$

Where:

ϕ_{LT} is given by:

$$\phi_{LT} = 0,5 \times [1 + \alpha_{LT} \times (\bar{\lambda}_{LT} - 0,2) + \bar{\lambda}_{LT}^2]$$

$$\phi_{LT} = 0,5 \times [1 + 0,49 \times (0,68 - 0,2) + 0,68^2]$$

$$\phi_{LT} = 0,85$$

α_{LT} is an imperfection factor, determined by Table 6.3 of (EN 1993-1-1, 2005).

For a Welded I-section with a buckling curve C, it is taken equal to 0,49.

Then:

$$\chi_{LT} = \frac{1}{0,85 + \sqrt{0,85^2 - 0,68^2}} = 0,74$$

$$N_u = \chi_{LT} \times A_{eff} \times \frac{f_y}{\gamma} = 0,74 \times 1,0 \times 0,027 \times \frac{430 \times 10^3}{1,1} = 7810 kN$$

Since $N_{Sd} = 3085 \text{ kN} < N_u = 7810 \text{ kN}$, the lateral torsional buckling of upper chord, considering the hypothesis of constant compression is verified.

4.9. Verification of Serviceability Limit States (SLS)

According to clause 3.4 of (EN 1990, 2002), Serviceability Limit States concern the functioning of the structure and its structural members under normal use, the comfort of people, as well as the appearance of the bridge, in such a way, that it avoid excessive deformations, and cracking of the concrete slab.

Thus, at Serviceability Limit State under global longitudinal bending, the following parameters have been checked:

- Deflection control;
- Stress limitations for structural steel, reinforcement, and concrete;
- Control of cracking for concrete.

4.9.1. Deflections

As it was already explained in 3.7.2, there exist no limit deflection on Eurocodes for road bridge so that such limits must be agreed with the owner of the bridge, or by reference to other sources. Thus, as indicated in that section, the limiting value of $(L/1200)$ related to the overload for frequent SLS combination of actions, has been adopted as the representative value to check the deformation of the bridge analysed in this numerical example. Then:

- Deflection value due to overload

Uniform distribute load UDL: 31,3 mm

Heavy vehicle Tsk: 28,3 mm

- Frequent SLS combination of actions

$$(31,3 \times 0,4) + (28,3 \times 0,75) = 33,75 \text{ mm}$$

- Limiting value

$$33,75 \text{ mm} < L/1200 = 41,67 \text{ mm}$$

4.9.2. Stress limitations

As it can be inferred by 3.7.1, the stress levels at SLS are verified for the characteristic SLS combination of actions, in order to ensure the bridge functioning under normal use and the comfort of users, limiting the deformations affecting the appearance and its vibrations, as well as to control the damage affecting its appearance, durability or its

functioning. On the following, the stress limitations refer to the structural steel and, concrete slab, and steel reinforcement are to be determined.

4.9.2.1. Structural steel

The stress limiting values for the characteristic SLS combination of actions are defined by clause 7.2.2 of (EN 1994-2, 2005), which on its turn refers to (EN 1993-2, 7.3). Thus, in order to ensure the elastic behaviour under service loads, the design stresses of structural steel, should be limited as follows:

- Direct stresses:

$$\sigma_{Ed,ser} \leq \frac{f_y}{\gamma_{M,ser}}$$

- Shear stresses:

$$\tau_{Ed,ser} \leq \frac{f_y}{\sqrt{3} \times \gamma_{M,ser}}$$

- Von Misses stresses:

$$\sqrt{\sigma_{Ed,ser}^2 + 3 \times \tau_{Ed,ser}^2} \leq \frac{f_y}{\gamma_{M,ser}}$$

Taking the aforementioned considerations, the stresses in the structural steel under characteristic SLS combination of actions obtained for each loading form, are summarised on the following table. It corresponds to the stresses in the top of upper flange, and to the stresses in bottom of the lower flange, obtained for the section over pier, considering the mechanical properties of the cracked section.

	M (kNm)	V (kN)	S (m³)	τ (N/mm²)	W_{top} (m³)	σ_{top} (kN/m²)	W_{bottom} (m³)	σ_{bottom} (kN/m²)
Steel	1484	180	0,045	5314,07	0,063	23537,93	0,110	13438,06
Concrete	7405	899	0,045	26540,81	0,063	117451,72	0,110	67054,47
Dead t=0	4555	631	0,045	18628,75	0,117	38992,27	0,126	36290,83
Load t=∞	4902	631	0,045	18628,75	0,117	41962,70	0,126	39055,47
UDL	5988	808	0,045	23854,25	0,117	51259,21	0,126	47707,90
TS	3217	516	0,045	15233,66	0,117	27538,56	0,126	25630,65
Pedestrian	536	72	0,045	2125,63	0,117	4588,33	0,126	4270,45
Thermal	3102	0	0,045	0,00	0,117	26554,12	0,126	24714,41
Shrinkage	4681	0	0,045	0,00	0,117	40070,87	0,126	37294,70

Table 4-13 - Stresses in structural steel

For the characteristic combination of actions, as described in 3.4.2.1, the direct stress in the upper and bottom flanges, as well as the shear stress, determined for combination with gr1a as leader variable action, which leads to the most unfavourable combined values, are given by:

$$\tau = (5314,07 + 26540,81 + 18628,75 + 23854,25 + 15233,66 + 2125,63 + 0 + 0) \times 10^{-3}$$

$$\tau = 91,70 \text{ N / mm}^2$$

$$\sigma_{top} = \left(\begin{array}{l} 25537,93 + 11745,72 + 41962,70 + 51259,21 + 27538,56 + 4588,33 \\ + 40070,87 + (0,6 \times 26554,12) \end{array} \right) \times 10^{-3}$$

$$\sigma_{top} = 322,34 \text{ N / mm}^2$$

$$\sigma_{bottom} = \left(\begin{array}{l} 13438,06 + 67054,47 + 39055,47 + 47707,90 + 25630,65 + 4270,45 \\ + 37294,70 + (0,6 \times 24714,41) \end{array} \right) \times 10^{-3}$$

$$\sigma_{bottom} = 249,28 \text{ N / mm}^2$$

Taking this into consideration, the aforementioned conditions may be checked:

$$\sigma_{top} = \sqrt{322,34^2 + 3 \times 91,70^2} = 359,35 \text{ N / mm}^2 \leq \frac{430}{1,0}$$

$$\sigma_{bottom} = \sqrt{249,28^2 + 3 \times 91,70^2} = 295,58 \text{ N / mm}^2 \leq \frac{430}{1,0}$$

The above verification are sufficient and guarantee the limit stresses at SLS, under characteristic combination of actions.

4.9.2.2. Concrete slab

The verification of stress limitations in concrete slab is performed for mid-span section, and is based on the characteristic combination of actions, with leading variable of the traffic load group gr1a. In addition, it is calculated both for short-term and long-term designs considering the mechanical properties of cross-sections defined on section 4.7.4.

$$\sigma_c = \left(\begin{array}{l} \frac{1}{19} \times \frac{2988 \times 0,823}{0,140} - \frac{1}{12,6} \times \frac{4681 \times 0,689}{0,155} \\ + \frac{1}{6,2} \times \frac{(5618 + 7007 + 504 + (0,6 \times 3102)) \times 0,475}{0,192} \end{array} \right) \times 10^{-3}$$

$$\sigma_c = 5,25 \text{ MPa} < 0,6 \times f_{ck} = 21 \text{ MPa}$$

Accordingly, the verification of stress limitations in concrete slab is verified.

4.9.2.3. Steel reinforcement

The verification of stress limitations in steel reinforcement is performed for the cross section over pier, and is based on the characteristic combination of actions with leading variable of the traffic load group gr1a. Taking this into consideration, the stresses in the reinforcement steel under characteristic SLS combination of actions, are summarised on the following table.

		M	W	σ
		(kNm)	(m³)	(kN/m²)
Dead	t=0	4555	0,101	45258,08
Load	t=∞	4902	0,101	48706,27
UDL		5988	0,101	59496,77
TS		3217	0,101	3164,11
Pedestrian		536	0,101	5325,70
Thermal		3102	0,101	30821,47
Shrinkage		4681	0,101	46510,42

Table 4-14 - Stresses in steel reinforcement

$$\sigma_s = \left(48706,27 + 59496,77 + 31964,11 + 5325,70 + 46510,42 \right) \times 10^{-3} \\ + (0,6 \times 30821,47)$$

$$\sigma_s = 210,50 \text{ MPa} < 0,8 \times f_{sk} = 400 \text{ MPa}$$

Accordingly, the verification of stress limitations in steel reinforcement is verified.

4.9.3. Cracking of concrete for longitudinal global bending

The verification of cracking of concrete is concerned for quasi-permanent SLS combination of action, according to (EN 1994-2, 2005) (7.4). In order to check the limiting values of cracking of concrete, the following points will be analysed:

- Maximum value of crack width;
- Minimum reinforcement area;
- Control of cracking under direct loads;
- Control of cracking under indirect loads.

- **Maximum value of crack width**

The maximum values of the crack width, depending on the exposure class are determined according to Table 7.1N of EN1992-1-1, 7.3.1. Taking in to account that the exposure class of the upper and lower reinforcement of the slab is XC3 and XC4, respectively, the recommended value of the maximum crack width W_{\max} should be limited to 0,3 mm.

- **Minimum reinforcement area**

The control of cracking at Serviceability Limit States is covered by clause 7.4.2 (1) of EN 1994-2, which requires a minimum reinforcement area given by:

$$A_{s,\min} = k_s \times k_c \times k \times f_{ct,ef} \times \frac{A_{ct}}{\sigma_s}$$

Where:

$f_{ct,ef}$ is the mean value of the tensile strength of the concrete effective at the time when the first cracked may be expected to occur. This value can be taken as those for f_{ctm} (EN 1992-1-1, 2004) (Table 3.1), taking into account the concrete strength class, thus it will be equal to 3,2 MPa.

A_{ct} is the cross-sectional area of the tensile zone of the concrete (due to direct loading and the primary effects of shrinkage). For simplicity, the cross-sectional area of the concrete may be adopted as the area determined by its effective width.

σ_s is the maximum stress allowed in the reinforcement immediately after cracking of the concrete. To satisfy the required width limits, this value may

be taken as its characteristic yield strength f_{sk} , according to EN-1994-2, 7.4.2. Thus, it will be equal to $f_{sk} = 500$ MPa.

k is the 0,8 reduction factor allowing for the effect of non-uniform self-equilibrating stresses.

k_c is a coefficient which takes account of the stress distribution within the section immediately prior to cracking and is given by:

$$k_c = \frac{1}{1 + h_c / (2 \times \bar{z}_{1,0})} + 0,3 \leq 1,0$$

For this example, taking into account that the deck slab is in tension, k_c is equal to 1,0.

k_s is the 0,9 reduction factor accounting for the reduction of tensile force in the deck slab due to local slip of the shear connection.

Then:

$$A_{s,\min} = 0,9 \times 1,0 \times 0,8 \times 3,2 \times \frac{(5,75 \times 0,25) \times 10^6}{500} = 6635,52 \text{ mm}^2 = 66,36 \text{ cm}^2$$

Hence the reinforcement concrete slab is formed by $\phi 20/130$ mm in the upper reinforcement level and $\phi 16/130$ in the lower reinforcement level, the reinforcement area is:

$$\left(\frac{3,14}{13,0} + \frac{2,01}{13,0} \right) \times 575 = 227,79 \text{ cm}^2 \gg A_{s,\min}$$

Thus, the minimum reinforcement area of the slab is verified.

○ Control of cracking under direct loading

Clause 7.4.3 of (EN 1994-2, 2005) covers the control of cracking under direct loading. According to this clause, where the minimum reinforcement calculated before is provided, the limitations of crack widths may generally be achieved by limiting the bar spacing according to Table 7.2 of (EN 1994-2, 2005) (7.4.3), or limiting the bar diameters according to Table 7.1 of (EN 1994-2, 2005) (7.4.2) of the slab steel reinforcement.

For a composite beam where the concrete slab is assumed to be cracked and not prestressed by tendons, stress in reinforcement increases due to the effects of tension stiffening of concrete between cracks compared with the stress based on a composite section neglecting concrete. Thus, according to (EN 1994-2, 2005) (7.4.3(3)) the tensile stress in reinforcement due to direct loading may be calculated as:

$$\sigma_s = \sigma_{s,0} + \Delta\sigma_s$$

With:

$$\Delta\sigma_s = \frac{0,4 \times f_{cm}}{\alpha_{st} \times \rho_s}$$

$$\alpha_{st} = \frac{AI}{A_a I_a}$$

Where:

$\sigma_{s,0}$ is the stress in the reinforcement caused by internal forces acting on the composite section, calculated neglecting concrete in tension.

Thus, the global stresses in steel reinforcement for quasi-permanent combination of actions due to dead loads ($t = \infty$), shrinkage and temperature is:

$$\sigma_{s,0} = \frac{M \times \nu}{I} = \frac{12685 \times (1,351 - (0,25/2))}{0,129} \times 10^{-3} = 120,46 \text{ MPa}$$

f_{ctm} is the mean tensile strength of the concrete, for normal concrete taken as 3,2 MPa (Table 3.1 of EN1992-1-1);

ρ_s is the reinforcement ration, given by:

$$\rho_s = \frac{A_s}{A_{ct}} = \frac{0,0228}{1,4375} = 0,0158$$

A_{ct} is the effective area of the concrete flange within the tensile zone; for simplicity the area of the concrete section within the effective width will be adopted (1,4375m²);

A_s is the total area of the all layers of longitudinal reinforcement within the effective area A_{ct} (0,0228 m²);

A, I are the area and the second moment of area, respectively, of the effective composite section neglecting concrete in tension (0,138 m² ; 0,129 m⁴);

A_a, I_a Are the corresponding properties of the structural steel section (0,115 m² ; 0,085 m⁴);

Thus:

$$\alpha_{st} = \frac{AI}{A_a I_a} = \frac{0,138 \times 0,129}{0,115 \times 0,085} = 1,82 \quad \Delta\sigma_s = \frac{0,4 \times 3,2}{1,82 \times 0,0158} = 44,51 \text{MPa}$$

$$\sigma_s = 120,46 + 43,56 = 127,5 \text{MPa}$$

Since the tensile stress on the reinforcement is less than 160 MPa, according to Table 7.2 of EN 1994-2, the maximum bar spacing for $w_k=0,3$ mm is 300 mm. Thus, the maximum bar spacing is verified ($127,5 < 300$ mm).

On its turn, for a tensile stress of 160 MPa, the maximum bar diameter is 32 mm according to Table 7.1 of EN 1994-2. Then:

$$\phi = 32 \times \frac{3,2}{2,9} = 35,3 \text{mm}$$

As it can be inferred by the above equation, the limit proposed by (EN 1994-2, 2005), (7.4.2 (3)) is checked, since the maximum bar diameter used is 20 mm.

o Control of cracking under indirect loading

The control of cracking under indirect loading is performed from the expression of the minimum reinforced area, considering the stress in the reinforcement due to shrinkage at the cracking instant, determined as:

$$\sigma_s = k_s \times k_c \times k \times f_{ct,ef} \times \frac{A_{ct}}{A_s}$$

For the cross-section at supports, this gives:

$$\sigma_s = 0,9 \times 1,0 \times 0,8 \times 3,2 \times \frac{(5,75 \times 0,25) \times 10^4}{227,79} = 145,40 \text{MPa}$$

The maximum bar diameters for high bond bars, is determined by eq. 7.3 of (EN 1994-2, 2005):

$$\phi = \phi^* \times \frac{2,9}{3,2} = 20 \times \frac{2,9}{3,2} = 18,125 \text{mm}$$

The maximum reinforcement stress is obtained by a linear interpolation in Table 7.1 of (EN 1994-2, 2005).

$$230,18 \text{MPa} > 145,40 \text{MPa}$$

The maximum allowable reinforcement stress of slab is higher than the existing stress, so this criterion is checked.

4.9.4. Connection

As it can be noted by section 3.6.4.1, shear connectors are required on the top flanges of the girders to provide the required transfer of composite action between the steel girder and concrete slab. Thus, the design process of shear connectors is to be performed on the following.

4.9.4.1. Design resistance of headed studs

The design value of the shear connectors is defined by (EN 1994-1-1, 2004) (6.6.3). Thus, for shear connectors with 19 mm diameter and 150 mm long, the design value is given by:

$$P_{Rd,1} = \frac{0,8 \times f_u \times \pi \times d^2 / 4}{\gamma_V}$$

$$P_{Rd,1} = \frac{0,8 \times 450 \times \pi \times 19^2 / 4}{1,25}$$

$$P_{Rd,1} = 81,7kN$$

$$P_{Rd,2} = \frac{0,29 \times \alpha_u \times d^2 \times \sqrt{f_{ck} \times E_{cm}}}{\gamma_V}$$

$$P_{Rd,2} = \frac{0,29 \times 1,0 \times 19^2 \times \sqrt{25 \times (34 \times 10^3)}}{1,25}$$

$$P_{Rd,2} = 91,4kN$$

$$P_{Rd} = \min(81,7; 91,4) = 81,7kN$$

4.9.4.2. Determination of number of shear connectors

The first step to determine the number of shear connectors, consists in the determination of the zones where the elastic resistance moment exceeds the moment acting on the structure, in order to determine where the structure behaviour remains elastic or plastic.

As described on section 3.6.1.2, the elastic resistance moment for a composite cross-section that behaves in an elastic manner, is determined by the summation of the bending moments at each stage of construction, as:

$$M_{El,Rd} = M_{a,Ed} + k \times M_{c,Ed}$$

Since for this numerical example, the bending moments acting on the structure, does not exceed the elastic resistance moment, the longitudinal shear at the steel-concrete interface, is determined by the following formula of mechanics:

$$V_{L,Ed} = \frac{V_{Ed} \times S}{I}$$

On the following table, the shear forces acting at an edge support, as well as the cross section properties necessities to obtain the longitudinal shear are to be presented.

	At edge support				
	maxV (kN)	n	I (m ⁴)	S (m ³)	V _{LE,d} (kN/m)
Distributed traffic load	515,54	6,2	0,154	0,071	237,68
Heavy vehicle	800	6,2	0,154	0,071	368,83
Pedestrian load	46,21	6,2	0,154	0,071	21,30
Dead load	333,28	19	0,123	0,048	130,06
Temperature	79,82	6,2	0,154	0,071	36,80
Shrinkage	-144,89	13	0,135	0,055	-59,03

Table 4-15 - Longitudinal shear at an edge support

Thus, for Ultimate Limit States (ULS), the longitudinal shear is obtained by:

$$V_{L,Ed} = 1,35 \times (237,68 + 368,83 + 21,30) + 1,35 \times (12,99) + 1,5 \times (0,6 \times 36,80)$$

$$V_{L,Ed} = 1056 \text{ kN/m}$$

Taking into account the design resistance of the shear connectors determined on the section 4.9.4.1, the number and spacing of shear connectors is determined as:

$$R = \frac{1}{0,15} \times 2 \times 81,7 = 1089,33 \text{ kN/m}$$

Thus, rows of 2 shear connectors placed at a spacing of 0,15 m are adopted to provide the connection on the steel and concrete interface.

The procedure above described, needs to be taken into consideration in order to calculate the distribution of shear connectors over all the length of the bridge. It should be noted that, in hogging moment regions, where the slab is in tension, longitudinal shear is calculated using uncracked section properties, which gives a safer value.

Figure 4-18 depicts, the curve representing the shear force per unit length, as well as the values of row spacing over a length corresponding to half of the bridge length (Symmetric structure).

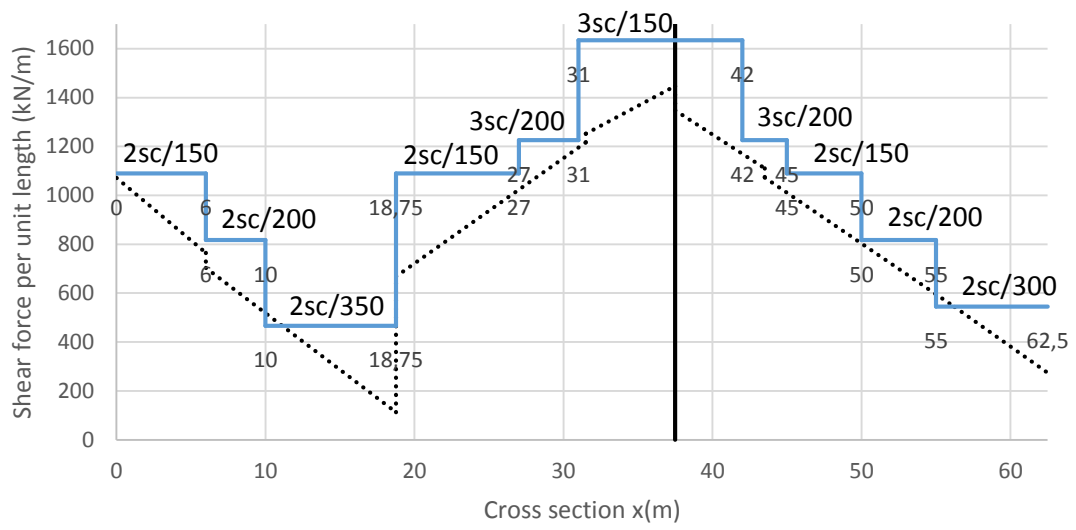


Figure 4-18 - ULS shear force per unit length resisted by the shear connectors

Chapter 5

Influence of the construction process on the serviceability behaviour of composite bridges

The goal of the study presented herein is to analyse and evaluate the structural response under service conditions of composite bridges when considering different construction processes. Taking this into consideration, short and long term stresses, deflections, as well as the effect of concrete cracking above supports are analysed.

The aforementioned study is made over the bridge designed on the previous chapter, considering five construction sequences. In order to study the structural response under service conditions of the bridge at each stage, analytical models capable to take into account the time dependent response of the structures at early ages and along the structure service life are necessary.

The models are solved through the analysis Program Midas/Civil 2015 (V2.2), in order to draw conclusions that lead to the most suitable construction solution depending on the most restrictive design criterion of the project. The study carried out on this chapter is based on the study developed by (Mari, Mirambell, & Estrada, 2002).

5.1. Description of the structural analysis

Clause 5.4.2.4 of Eurocode 4, part 2 states that an appropriate analysis shall be made to cover the effects of staged construction, in order to achieve the correct profile of the completed bridge, unless all the cross sections are class 1 or 2 and there is no allowance for lateral torsional buckling.

In the current structural analysis, five different construction sequences will be analysed with the main purpose of comparing the structural response of the bridge on each construction sequence. The structural description, as well as the material properties of the bridge presented on the previous chapter, are adopted in the current structural analysis.

Bearing in mind that the verification of the serviceability limit states requires the realistic evaluation of internal forces, support reactions, stress and strains, together with crack widths and displacements, it is essential to take into account the following aspects that affects the structure's response: (Mari, Mirambell, & Estrada, 2002)

- The cracking of concrete under tension, in such a way, that it reduces the structure stiffness, modifies the stress distribution between the concrete slab and the steel girder and, in the case of continuous bridges, it also affects the distribution of internal forces. In the current study, three methods for taking into account cracking of concrete above intermediate supports are compared:
 - Method 1 (uncracked analysis): first an uncracked analysis is carried out and the extent of cracking is determined, followed by another analysis using cracked section properties in these regions;
 - Method 2 (simplified method): it is assumed that, the concrete is cracked adjacent to internal supports over 15% of the span;
 - Method 3: this calculation method assumes an uncracked section and a default redistribution of 10% of the support moments into the spans. (Lebet & Hirt, 2013)
- The difference in the rheological behaviour between the component materials: unlike steel, concrete suffers from time-dependent strains due to shrinkage and creep and its mechanical characteristics evolve with time, which leads to deflections and stress re-distribution changes during and after the construction process. MIDAS/Civil can reflect time dependent concrete properties such as creep, shrinkage and compressive strength, as explained on section 5.2.2
- The construction process: since the structural configuration continuously changes with different loading and support conditions, and each construction stage affects the subsequent stages, the design of certain structural components may be governed during the construction. Accordingly, without consideration of construction process, the analysis for the post-construction stage will not be reliable. The five construction processes considered are presented and explained on section 5.3.

In order to capture the time-dependent behaviour of the bridge under service conditions, the structural analysis strategy consists of a time step-by-step procedure, in which the time domain is divided into a number of intervals. A time forward integration is performed in which increments of displacements, stresses and other structural quantities are successively added to the previous totals as forward in the time domain. Thus, at each time step, the structure is analysed under three types of cycles defined, each one enclosing the previous one:

- Construction stages;
- Time intervals;
- Load steps.

This structural analysis is performed by the analysis program Midas/Civil 2015 (V2.2).

5.2. General description of MIDAS/Civil

The structural analysis, as described above has been incorporated into the computer program MIDAS/Civil 2015 (V2.2). MIDAS/Civil is an analysis and design software for structural engineering that offer special features for the analysis of any bridge structure. It has been developed by the Korean structural software development company MidasSoft, Inc, and its reliability has been established through applying them to thousands of real projects. (Analysis for civil structures)

Midas/Civil offers many special features for the analysis and design of bridges, such as:

- Construction stage analysis;
- Time-dependent analysis feature;
- Solution for unknown loads using optimization technique;
- Analysis of prestressed concrete box girders;
- Moving load analysis for bridge structures;
- Hydration heat analysis;
- Composite steel bridge analysis considering section properties of pre- and post-combined sections;
- ILM/MSS/FCM bridge wizard (automatic generation of the model data of a prestressed or post-tensioned box bridge constructed by: incremental launching method (ILM), a movable scaffolding system (MSS) or by free cantilever method (FCM));
- Cable-stayed bridge wizard (automatic generation of two-dimensional cable-stayed bridges).

Although, it is not intention to use all these features. Actually, the first two specialities are considered and explained on the following, in order to perform the construction stage analysis.

5.2.1. Definition of construction stages

In order to define construction activities MIDAS/Civil provides the *Composite Section for Construction Stage* command for performing the construction stage analysis of a composite section, which allows the activation and deactivation of elements, activation and deactivation of loadings at certain points in time, as well as it allows changes in boundary conditions. Taking this into consideration, the procedure to perform construction stage analysis of a composite bridge is as follows:

1. Define the material and section properties;
2. Define Structure Groups, Boundary Groups and Load Groups;
3. Define construction stages;
4. Activate the Boundary Groups and Load Groups corresponding to each construction stages;
5. Activate the flooring sections corresponding to each construction stage as per the construction sequence for floor slab;
6. Review the analysis results for each construction stage. (Construction Stage Analysis of a Bridge Using a Composite Section)

5.2.2. Consideration of time-dependent material behaviour

As it was already mentioned, deflections and stress redistributions continue to change during and after the construction of composite bridges due to varying time-dependent properties, such as concrete creep, shrinkage, and modulus of elasticity (aging). MIDAS/Civil allows to performing the option of a time-dependent construction stage analysis considering the following time effects on materials: (Construction Stage Analysis of a Bridge Using a Composite Section)

- Creep in concrete members having different maturities;
- Shrinkage in concrete members having different maturities;
- Compressive strength gains of concrete members as a function of time.

The creep and shrinkage effects as well as the compressive strength gain properties of concrete in MIDAS/Civil can be defined by choosing one model code. When the European code is selected for the determination of creep and shrinkage the following input parameters are required:

- Characteristic compressive cylinder strength of concrete at the age of 28 days (f_{ck});

- Relative humidity of ambient environment;
- Notional size of the members ($h=2A_c/u$);
- Type of cement (Class S, N or R);
- Age of concrete at beginning of shrinkage.

Based on these input parameters, MIDAS/Civil automatically computes the creep and shrinkage coefficients. Accordingly, Figure 5-1 and Figure 5-2 illustrates the creep coefficients and shrinkage strain respectively, for the current construction structural analysis.

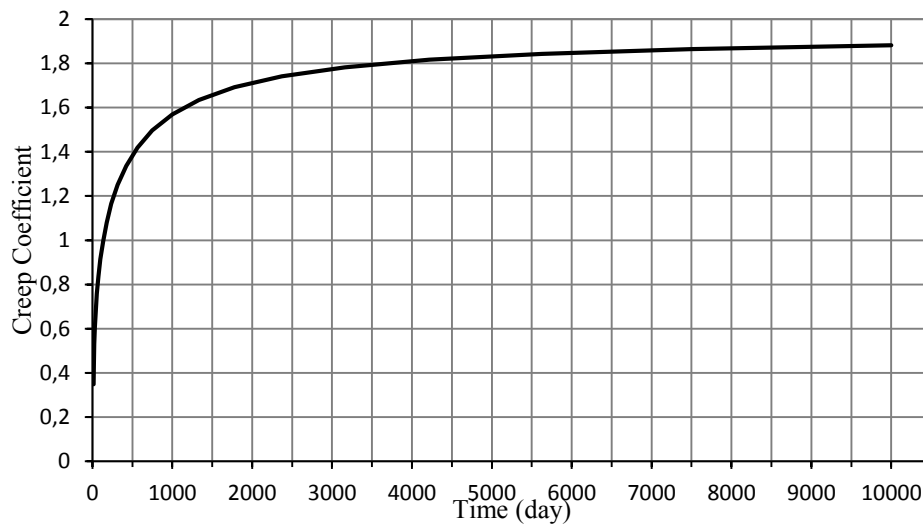


Figure 5-1 - Creep Coefficient

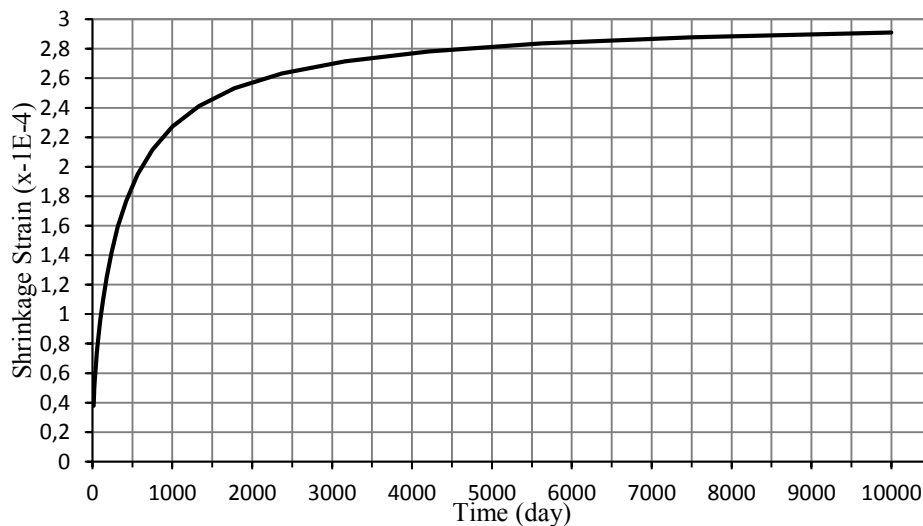


Figure 5-2 - Shrinkage Strain

On its turn, when the European code is selected for the determination of compressive Strength the following input parameters are required:

- Mean compressive strength of concrete at the age of 28 days;
- Cement type: (Class R: 0.20, Class N: 0.25, Class S: 0.38).

Based on these input parameters, MIDAS/Civil automatically computes the compressive strength. Accordingly, Figure 5-3 illustrate the compressive strength, for the current construction structural analysis.

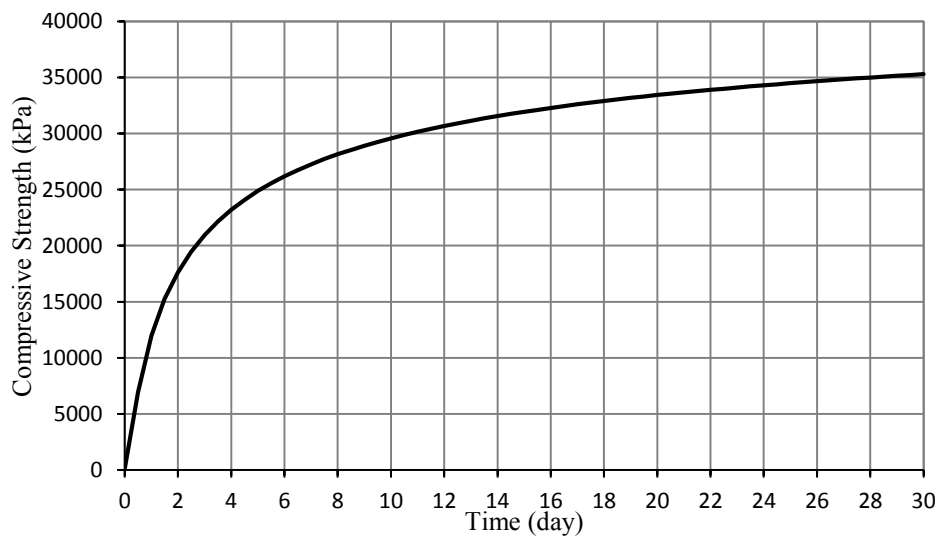


Figure 5-3 - Compressive strength

5.2.3. Running a construction stage analysis by MIDAS/Civil

Bearing in mind the above considerations, on the following, a summary of the procedure used in MIDAS/Civil for carrying out a time dependent analysis reflecting construction stages is presented: (Analysis for civil structures)

1. Create a structural model. Assign elements, loads and boundary conditions to be activated or deactivated to each construction stage together as a group;
2. Define time dependent material properties such as creep and shrinkage. The time dependent material properties can be defined using the standards such as ACI, CEB-FIP, or European;
3. Link the define time dependent material properties to the general material properties. By doing this, the changes in material properties of the relevant concrete members are automatically calculated;

4. Considering the sequence of the real construction, generate construction stages and time steps;
5. Define construction stages using the element groups, boundary condition groups and load groups previously defined;
6. Carry out a structural analysis after defining the desired analysis condition;
7. Combine the results of the construction stage analysis and the completed structure analysis.

5.3. Considered construction process and loads applied at each stage

Steel-concrete Composite bridges allows several construction processes, which may be influenced by many different parameters, such as the access, temporary support arrangements, and the need to minimise work during road or railway closures. In the current study, five different construction processes have been considered, which in turn differ in the execution sequence for the concrete slab and in the existence or not of propping. These are:

1. Propped bridge: this solution correspond to the “pure” composite solution, in which the concrete slab is executed with the bridge completely propped. The slab is concreted in five phases with 6 days interval between each one, with lengths of 25 meters.
2. Alternate slab concreting: after the installation of the steel structure, the concrete is poured on site casting the slab elements in the mid-span sections before the pier sections. It corresponds to a solution that leads to a reduction of stresses in the slab in the support zones.
3. Continuous slab concreting: once the steel structure is assembled, the slab is concreted in five phases with 6 days interval between each one, with lengths of 25 meters, starting out from an abutment and arriving at the other without any alteration. This is a simple method, because the mobile formwork always moves in the same direction. However, this is an unfavourable option from the point of view of stresses, particularly above the intermediate supports.
4. Simultaneous slab concreting: this is an option, in which the concrete is pour over the full length of the bridge at once, without the steel girder being propped. Although, it is not a common solution for practical reasons.

5. Propped bridge 2: this construction process consists firstly of concreting the span regions above the temporary supports, with lengths of 25 meters in 3 phases with 6 days interval between each one, followed by the removing of temporary supports. After that, concreting support regions takes place. This method allows some of self-weight of the concrete in the spans to be resisted by composite cross sections, as well as it reduces the tensile stresses at the support regions.

Figure 5-4 to Figure 5-8, shows the schematic construction procedures considered in the current study, as well as the loads applied at each stage. Unlike the *Simultaneous Slab Concreting*, in which the slab is concreting at once, concrete is poured on site casting the slab elements in a specific order, where the total length of the bridge (125 m) is split into 5 identical 25 meters concreting segments. The time interval between each concreting stage is intended to be as 6 work days. The first day is devoted to the concreting, the next 3 days to its hardening and the last 2 days to moving the formwork. This sequence respects a minimum concrete strength of 20 MPa before removal of the formwork. (Composite highway bridge design: Worked Examples, 2014)

The Dead Load, consisting of asphalt layer, waterproofing layer, pedestrian footway, parapets, safety barriers, kerbs and edge beam, with a weight taken as being 25,25 kN, was placed after the final phase of slab concreting. These permanent loads are maintained in the analysis for 10000 days, so that creep, and shrinkage takes place. In order to clarify the results, the variable loads were considered as being due only to the traffic, as defined on section 4.5.2. The traffic load is applied at long term, at the most unfavourable position, which is:

- To obtain the maximum deflections and positive moments at the central spans, distributed load at the central span, and heavy vehicle in the centre of the central span;
- To obtain the maximum negative moments in the support, distributed load in spans 1 and 2, and heavy vehicle at 55,44 meters from the abutment.

Table 5-4 to Table 5-8, shows the inputs parameters to perform the construction stage analysis in MIDAS/Civil. Taking this into consideration, on the following, a brief reference to the Loads considered is presented:

DL(BC)1	Self-weight of steel structure;
DL(BC)2	Self-weight of concrete slab at construction stage 1;
DL(BC)3	Self-weight of concrete slab at construction stage 2;
DL(BC)4	Self-weight of concrete slab at construction stage 3;
DL(BC)5	Self-weight of concrete slab at construction stage 4;
DL(BC)6	Self-weight of concrete slab at construction stage 5;
DL(AC)	Dead load applied after composite action;
LL(Trf)	Live load due to traffic.

Table 5-1 - Loads applied at each stage

In addition to the input parameters described on Table 5-4 to Table 5-8, *Section Stiffness Scale Factors* are included in Boundary Groups, at the moment of the concrete cracking. Section Stiffness Scale Factor is a function used for reducing flexural stiffness of the members. This scale factor is applied to the calculation for displacements, member forces, and stress calculations, in order to reflect cracked sections of concrete. Table 5-2 and Table 5-3 shows the required Moment of Inertia and Cross-sectional area Scale factors to be applied to each stiffness component.

Classification	Moment of Inertia I_{yy}		Scale factor for I_y , I_{yy_2}/I_{yy_1}
	I_{yy_1} (Full width)	I_{yy_2} (Cracked section)	
Section Type 1	0,324354142	0,12857302	0,396397035
Section Type 2	0,217892368	0,105537333	0,484355346

Table 5-2 - Area moment of inertia about the element local y-axis Scale factor

Classification	Areas		Scale factor for A , A_2/A_1
	A_1 (Full width)	A_2 (Cracked section)	
Section Type 1	1,552	0,137684954	0,088714532
Section Type 2	1,51936	0,105044954	0,069137633

Table 5-3 - Cross-sectional area Scale factor

5.3.1. Propped bridge

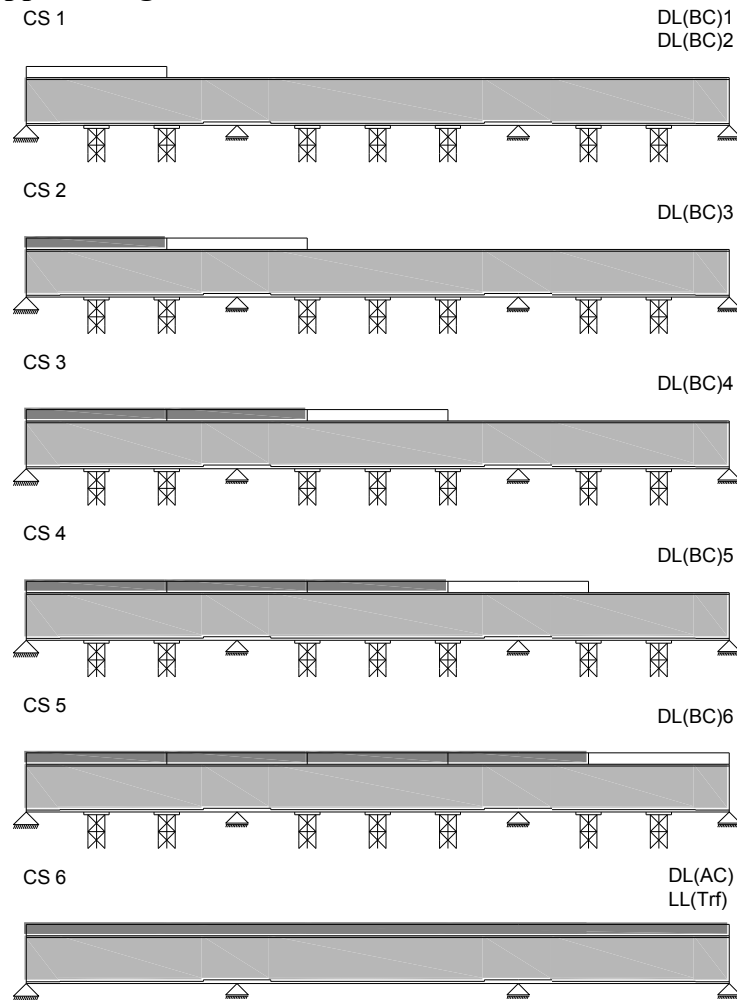


Figure 5-4 - Schematic representation of Propped bridge construction process

Cosnt. Stage	Structure Group	Boundary Group	Load Group Activation		Load Group Deactivation	Duration	Remark
			Group	Step			
CS1	S1	Bgroup Temporary	DL(BC)1	First	-	3	Non-composite
			DL(BC)2	First	-		
CS2	S2	-	DL(BC)3	First	-	6	Composite in CS1
CS3	S3	-	DL(BC)4	First	-	6	Composite in CS2
CS4	S4	-	DL(BC)5	First	-	6	Composite in CS3
CS5	S5	-	DL(BC)6	First	-	6	Composite in CS4
CS6	S6	-	DL(AC)	28	Temporary	10000	Composite in CS5
			LL(Trf)	Last			

Table 5-4 - Input parameters to perform Propped bridge construction process

5.3.2. Alternate slab concreting

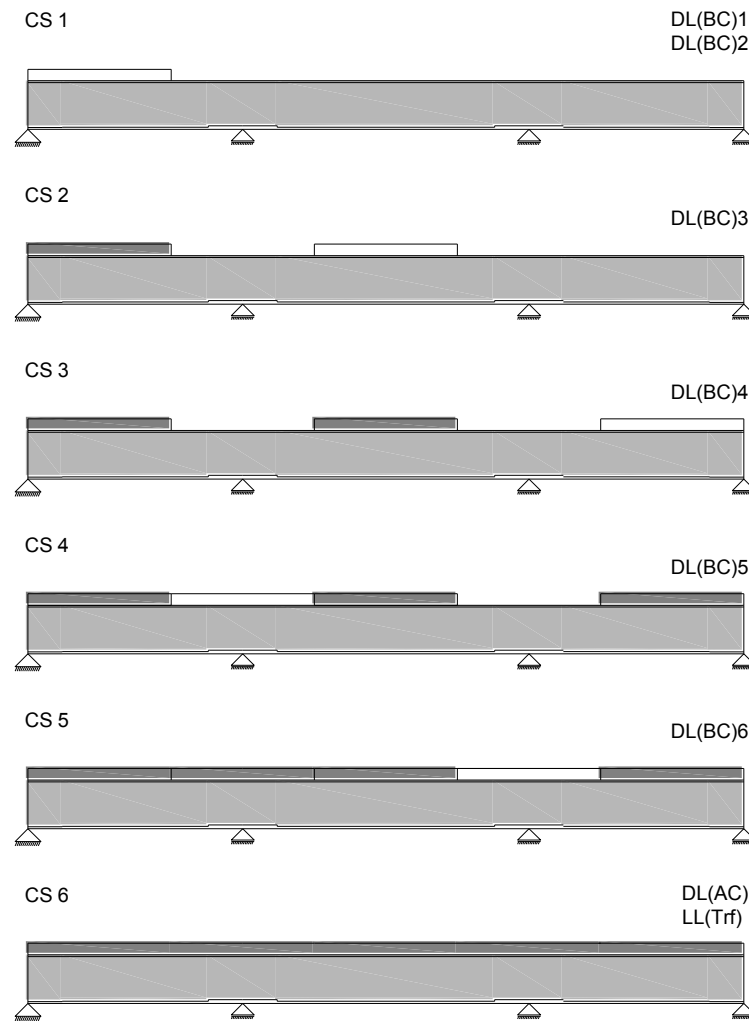


Figure 5-5 - Schematic representation of Alternate slab concreting

Cosnt. Stage	Structure Group	Boundary Group	Load Group Activation		Load Group Deactivation Group	Duration	Remark
			Group	Step			
CS1	S1	Bgroup	DL(BC)1	First	-	3	Non-composite
			DL(BC)2	First	-		
CS2	S2	-	DL(BC)3	First	-	6	Composite in CS1
CS3	S3	-	DL(BC)4	First	-	6	Composite in CS2
CS4	S4	-	DL(BC)5	First	-	6	Composite in CS3
CS5	S5	-	DL(BC)6	First	-	6	Composite in CS4
CS6	S6	-	DL(AC)	28	-	10000	Composite in CS5
			LL(Trf)	Last			

Table 5-5 - Input parameters to perform Alternate slab concreting

5.3.3. Continuous slab concreting

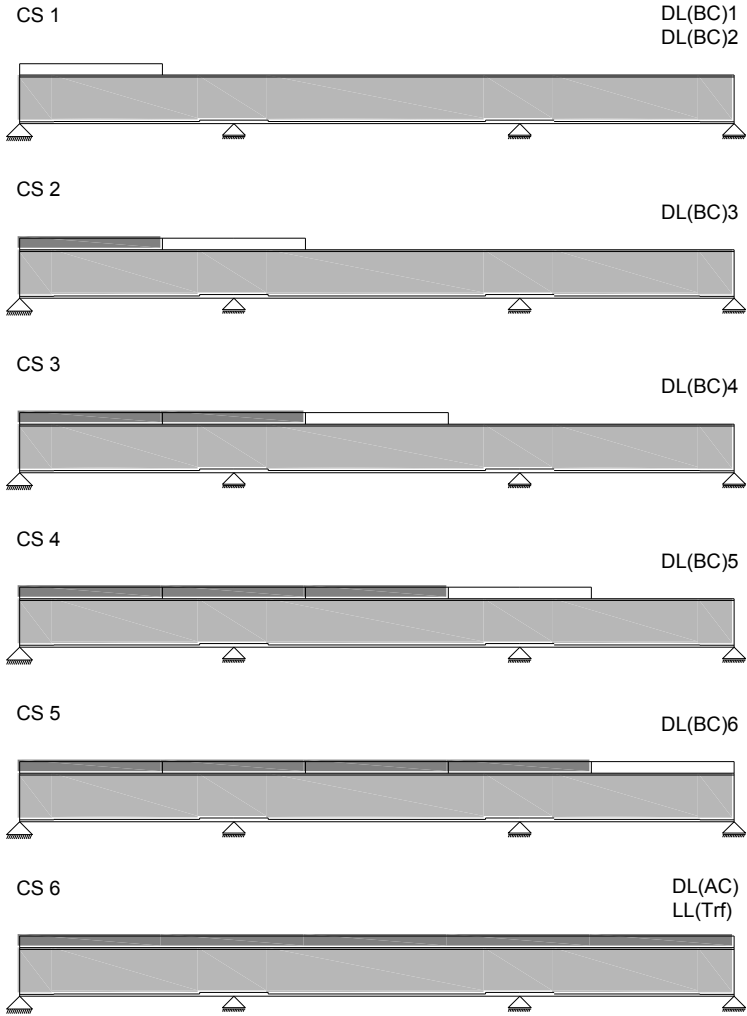


Figure 5-6 - Schematic representation of Continuous slab concreting

Cosnt. Stage	Structure Group	Boundary Group	Load Group Activation		Load Group Deactivation Group	Duration	Remark
			Group	Step			
CS1	S1	Bgroup	DL(BC)1	First	-	3	Non-composite
			DL(BC)2	First			
CS2	S2	-	DL(BC)3	First	-	6	Composite in CS1
CS3	S3	-	DL(BC)4	First	-	6	Composite in CS2
CS4	S4	-	DL(BC)5	First	-	6	Composite in CS3
CS5	S5	-	DL(BC)6	First	-	6	Composite in CS4
CS6	S6	-	DL(AC)	28	-	10000	Composite in CS5
			LL(Trf)	Last			

Table 5-6 - Input parameters to perform Continuous slab concreting

5.3.4. Simultaneous slab concreting

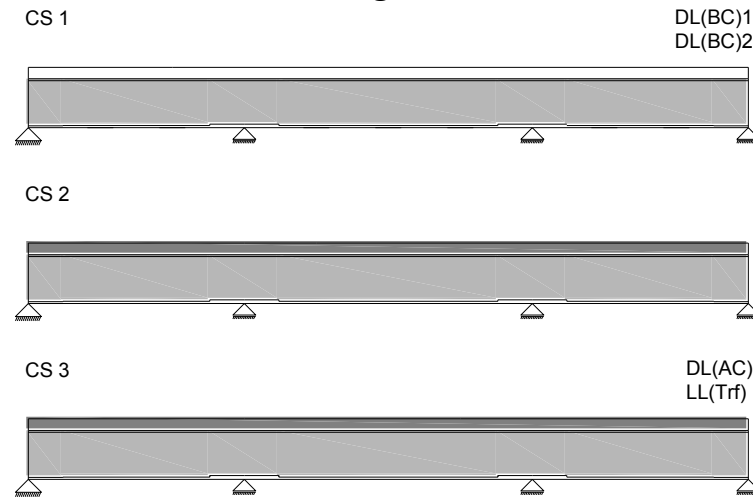


Figure 5-7 - Schematic representation of Simultaneous slab concreting

Cosnt. Stage	Structure Group	Boundary Group	Load Group Activation		Load Group Deactivation	Duration	Remark
			Group	Step	Group		
CS1	S1	Bgroup	DL(BC)1	First	-	3	Non-composite
			DL(BC)2	First	-		
CS2	-	-	-	-	-	28	Composite
CS3	-	-	DL(AC)	First	-	10000	Composite
			LL(Trf)	Last			

Table 5-7 - Input parameters to perform Simultaneous slab concreting

5.3.5. Propped bridge 2

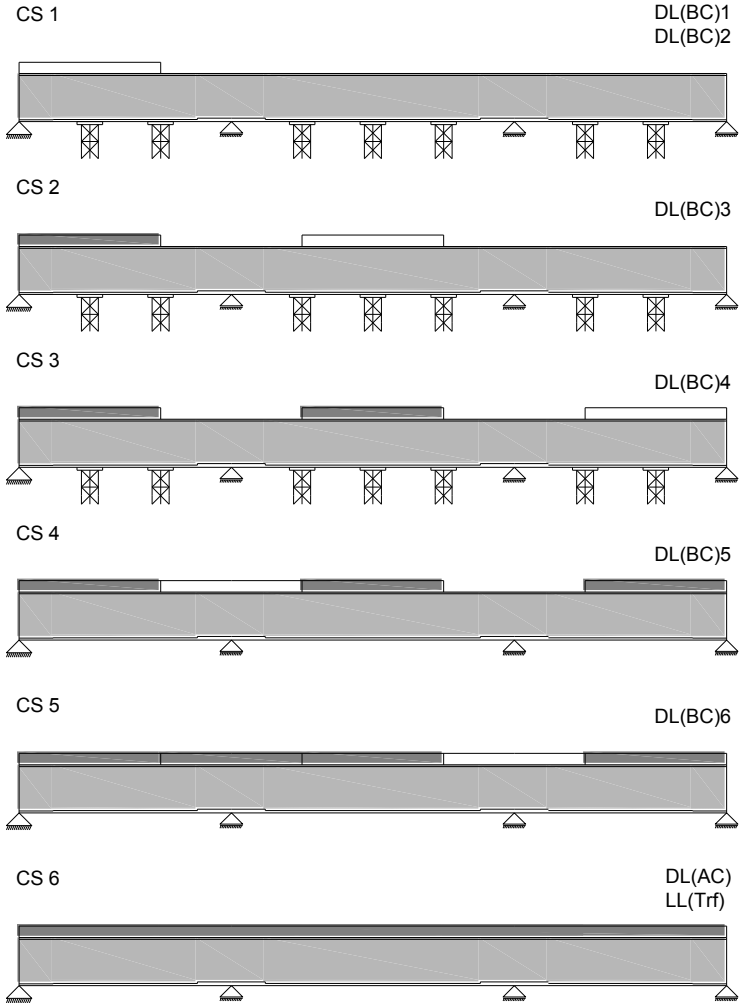


Figure 5-8 - Schematic representation of Propped bridge alternate slab concreting

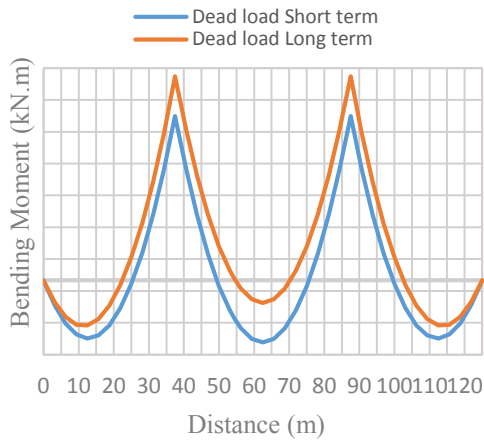
Cosnt. Stage	Structure Group	Boundary Group	Load Group Activation		Load Group Deactivation Group	Duration	Remark
			Group	Step			
CS1	S1	Bgroup	DL(BC)1	First	-	3	Non-composite
		Temporary	DL(BC)2	First	-		
CS2	S2	-	DL(BC)3	First	-	6	Composite in CS1
CS3	S3	-	DL(BC)4	First	-	6	Composite in CS2
CS4	S4	-	DL(BC)5	First	Temporary	6	Composite in CS3
CS5	S5	-	DL(BC)6	First	-	6	Composite in CS4
CS6	S6	-	DL(AC)	28	-	10000	Composite in CS5
			LL(Trf)	Last			

Table 5-8 - Input parameters to perform Propped bridge alternate slab concreting

5.4. Conclusions related to the influence of the construction sequence

The results obtained after carrying out the analysis with MIDAS/Civil for the considered construction processes, are displayed and duly commented below.

5.4.1. Longitudinal bending moments



By observing the Figure 5-9, it is possible to conclude that due to the effect of creep and shrinkage under the dead load, time-dependent longitudinal internal forces are developed; thus, a time-dependent longitudinal bending moment redistribution arises, increasing the negative bending moments, and reducing the positive ones.

Figure 5-9 - Bending moments due to Dead load at short and long term

The results obtained for bending moments at interior span, as well as at central support, due to the different actions on the bridge, namely dead loads and the traffic loads are displayed in Figure 5-10, Figure 5-11 and in Table 5-9. From the observation of the results it is possible to conclude that a significant reduction with time of the positive moments takes place, varying between 30,8% for the Continuous slab concreting and 46,2% for the Propped 2 case. On its turn, an increment of the negative bending moments between 16,0% for the Continuous slab concreting and 25,4% for the propped 2 case is observed.

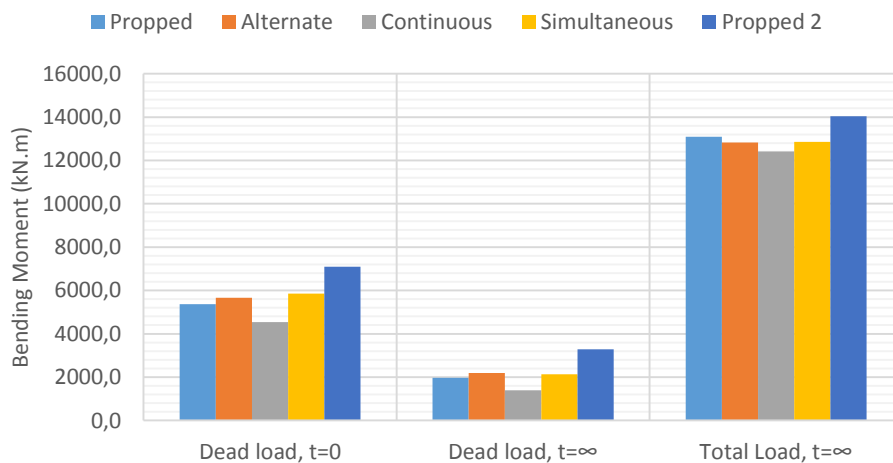


Figure 5-10 - Bending moments at central span

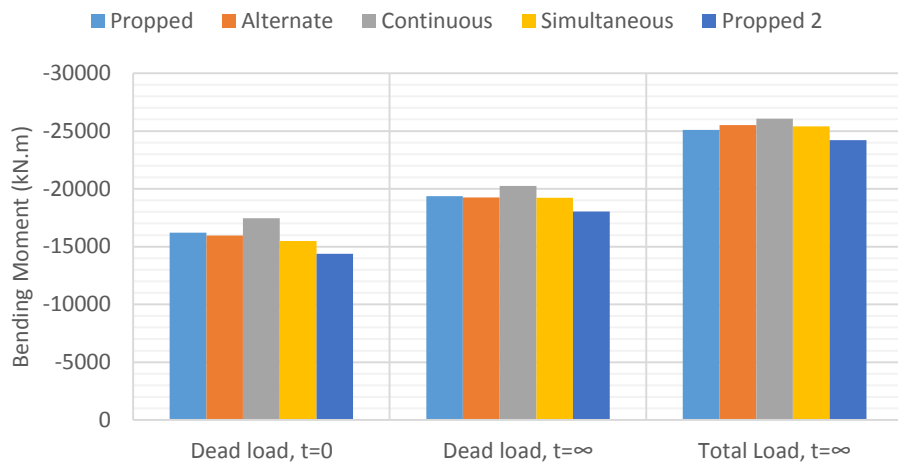


Figure 5-11 - Bending moments at support

Sequence of slab concreting	Propped	Alternate	Continuous	Simultaneous	Propped 2
Moment at central span (kN.m)					
Dead load, t=0	5369,2	5660,3	4543,8	5849,8	7100,4
Dead load, t=∞	1974,1	2188,0	1398,9	2127,2	3280,0
Redistribution (%)	-36,8	-38,7	-30,8	-36,4	-46,2
Live Load, t=∞	11115,7	10641,3	11015,0	10733,9	10755,6
Total Load, t=∞	13089,8	12829,3	12413,9	12861,1	14035,7
Moment at support (kN.m)					
Dead load, t=0	-16195,54	-15969,04	-17456,06	-15493,09	-14391,45
Dead load, t=∞	-19361,52	-19267,85	-20240,7	-19215,63	-18049,37
Redistribution (%)	19,5	20,7	16,0	24,0	25,4
Live Load, t=∞	-5733,6	-6251,9	-5814,7	-6191,5	-6158,4
Total Load, t=∞	-25095,14	-25519,78	-26055,37	-25407,15	-24207,78

Table 5-9 - Bending moments at central span and at support sections

Comparison of the results illustrates that whether for bending moments at central span and at support, Propped 2 case and Continuous slab concreting originates the extreme bending moment values due to the different action on the bridge, in its final state.

Thus, while the maximum negative, and the minimum positive bending moment are obtained for the Continuous slab concreting, the minimum negative and the maximum positive bending moments are obtained for the Propped 2 case.

5.4.2. Deflections and stresses at critical sections

The deflection values at central span and the most significant stress values in the concrete and steel in the sections of the central span and the support are summarised in Table 5-10 for each construction process.

Sequence of slab concreting	Propped	Alternate	Continuous	Simultaneous	Propped 2
Deflection at central span (mm)					
Dead load, t=0	29,3	72,9	58,3	73,0	54,0
Dead load, t=∞	28,4	68,2	55,8	68,7	50,8
Delayed deflection, t=∞	-0,9	-4,7	-2,4	-4,3	-3,2
Live Load, t=∞	57,8	54,4	57,0	55,0	55,2
Total Load, t=∞	86,2	122,6	112,9	123,7	106,0
Stresses at central span (MPa)					
<u>Concrete</u>					
Dead load, t=0	-2,1	-0,302	-0,0802	-0,423	-2,63
Dead load, t=∞	0,0752	1,59	1,69	1,63	-0,247
Total Load, t=∞	-4,71	-2,99	-3,05	-3	-4,88
<u>Bottom steel plate</u>					
Dead load, t=0	58,5	74,5	61,1	75,9	77,7
Dead load, t=∞	28,7	42,3	32,6	41,7	43,5
Total Load, t=∞	147	155	149	156	158
Stresses at support (MPa)					
<u>Bottom steel plate</u>					
Dead load, t=0	-113	-128	-133	-125	-114
Dead load, t=∞	-135	-149	-151	-148	-137
Total Load, t=∞	-275	-300	-293	-298	-286

Table 5-10 - Deflections and stresses at the critical sections

From the above table and Figure 5-11 it is visible that deflection at central span reach higher values for the Simultaneous and Alternate slab concreting case, and as it would be expected, the smaller deflection values are obtained for the Propped one. In addition to the construction process that affects significantly the total deflection, it is possible to observe the effect of the live load for each case, which varies between 54,4mm and 57,8mm.

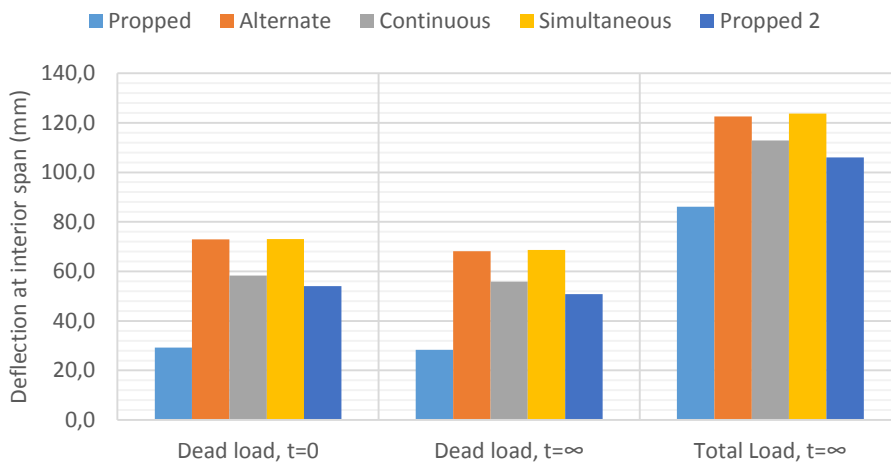


Table 5-11 - Deflection values at central span (mm)

Attention must be called to the fact that in deflection of the deck at central span under Dead load at long term, a deflection reduction is observed, which is comprised between 0,9% and 4,7% for the Propped and Continuous slab concreting case, respectively. The cause for these results is presented below.

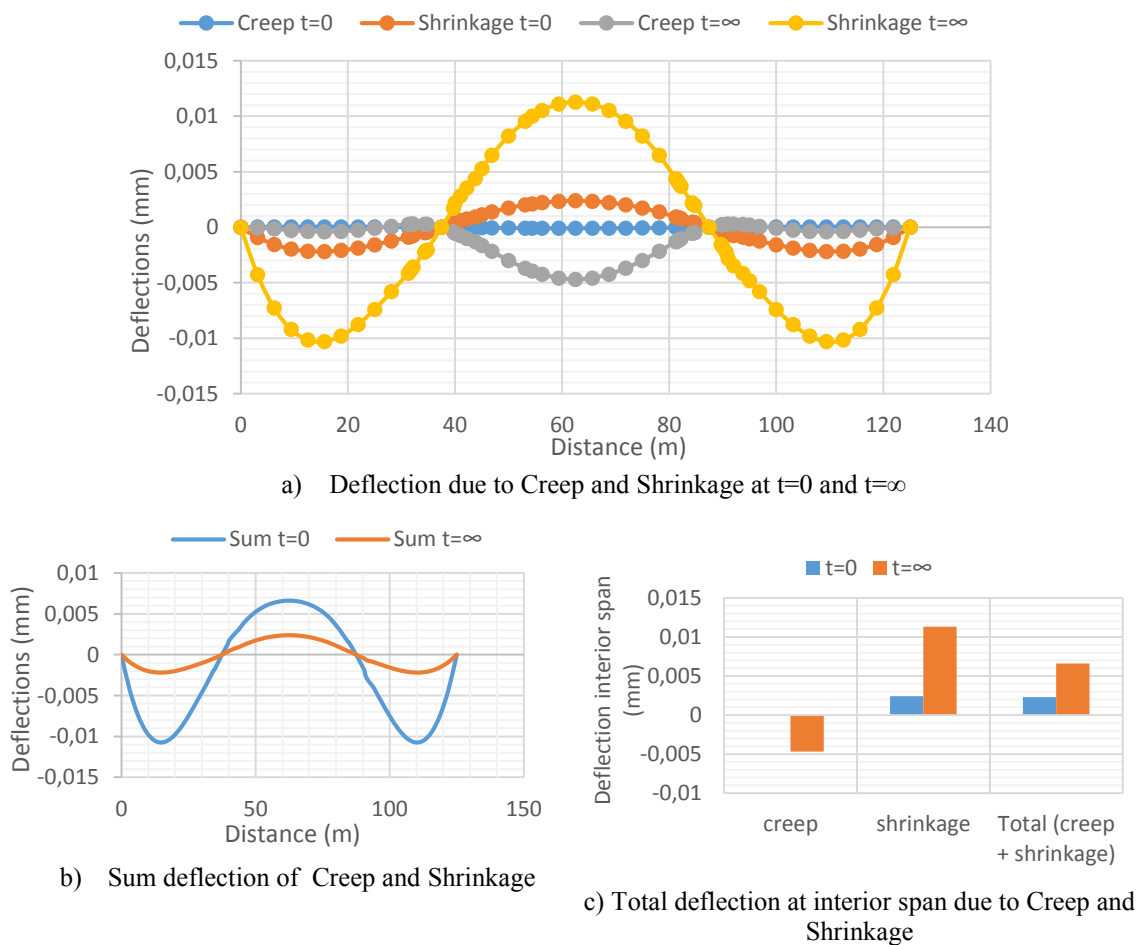


Figure 5-12 - Deflections due to Creep and Shrinkage in the bridge deck

From the results displayed in Figure 5-12, it is possible to observe that the time-dependent deformations due to the creep increases the deflections in the central span while the shrinkage reduces the deformation at central span. Figure 5-12 a) shows the total deflections due to the sum of Creep and Shrinkage in the bridge deck, for the Simultaneous Slab concreting case. As it can be inferred, the sum of the time-dependent deformations due to Creep and Shrinkage leads to a negative deflection in the exterior spans and to a positive deflection in the central span. The evolution of the total deflection at interior span due to the effect of Creep and Shrinkage at $t=0$ and $t=\infty$ is represented in Figure 5-12 c).

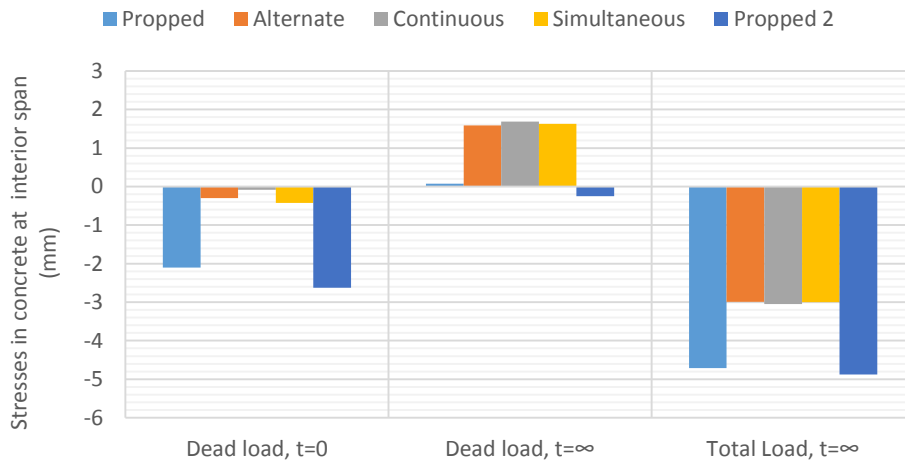


Figure 5-13 - Time evolution of the stresses in the concrete slab at the centre of the central span

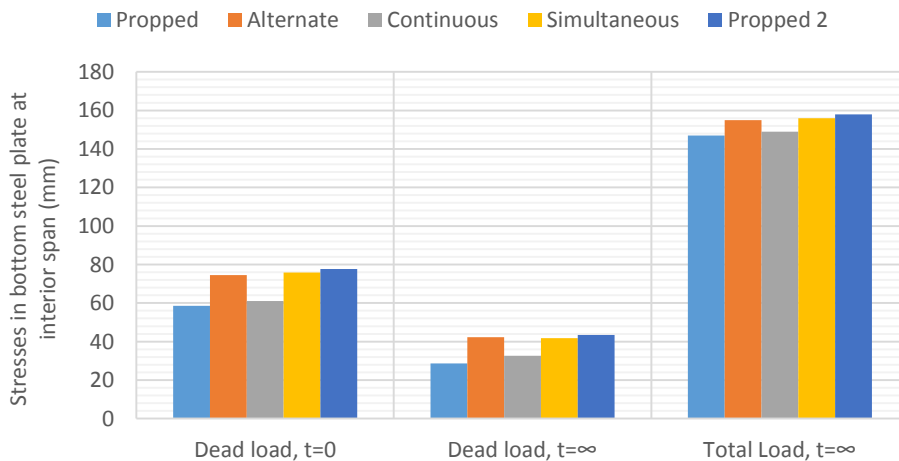


Figure 5-14 - Time evolution of the stresses in the bottom steel plate at the centre of the central span

Figure 5-13 and Figure 5-14, shows the time evolution of the stresses in the concrete slab and in the bottom steel plate at the centre of the interior span, respectively. From the results displayed it is possible to observe that due to the effect of creep and shrinkage, the

compression stress in concrete slab increases while the tension in the bottom steel plate is reduced. By other hand, as it would be expected, the maximum compression stresses in the concrete slab at interior span are observed for the Propped and Propped 2 case while the minimum stress is registered in the Alternate slab concreting. The Bottom steel plate arises the maximum tensile stresses in the Propped 2 and in the Simultaneous slab concreting, whereas the Propped case corresponds to the minimum tensile stress in the bottom steel plate.

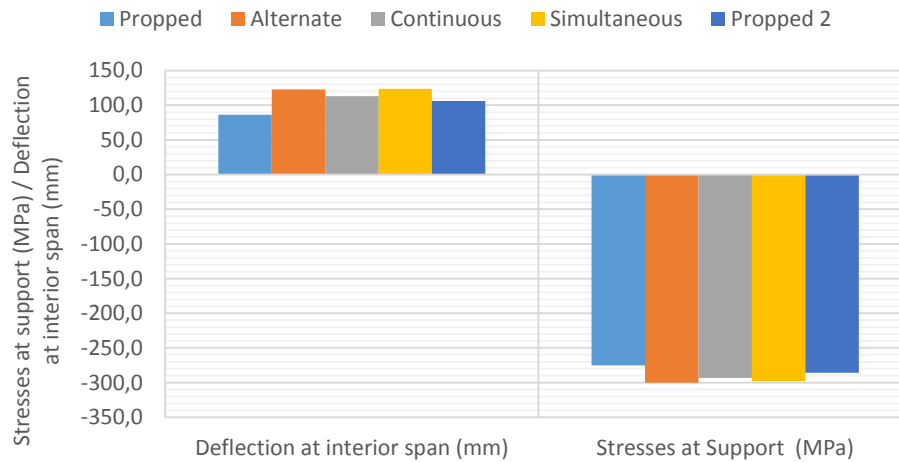


Figure 5-15 - Final deflections at interior span and bottom steel stresses at support

Figure 5-15 summarises the final values of deflections at interior span and stresses at bottom steel plate. The comparison between the results illustrates that whether for the deflection at interior span or for the compression in the bottom steel support, Alternate and Continuous slab concreting originates higher values of deflection and compression stresses, while the Propped case leads to the smaller results.

5.4.3. Effect of calculation method used to take into account the concrete cracking above supports

As it was already explained, the influence of the calculation method used to take into account the cracking of the concrete above the intermediate supports is estimated by comparing the distribution of internal moments at central span and at support zones. In the Table 5-12, bending moments at central span and at support resulting from the “exact” calculation method are compared with the results predicted by two “non-exact” methods.

Sequence of slab concreting	Method 1: "exact calculation"		Method 2: Simplified method		Method 3: Redistribution of 10%	
Moment at central span						
	(kN.m)	(%)	(kN.m)	(%)	(kN.m)	(%)
Propped	13089,80	100,0				
Alternate	12829,34	98,0				
Continuous	12413,89	94,8	13261,76	101,3	13045,23	99,7
Simultaneous	12861,08	98,3				
Propped 2	14035,65	107,2				
Moment at support						
	(kN.m)	(%)	(kN.m)	(%)	(kN.m)	(%)
Propped	-27342,25	100,0				
Alternate	-27917,24	102,1				
Continuous	-28339,46	103,6	-27167,54	99,4	-26379,693	96,5
Simultaneous	-27750,69	101,5				
Propped 2	-26546,92	97,1				

Table 5-12 - Influence of the bending moments on the bending moments

In Figure 5-16, the bending moments at interior span are depicted for the analysis taking into account the three calculation methods. It can be observed that Method 2 and Method 3 are similar and give results that are by the safety side, when comparing with the Method 1. The only exception is noted for Propped 2 case, which originates a higher bending moment value than the Method 2 and 3.

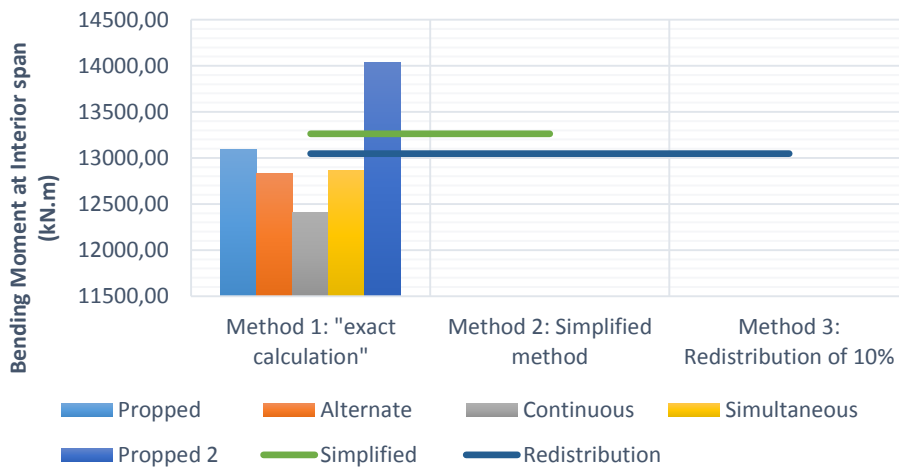


Figure 5-16 - Influence of the calculation method on the bending moments at Central Span

On its turn, by observing the Figure 5-17, it is possible to conclude that for the bending moment at support, Method 2 and 3 do not give accurate results.

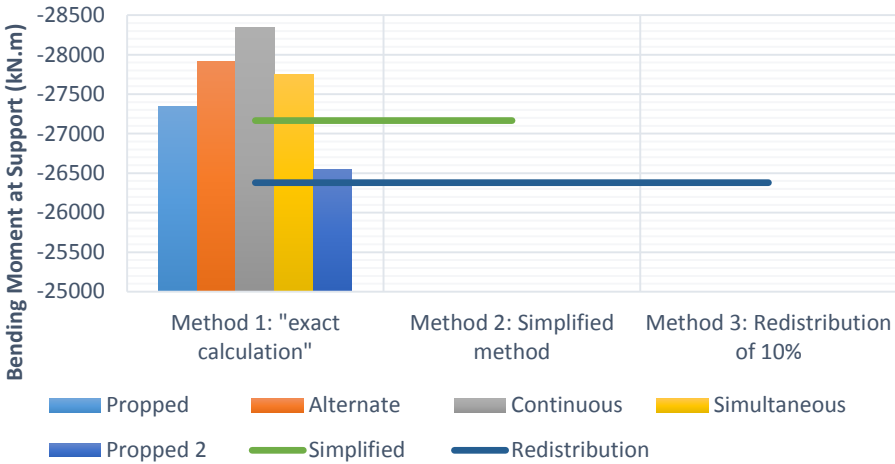


Figure 5-17 - Influence of the calculation method on the bending moments at Support

5.4.4. Final considerations

Based on the study carried out throughout this structural analysis, it is possible to prove that the issue to analyse the correct profile of a composite bridge not only concerns the analysis of post-construction, but also requires an appropriate analysis to cover the effects of staged construction.

The results obtained allows to conclude that the Propped case corresponds to the most rigid solution, since all the span works as a composite section under the self-weight of concrete slab, right from the beginning.

In what concerns the deflections at centre of the interior span, as it would be expected, the Simultaneous and the Alternate slab concreting corresponds to the cases that leads to the most significant deflection values. These two concreting cases also leads to the higher stresses in the bottom steel plate at support section.

Finally, it is possible to conclude that Method 2 and 3 gives accurate results for the calculation of bending moments at interior span, with exception of the Propped 2 case, while for the section at support, these two methods give results that are not by the safety side.

Chapter 6 Conclusion

The thesis presented herein provided a general overview of the composite bridges designing according to the methodologies proposed by Eurocodes.

As it was demonstrated, composite bridge designing is a long and complex process that involves several variables and conditions, starting with consideration of an appropriate design criterion, followed by a definition and combination of actions, until determination of resistances, durability and serviceability. Bearing in mind the earlier considerations, it can be concluded that covering all topics related to the composite bridge designing on this thesis, is clearly not possible. Thus, it was decided to focus this work on the design of a twin-girder bridge superstructure, with an emphasis on their verification part of the design.

The numerical example have been developed, in order to provide as comprehensive a coverage as possible of composite bridge designing, highlighting the various actions acting on the bridge, and how they are modelled, as well as the verification at ultimate and at serviceability limit states of the deck cross section.

Through a structural analysis, the influence of the construction process on the serviceability behaviour of composite bridges have been studied. Short and long term stresses, deflections as well as the effect of concrete cracking above supports have been analysed and evaluated. The following conclusions can be drawn from this study:

1. Due to the effect of concrete creep and shrinkage, a time-dependent longitudinal bending moment redistribution arises, increasing the negative bending moments, and reducing the positive ones;
2. Simultaneous and the Alternate slab concreting corresponds to the cases that leads to the most significant deflections at centre of the central span, as well as to the higher stresses in the bottom steel plate at support section;
3. Method 2 and 3 do not give accurate results for the calculation of bending moments for the sections at support;
4. Furthermore, this study proves that an appropriate analysis should be taken into consideration, in order to cover the effects of staged construction.

Future developments

As it was already mentioned, this dissertation provides a didactical understanding related to the composite bridge designing according to the methodologies proposed by Eurocodes, giving emphasis to the verification part of the design.

It would be interesting to apply the acquired knowledge to a real case study, in order to carry out a conceptual design of a composite bridge. Taking this into account, the following aspects should be taken into consideration:

- Piers, abutments and bearings designing;
- Geotechnical aspects of bridge design;
- Overview of seismic issues for bridge design.

References

Analysis for civil structures. MIDAS/Civil.

Chatterjee, S. (2003). *The design of modern steel bridges, Second edition*. Blacked Science Ltd.

Collings, D. (2005). *Steel-concrete Composite Bridges*. London: Thomas Telford Limited.

COMBRI Design Manual. (2008). *Part I: Application of Eurocode rules*. Germany: Poject partners.

Composite highway bridge design. (2010). *Designing to the Eurocodes (P356)*. Berkshire: The Steel Construction Institute.

Composite higway bridge design: Worked Examples. (2014). The steel construction Institute.

Comprobación de un tablero mixto: Comisión 5 - Grupo de trabajo 5/3 "Puentes mixtos". (2006). ACHE (Asociación Científico - técnica del Hormigón Estructural).

Construction Stage Analysis of a Bridge Using a Composite Section. MIDAS/Civil .

Davaine, L., Imberty, F., & Raoul, J. (2007). *Eurocodes 3 and 4: Application to steel-concrete composite road bridges* . Sétra - Service d'Estudes techniques des routes et autoroutes.

EN 1990. (2002). *Eurocode - Basis of structural design*. Brussels: CEN (European Committee for Standardization).

EN 1991-1-1. (2002). *Eurocode 1: Actions on structures - Part 1-1: Densities, self-weight, imposed loads for buildings*. Belgium: CEN (Europeen Committee for Standardization).

EN 1991-1-5. (2003). *Eurocode 1: Actions on structures - Part 1-5: General actions - Thermal actions*. Brussels: CEN (European Committee for standardization).

- EN 1991-1-6. (2005). *Eurocode 1: Part 1-6: General actions - Actions during execution*. Brussels: CEN (European Committee for Standardization).
- EN 1991-2. (2003). *Eurocode 1: Actions on structures - Part 2: Traffic loads on bridges*. Belgium, Brussels: CEN (European Committee for Standardization).
- EN 1992-1-1. (2004). *Eurocode 2: Design of concrete structures - Part 1-1: General rules and rules for buildings*. Brussels: CEN (European Committee for Standardization).
- EN 1992-2. (2005). *Eurocode 2: Design of concrete structures - Part 2: Concrete bridges - Design and detailing rules*. Brussels: CEN (European Committee for Standardization).
- EN 1993-1-1. (2005). *Eurocode 3: Design of steel structures - Part 1-1: General rules and rules for buildings*. Belgium: CEN.
- EN 1993-1-5. (2006). *Eurocode 3 - Design of steel structures - Part 1-5: Plated structural elements*. Brussels: CEN (European Committee for Standardization).
- EN 1993-1-9. (2005). *Eurocode 3: Design of steel structures - Part 1-9: Fatigue*. Brussels: CEN (European Committee for Standardization).
- EN 1993-2. (2006). *Eurocode 3 - Design of steel structures - Part 2: Steel bridges*. Brussels: CEN (European Committee for Standardization).
- EN 1994-1-1. (2004). *Eurocode 4: Design of composite steel and concrete structures - Part 1-1: General rules, and rules for buildings*. Belgium: CEN (European Committee for Standardization).
- EN 1994-2. (2005). *Eurocode 4: Design of composite steel and concrete structures - Part 2: General rules and rules for bridges*. Brussels: CEN (European Committee for Standardization).
- EN 1998-1. (2004). *Eurocode 8: Design of structures for earthquake resistance - Part 1: General rules, seismic actions and rules for buildings*. Brussels: European Committee for Standardization.
- EN 1998-2. (2011). *Eurocode 8 - Design of structures for earthquake resistance - Part 2: Bridges*. Brussels: CEN (European Committee for Standardization).

- Lebet, J.-P., & Hirt, M. A. (2013). *Steel Bridges: Conceptual and Structural Design of Steel and Steel-Concrete Composite Bridges*. Switzerland: EPFL Press.
- Mari, A., Mirambell, E., & Estrada, I. (2002). Effects of construction process and slab prestressing on the serviceability behaviour of composite bridges. *Journal of Constructional Steel Research*.
- Recomendaciones para el proyecto de puentes mixtos para carreteras RPX - 95*. (2003). Madrid: Dirección general de carreteras: Ministerio de fomento.
- Sétra - Service d'études sur les transports, les routes et leurs aménagements. (2010). *Steel-Concrete Composite Bridges: Sustainable Design Guide*. Ministère de l'Écologie, de l'énergie du Développement durable et de la Mer.
- Steel Bridge Group. (2010). *Guidance Notes on Best Practice in Steel Bridge Construction*. Berkshire: The Steel Construction Institute.
- Vayas, I., & Iliopoulos, A. (2013). *Design of Steel-Concrete Composite Bridges to Eurocodes*. CRC Press.
- Weingardt, R. G. (2005). *Engineering legends: great America civil engineers*. Reston, Virginia: American Society of Civil Engineers.

Appendix

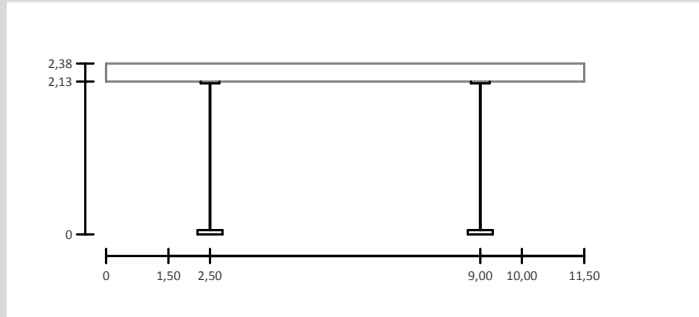
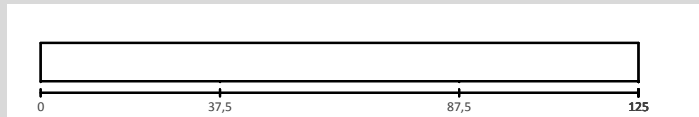
Excel spreadsheet for the Design of Composite Steel and Concrete Bridges according to Eurocodes

1 Description

1.1 Geometry

Number spans	3,00
Span 1	37,50
Span 2	50,00
Span 3	37,50
Span 4	0,00
Span 5	0,00
Span 6	0,00

Number of carriageway wide (m)	2,000
Number of footway wide (m)	4,250
Deck Slab thick (m)	2,000
Deck Slab Cantilevers (m)	1,500
Space btw main beams (m)	0,250
Steel beam depth (m)	2,500
Flange sup. b(m)	6,500
Flange sup. h(m)	2,125
Flange inf. b(m)	0,450
Flange inf. h(m)	0,025
Web b(m)	0,600
Web h(m)	0,060
Web b(m)	0,015
Web h(m)	2,040



1.2 Materials

Structural Steel:

S355	$t \leq 40\text{mm}$	$f_y = 355$	N/mm^2	EN 1993-1, 3.2
S460	$40 < t \leq 80\text{mm}$	$f_y = 430$	N/mm^2	EN 1993-1, 3.2
		$E_a = 210$	N/mm^2	EN 1993-1, 3.2

Concrete:

C35/45	$f_{ck} = 35$	N/mm^2	EN 1992-1-1
	$E_{cm} = 34$	KN/mm^2	EN 1992-1-1
	$f_{cm} = 43$	N/mm^2	EN 1992-1-1
	$f_{ctm} = 3,2$	N/mm^2	EN 1992-1-1

Reinforcing Steel:

A500 NR	$f_{sk} = 500$	N/mm^2	EN 1992-1-1
	$E_s = 210$	KN/mm^2	EN 1994-2, 3.2.2

Connectors:

$f_u = 450$	N/mm^2
$\Phi = 19$	mm
$h = 125$	mm

1.3 Main Beams - Final dimensions for the elements of the plate girders and Diaphragms

Span 1:

Transverse stiffeners:	distance :	2,083 m
		3,125 m

Intermediate diaphragms:	distance :	6,250 m
---------------------------------	------------	---------

Longitudinal stiffeners:	distance :	6,250 m
---------------------------------	------------	---------

Span 2:

Transverse stiffeners:	distance :	3,125 m
-------------------------------	------------	---------

Intermediate diaphragms:	distance :	6,250 m
---------------------------------	------------	---------

Longitudinal stiffeners:	distance :	6,250 m
---------------------------------	------------	---------

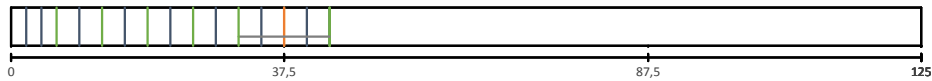
Span 3:

Transverse stiffeners:	distance :	2,083 m
		3,125 m

Intermediate diaphragms:	distance :	6,250 m
---------------------------------	------------	---------

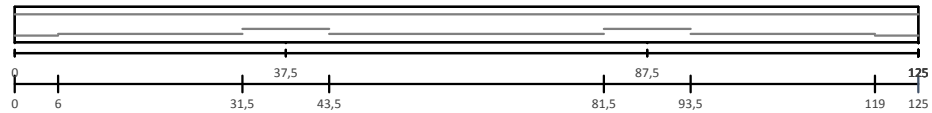
Longitudinal stiffeners:	distance :	6,250 m
---------------------------------	------------	---------

a) Stiffeners distribution



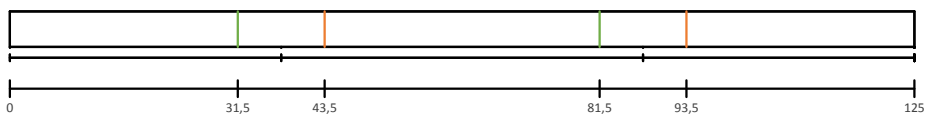
b) Plate thickness

	b	h	
Top flange:	500	45	mm
Lower flange:	700	40	mm
	700	50	mm
	700	80	mm



c) Web thickness

tw		
12	mm	—
18	mm	—



1.4 Stages of construction

- 1 Steel frame launching
- 2 Concreting slab construction at once without stopping
- 3 Dead load application at once, 15 days after concreting stage

2 Standards used

EN 1990	Basis of Structural Design
EN 1991	Actions on structures
EN 1991-1-1	Permanent actions
EN 1991-1-5	Thermal actions
EN 1991-2	Traffic loads
EN 1992	Design of concrete structures
EN 1992-1-1	General rules
EN 1992-1-1	Concrete bridges
EN 1993	Design of steel structures
EN 1993-1-1	General rules
EN 1993-1-5	Stiffened Plates
EN 1993-2	Steel bridges
EN 1994	Design of composite steel and concrete bridges
EN 1994-1-1	General rules
EN 1994-2	Composite bridges

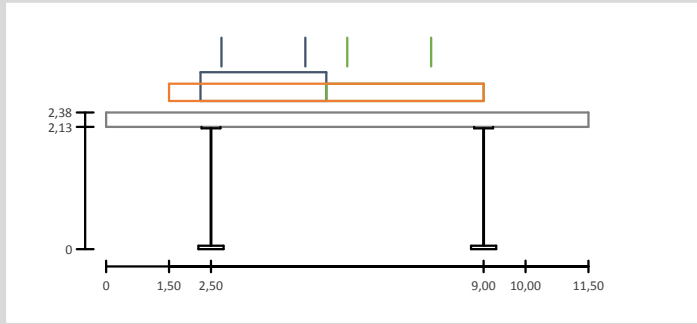
3 Actions

Permanent loads:	kN/m ²	m	kN/m
Steel structure:	1,00	1,00	7,20
Concrete slab:	6,25	5,75	35,94
Dead load:	1,00	1,00	25,25

Traffic loads:		
Carriageway Width w	8,5	m
Number of notional lanes	2	
Width of a notional lane w1	3	m
Width of the remaining area	2,5	m
Width of the marginal strip	0,75	m

Load model 1 (LM1)

Location	TS	UDL system
	Q _{ik} [kN]	q _{ik} [kN/m ²]
Lane number 1	300	9
Lane number 2	200	2,5
Lane number 3	100	2,5
Other lanes	0	2,5
Remaining area	0	2,5



Uniforme Traffic load 32 kN/m
 Heavy vehicle 800 kN

Thermal actions:

EN 1991-1-5

Temperature difference component:

EN 1991-1-5, 6.1.4

Approach 1

Type of deck:	Top warmer than bottom $\Delta T_{M,heat}$ (°C)	Bottom warmer than top $\Delta T_{M,cool}$ (°C)
Type 2: Composite bridges	15	-15

Shrinkage:

EN 1992-1-1, 3.1.4

Drying shrinkage

EN 1992-1-1, B.2

Ac 2,875 m²
 u 23,5 m
 h₀ 244,68 mm
 kh 0,8050

RH 70 %
 β_{RH} 1,018

Cement class

α_{ds1} 4
 α_{ds2} 0,12
 $\epsilon_{c,d0}$ 0,000414

t 56 dias
 t_s 1 dias
 $\beta_{ds}(t,t_s)$

t = ∞ 1

t = ∞ $\epsilon_{c,d=}$ 0,000334

Creep:

EN 1992-1-1, 3.1.4

α_1 0,865804
 α_2 0,959666
 α_3 0,902194

φ_{RH} 1,358195

$\beta(f_{cm})$ 2,561976

t₀ = 15

$\beta(t_0)$ 0,549822

φ_0 1,913194

β_h 608,4815

t[∞] = 10000

β_{∞} 0,982435

t = ∞ $\varphi(\infty)$ 1,87959

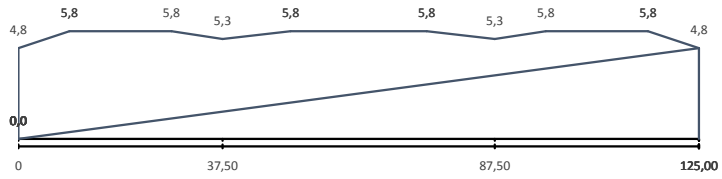
Construction loads:

EN 1991-1-6, 4.11.1

Personal and hand tools 1 kN/m²
 Formwork and load bearing memb 0,5 kN/m²
 Weigth of fresh concrete 0,25 kN/m²
 1,75 kN/m²

4 Effective width of flanges for shear lag

Number spans	3,00
Span 1	37,50
Span 2	50,00
Span 3	37,50
Span 4	0,00
Span 5	0,00
Span 6	0,00
be	5,75
b0	0,20
b1	2,40
b2	3,15



5 Global Analysis

5.1 Effecto of Creep

Short term effects:

$n_0 = 6,2 \quad 6,2$

Long term effects:

Permanent Load:

$n = 19$

Shrinkage:

$n = 13$

5.2 Effecto of Cracking of concrete

Ratio of the lengths of spans:

Span : 37,50

Span : 50,00

Ratio : 0,8

Ratio $\geq 0,6$:

OK

Adjacent support Spans (15%):

Span : 37,50 5,6

Span : 50,00 7,5

Adopted: 6,0

5.3 Mechanical characteristics of sections

Section Type 1: Section over pillar

Deck Slab: $h = 0,25 \text{ m}$

$b_{eff} = 5,75 \text{ m}$

Upper Flange: $h = 45 \text{ mm}$

$b = 500 \text{ mm}$

Lower Flange: $h = 80 \text{ mm}$

$b = 700 \text{ mm}$

Web: $h = 2000 \text{ mm}$

$b = 18 \text{ mm}$

Reinforcement: Top = $\phi // 20 \quad 0,13$

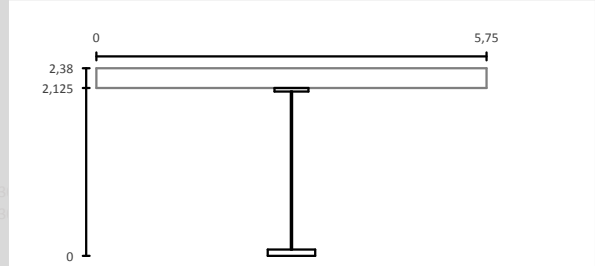
Bottom = $\phi // 16 \quad 0,13$

$n^{\circ} \phi$ Top 45 14137,17

$n^{\circ} \phi$ bottom 45 9047,787

v top 50 mm

v bottom 65 mm

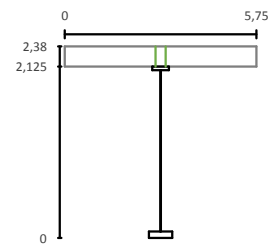
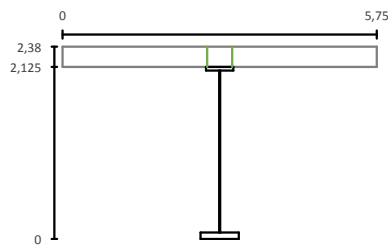
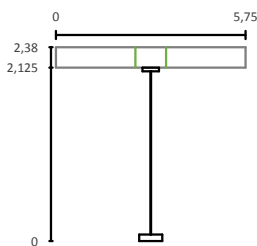


	Steel Section	Homogenized section			Cracked Section
		$n = 6,2$	$n = 13$	$n = 19,0$	
Area [m ²]	0,115	0,347	0,229	0,190	0,138
Inertia [m ⁴]	0,085	0,253	0,210	0,185	0,129
v [m]	1,353	0,612	0,864	1,014	1,351
v' [m]	0,772	1,763	1,511	1,361	1,024

$n = 6,2$

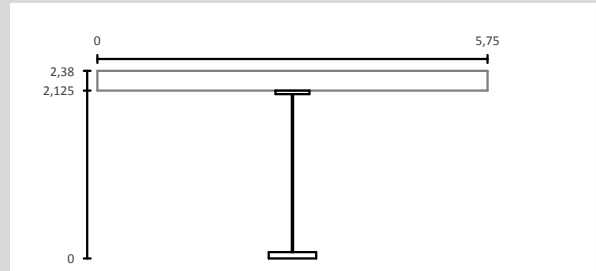
$n = 13$

$n = 19$

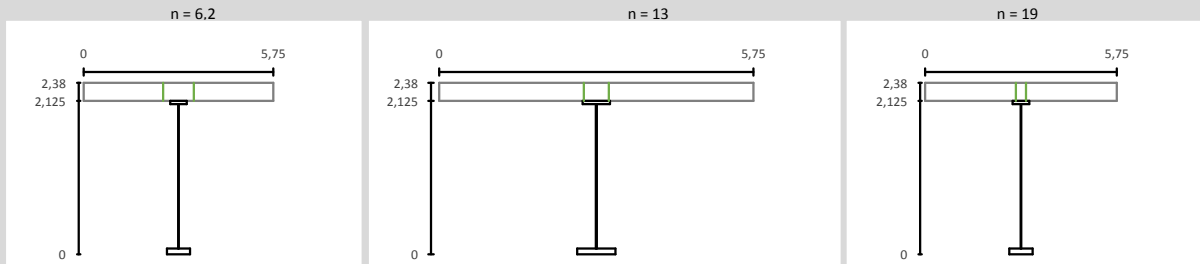


Section Type 2: Section over abutments

Deck Slab: h = 0,25 m
 beff = 5,75 m
 Upper Flange: h = 45 mm
 b = 500 mm
 Lower Flange: h = 40 mm
 b = 700 mm
 Web: h = 2040 mm
 b = 12 mm
 Reinforcement: Top = ϕ //
 Bottom = ϕ //
 $n^\circ \phi$ Top
 $n^\circ \phi$ bottom

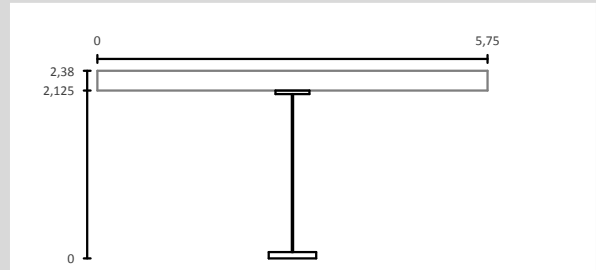


	Steel Section	Homogenized section		
		n = 6,2	n = 12,6	n = 19,0
Area [m ²]	0,075	0,308	0,189	0,151
Inertia [m ⁴]	0,063	0,154	0,135	0,123
v [m]	1,141	0,433	0,626	0,754
v' [m]	0,984	1,942	1,749	1,621

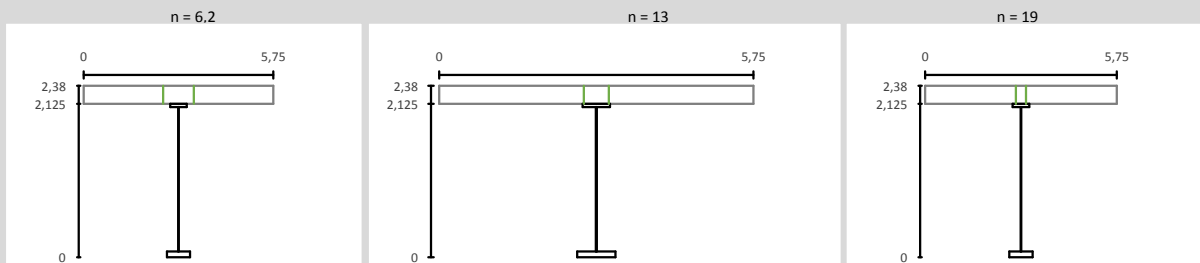


Section Type 3: Section in central span

Deck Slab: h = 0,25 m
 beff = 5,75 m
 Upper Flange: h = 45 mm
 b = 500 mm
 Lower Flange: h = 50 mm
 b = 700 mm
 Web: h = 2030 mm
 b = 12 mm
 Reinforcement: Top = ϕ //
 Bottom = ϕ //
 $n^\circ \phi$ Top
 $n^\circ \phi$ bottom



	Steel Section	Homogenized section		
		n = 6,2	n = 12,6	n = 19,0
Area [m ²]	0,082	0,314	0,196	0,158
Inertia [m ⁴]	0,068	0,192	0,155	0,140
v [m]	1,219	0,475	0,686	0,823
v' [m]	0,906	1,900	1,689	1,552



5.4 Calculation model

		Type 1	Type 2	Type 3
Self-weight of steel		Steel section	Steel section	Steel section
Self-weight of concrete		Steel section	Steel section	Steel section
Dead Load	t = 0	Cracked Section	n = 6,2	n = 6,2
	t = ∞	Cracked Section	n = 19	n = 19
Traffic loads		Cracked Section	n = 6,2	n = 6,2
Pedestrian traffic		Cracked Section	n = 6,2	n = 6,2
Thermal actions		Cracked Section	n = 6,2	n = 6,2
Shrinkage		Cracked Section	n = 13	n = 13

5.5 Stresses and displacements

	Over Pier		Mid Span		
	M (kN.m)	V (kN)	M (kN.m)	V (kN)	
Self-weight of steel	-1484	180	766	0	
Self-weight of concrete	-7405	899	3826	0	
Dead	t = 0	-4555	631	3335	0
Load	t = ∞	-4902	631	2988	0
Distributed traffic		-5988	808	5618	0
Heavy vehicle		-3217	516	7007	400
		0	800		
Pedestrian traffic		-536	72	504	0
Thermal	Heat	3102	0	3102	0
Action	Cool	-3102	0	-3102	0
Shrinkage		-4681	0	-4681	0

	t = 0 (mm)	t = ∞ (mm)
Self-weight of steel	8,8	8,8
Self-weight of concrete	43,9	43,9
Dea loads	15,3	17,7
Distributed traffic	31,3	31,3
Heavy vehicle	28,3	28,3
Pedestrian traffic	2,8	2,8

5.6 Partial factors on actions

Actions: (ULS)

	γ
Permanent action	1,35
Traffic load	1,35
Thermal action	1,5
Shrinkage	1

Factors on strength:

Material	γ	
Structural steel	γM0	1
	γM1	1,1
Concrete	γc	1,5
Reinforcement	γs	1,15

Factors for combination values:

	ψ0	ψ1	ψ2
Uniform overload	0,40	0,40	0,00
Heavy vehicle	0,75	0,75	0,00
Thermal action	0,60	0,60	0,50

5.7 Combination of actions

5.7.1 ULS

$$\begin{aligned}
 & + 1.35 \{ UDL_k + TS_k + q_{R,comb} \} + 1.5 \min \{ F_w'; 0.6 \cdot F_{VK,T} \} \\
 & + 1.35 \{ UDL_k + TS_k + q_{R,comb} \} + 1.5 \{ 0.6 \cdot T_k \} \quad \text{a)} \\
 & + 1.35 \text{ gr1b} \\
 & + 1.35 \text{ gr2} + 1.5 \{ 0.6 \cdot T_k \} \\
 & + 1.35 \text{ gr3} + 1.5 \{ 0.6 \cdot T_k \} \text{ [or } + 1.35 \text{ gr4} + 1.5 \{ 0.6 \cdot T_k \} \text{]} \\
 & + 1.35 \text{ gr5} \\
 & + 1.5 F_{VK} \\
 & + 1.5 T_k + 1.35 \{ 0.4 \cdot UDL_k + 0.75 \cdot TS_k + 0.4 \cdot q_{R,comb} \} \quad \text{b)}
 \end{aligned}$$

1.35 G_{k,sup} (or 1.0 G_{k,int})
+ (1.0 or 0.0) S

5.7.1.1 Mid span section

a)	Msd =	26067,95	kN.m
	Vsd =	540,00	kN
b)	Msd =	20605,47	kN.m
	Vsd =	405,00	kN

5.7.1.2 Pier section

1ª hypothesis: Mmáx. - Vcon

a)	Msd =	-39241,00	kN.m
	Vsd =	4193,10	kN
b)	Msd =	-34732,02	kN.m
	Vsd =	3306,15	kN

2ª hypothesis: Mcon. - Vmáx.

a)	Msd =	-34898,05	kN.m
	Vsd =	4576,50	kN
b)	Msd =	-31474,81	kN.m
	Vsd =	3593,70	kN

Section	Actions	M (kN.m)	V (kN)
Mid span	Vmax-Vco	26067,95	540,00
Over pier	Vmax-Vco	-39241,00	4193,10
	Mcon-Vma	-34898,05	4576,50

6 Verification of ULS

6.1 In midspan section

6.1.1 Classification of cross section

beff =	5,75	m
fck =	35	N/mm ²
γc =	1,5	
fy =	430	N/mm ²
γa =	1	
fytf =	430	N/mm ²
fyw =	355	N/mm ²
fybf =	430	N/mm ²

Steel Top Flange

Class 1

Web

Slab Strength

Nc = 28510,417 kN

The neutral plastic axis is located in the steel top flange

Steel Strength

Ns = 33373 kN
2*bf*tf*fy/ga = 19350 kN
Ns-Nc = 4862 kN

Class 1

Section

Class 1

6.1.2 Resistance of cross section of beam

Plastic resistance moment of the composite cross-section

Location of the Plastic Neutral Axis

Zpl = 0,261 mm
h = 2375,000 mm

Mpl,Rd = 44526 kN.m

Msd = 26068 kN.m

The plastic resistance of the composite cross section it' is checked

6.1.3 Resistance to shear buckling and in-plane forces applied to web

ε = 0,814
a = 3125 mm
hw = 2030 mm
a/hw = 1,539
ktsl = 0
fy = 355
η = 1,2
kτ = 7,028

$$\frac{31}{\eta} \varepsilon \sqrt{f_{cr}} = 55,7$$
$$\frac{i_w}{t_w} = 169,2$$

It is necessary to check the resistance to shear buckling

Web contribution

hw = 2030 mm
tw = 12 mm
σE = 6,6 N/mm²
τcr = 46,6 N/mm²
λw = 2,10
χw = 0,49
fyw = 355 N/mm²

Vbw,Rd = 2224 kN

Flange contribution

bf = 700 mm
tf = 50 mm
fyf = 430 N/mm²
a = 3125 mm
c = 996 mm
Med = 26068 kN.m
Ns = 15050 kN
yg = 138 mm
h = 2212 mm
Mf,Rd = 33200 kN.m

Vbf,Rd = 264 kN

Resistance to shear buckling

V_{b,Rd} =	2488	kN
V_{sd} =	540	kN
OK		

6.1.4 Interaction M-V

VRd =	2488	kN
Vsd =	540	kN
η₃ =	0,22	

Provided that n₃ does not exceed 0,5, the design resistance to bending moment and axial force need not be reduced to allow for the shear force.

6.2 Section over pier

6.2.1 Classification of cross section

Classification of lower flange (compression)

tf =	80	mm
bf =	700	mm
tw =	18	mm
c =	341	mm
fy =	430	N/mm ²
ε =	0,74	
c/tf =	4,2625	

Class 1

Classification of web

tw =	18	mm
c =	2000	mm
c/tw =	111,11111	
fy =	355	N/mm ²
ε =	0,81	

Calculation of the position of the neutral plastic axis

Reinforcement: Top = φ // 20 0,13

Bottom = φ // 16 0,13

n^o φ Top 41 12880,53

n^o φ botto 41 8243,539

Nφ _{upp} =	5600	kN
N ^o φ _{low} =	3584	kN
N _{fy,flupp} =	430	N/mm ²
N _{flupp} =	9675	kN
N _{fy,flflow} =	430	N/mm ²
N _{flflow} =	24080	kN
N _{web} =	12780	kN

x =	0,704		α =	0,30
	27860			
	27860			
f _{np} =	672	mm		

tw =	18	mm
c =	2000	mm
c/tw =	111,11111	

Class 2

Section

Class 2

6.2.2 Resistance of cross section of beam

Plastic resistance moment of the composite cross-section

			Z (m)
Nφ _{upp} =	5600	kN	2,275
N ^o φ _{low} =	3584	kN	2,155
N _{flupp} =	9675	kN	2,063
N _{web} =	12780	kN	1,336
			0,336

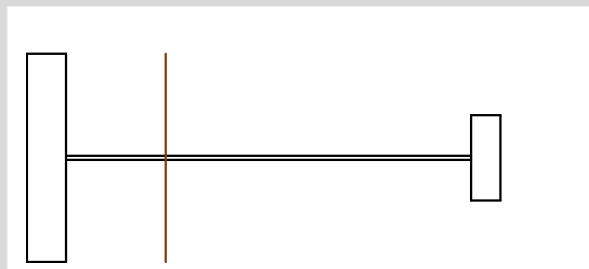
M_{pl,Rd} = -51172 kN.m

M_{sd} = -39241 kN.m

The plastic resistance of the composite cross section it is checked

6.2.3 Resistance to shear buckling and in-plane forces applied to web

tw =	18	mm
ε =	0,81	
1/2 IPE 400		
hw =	186,5	mm
tw =	8,6	mm
bf =	180	mm
tf =	13,5	mm
V =	63,88632	mm
V' =	154,1137	mm
I =	85091415	mm ⁴
A1 (mm ²)	7908,353	
A2 (mm ²)	1603,9	
A3 (mm ²)	2430	
I1 (mm ⁴)	213525,5	
I2 (mm ⁴)	4648938	
I3 (mm ⁴)	36905,63	
A (mm ²)	11942,25	



hw = 2000 mm
 a = 3125,00 mm
 tw = 18 mm
 η = 1,2
 a/hw = 1,56
 Kτ = 23,34

Ktsl = 16

auxiliar values
 kτ = 23,34209
 kτ = 22,55095

$$\frac{31}{\eta} \varepsilon \sqrt{k_{\tau}} = 101,5$$

$$\frac{h_w}{t_w} = 111,1$$

It is necessary to check the resistance to shear buckling

Web contribution

hw = 2000 mm
 a = 3125 mm
 a/hw = 1,56

hw1 = 1400 mm
 a = 3125 mm
 a/hw1 = 2,23

Kτ = 6,14

λw1 = 0,76
 λw2 = 1,03
 λw = 1,03
 χw = 0,80
Vbw,Rd = 5366,21 kN

Flange contribution

bf = 700 mm
 tf = 80 mm
 fyf = 430 N/mm²
 fyf = 355 mm
 a = 3125 mm
 c = 1158,0888 kN.m
 Med = 39241
Vbf,Rd = 87 kN

Resistance to shear buckling

Vb,Rd = 5453 kN
Vsd = 4577 kN
OK

6.1.4 Interaction M-V

Maximum V

VRd = 5453 kN
Vsd = 4577 kN
η3 = 0,84

If n3 is more than 0,5 the combined effects of bending and shear in the web should be considered.

MPI,Rdd = 51172 kN
MSd = 34898 kN
η1 = 0,68

$$\bar{\eta}_1 + \left(1 - \frac{M_{f,Rd}}{M_{pl,Rd}}\right) (2\bar{\eta}_3 - 1)^2 \leq 1,0 \quad 0,83 \quad \text{OK}$$

Maximum M

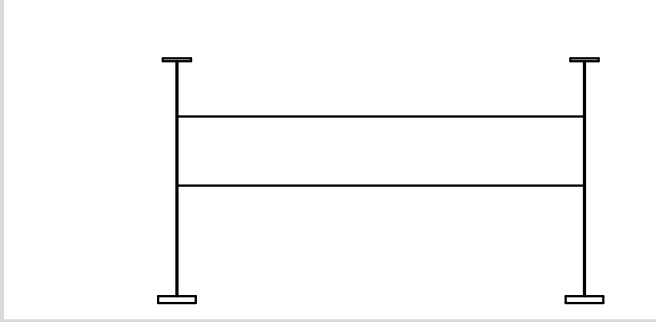
VRd = 5453 kN
Vsd = 4577 kN
η3 = 0,84

If n3 is more than 0,5 the combined effects of bending and shear in the web should be considered.

MPI,Rdd = 51172 kN
MSd = 34898 kN
η1 = 0,68

$$\bar{\eta}_1 + \left(1 - \frac{M_{f,Rd}}{M_{pl,Rd}}\right) (2\bar{\eta}_3 - 1)^2 \leq 1,0 \quad 0,83 \quad \text{OK}$$

6.3 Lateral torsional buckling



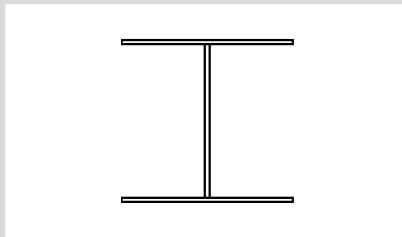
6.3.1 Mechanical Characteristics

Cross bracing

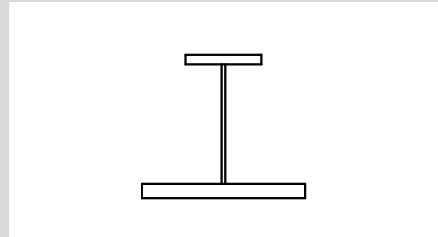
$h_1(m) =$	0,8	$h_2(m) =$	1,32
		b	h
Upper flange =	350	15	mm
Lower flange =	350	15	mm
Web =	10	570	mm

Stiffener

	b	h	
Upper flange =	204	12	mm
Lower flange =	439,3529173	18	mm
Web =	10	150	mm



A =	16200	mm ²
I _y =	0,0	mm ⁴
EI =	0	kN.m ²



A =	11856,35	mm ²
I _y =	0	mm ⁴
EI =	0	kN.m ²

6.3.2 Upper chorder (Only during construction)

h = hv =	0,8
bq =	6,5
Cd =	41192 kN/m

6.3.3 Lower chord

h = hv =	1,32
bq =	6,5
Cd =	11097,44 kN/m

6.3.4 Simplified method

L =	50	m
ℓ =	6,25	m
I =	0,000469	m ⁴
Cd =	42077,43	kN/m
C =	6732,389	kN/m ²
γ =	427453,3	
m =	132,4874	
NE =	388,6157	kN
N _{crit} =	51486,68	kN
lk =	4,343929	m
lk =	6,250	m
N _{crit} =	24871	kN

Support section

Md =	14797,4	kN.m
v =	1,352718	m
l =	0,085285	m
σ _{sup} =	234,7036	Mpa
bf =	500	mm
hf =	45	mm
tw =	18	mm
fyf =	430	N/mm ²

Mid Span section

Md =	7646,4	kN.m
v =	1,219495	m
l =	0,068369	m
σ _{sup} =	136,388	Mpa
bf =	500	mm
hf =	45	mm
tw =	12	mm
fyf =	430	N/mm ²

N _{sd} =	3068,73	kN
F _{Ed} =	30,6873	kN

A= 0,027 m²
 λ_{LT} = 0,686
 α_{LT} = 0,490
 ϕ_{LT} = 0,854
 χ_{LT} = 0,734
 Nu = 7799

Nu = 7799
 Nsd= 3069
 OK

7 Verification of SLS

7.1 Deformations

Deflection value due to overload:

UDL: 31,3 mm
 Tsk: 28,3 mm

Frequent SLS combination of actions:

33,745 mm

Limiting value:

L/1200: 41,67 mm

OK

7.2 stresses

7.2.1 Steel section - over pillar

	Over Pier		S	τ	Wsup	σ_{sup}	Winf	σ_{inf}	
	M (kN.m)	V (kN)	(m3)	kPa	(m3)	kPa	(m3)	kPa	
Self-weight of steel	1484	180	0,045321	5314,066	0,0630	23537,93	0,1104	13438,06	
Self-weight of concrete	7405	899	0,045321	26540,81	0,0630	117451,7	0,1104	67054,47	
Dead Load	t = 0	4555	631	0,045321	18628,75	0,1168	38992,27	0,1255	36290,83
	t = ∞	4902	631	0,045321	18628,75	0,1168	41962,7	0,1255	39055,47
Distributed traffic	5988	808	0,045321	23854,25	0,1168	51259,21	0,1255	47707,9	
Heavy vehicle	3217	516	0,045321	15233,66	0,1168	27538,56	0,1255	25630,65	
Pedestrian traffic	536	72	0,045321	2125,626	0,1168	4588,333	0,1255	4270,447	
Action	3102	0	0,045321	0	0,1168	26554,12	0,1255	24714,41	
Shrinkage	4681	0	0,045321	0	0,1168	40070,87	0,1255	37294,7	

τ = 91,70 MPa
 σ_{sup} = 322,34 MPa
 σ_{inf} = 249,28 MPa

f_y
 $\sigma_{Ed,ser,sup}$ = 359,35
 $\sigma_{Ed,ser,inf}$ = 295,58

430
 430

OK
 OK

7.2.2 Concrete - Mid-Span

	M (kN.m)	n	l	v	σ	
Dead Load	t = 0	3335	6,18	0,191809	0,474992	0
Load	t = ∞	2988	18,957453	0,139527	0,822964	929,6604
Distributed traffic		5618	6,18	0,191809	0,474992	2251,185
Heavy vehicle		7007	6,18	0,191809	0,474992	2807,771
Pedestrian traffic		504	6,18	0,191809	0,474992	201,9575
Thermal	Heat	3102	6,18	0,191809	0,474992	745,8003
Action	Cool	-3102	6,18	0,191809	0,474992	0
Shrinkage		-4681	12,568726	0,154615	0,685871	-1652,105

0,6f_{ck} = 21 Mpa
 σ = 5,284269 Mpa

OK